

Distribution Agreement

In presenting this thesis or dissertation as a partial fulfillment of the requirements for an advanced degree from Emory University, I hereby grant to Emory University and its agents the non-exclusive license to archive, make accessible, and display my thesis or dissertation in whole or in part in all forms of media, now or hereafter known, including display on the world wide web. I understand that I may select some access restrictions as part of the online submission of this thesis or dissertation. I retain all ownership rights to the copyright of the thesis or dissertation. I also retain the right to use in future works (such as articles or books) all or part of this thesis or dissertation.

Signature:

Rachel A. Pearson

Date

Impact of HIV infection and antiretroviral therapy on *Mycobacterium tuberculosis*-specific CD4
T cell responses

By

Rachel A. Pearson
Doctor of Philosophy

Graduate Division of Biological and Biomedical Sciences
Immunology and Molecular Pathogenesis

Cheryl L. Day, Ph.D.
Advisor

Ann M. Chahroudi, M.D., Ph.D.
Committee Member

Karen N. Conneely, Ph.D.
Committee Member

Eliver E. B. Ghosn, Ph.D.
Committee Member

Jacob E. Kohlmeier, Ph.D.
Committee Member

Christopher D. Scharer, Ph.D.
Committee Member

Accepted:

Kimberly Jacob Arriola, Ph.D., MPH
Dean of the James T. Laney School of Graduate Studies

Impact of HIV infection and antiretroviral therapy on *Mycobacterium tuberculosis*-specific CD4
T cell responses

By

Rachel A. Pearson
B.S., Columbus State University, 2017
M.S. Columbus State University, 2019

Advisor: Cheryl L. Day, Ph.D.

An abstract of
A dissertation submitted to the Faculty of the
James T. Laney School of Graduate Studies of Emory University
in partial fulfillment of the requirements for the degree of
Doctor of Philosophy
in Graduate Division of Biological and Biomedical Science
Immunology and Molecular Pathogenesis
2025

Abstract

Impact of HIV infection and antiretroviral therapy on *Mycobacterium tuberculosis*-specific CD4 T cell responses

By Rachel A. Pearson

HIV is the strongest known risk factor for tuberculosis (TB), largely due to its profound disruption of *Mycobacterium tuberculosis* (Mtb)-specific CD4 T cell immunity. This dissertation investigates how HIV infection and the timing of antiretroviral therapy (ART) affect the function and transcriptional profile of Mtb-specific CD4 T cells and examines the broader epigenetic and transcriptional landscape of total peripheral CD4 T cells in individuals with and without HIV.

In a unique longitudinal analysis, we profiled Mtb-specific CD4 T cells before and after HIV acquisition using flow cytometry and single-cell RNA sequencing. We observed early and preferential depletion of Mtb-specific effector subsets, including Th1 and Th17 cells, alongside reduced cytokine production and increased representation of *TCF7*⁺ stem-like cells. Transcriptional dysregulation following HIV infection was marked by enrichment of WNT and hypoxia signaling pathways and downregulation of antigen processing, cytokine signaling, and migration programs. These findings suggest that HIV rapidly impairs the differentiation and function of Mtb-specific CD4 T cells.

In a separate cross-sectional analysis, we performed RNA-seq, ATAC-seq, and reduced representation bisulfite sequencing (RRBS) on total CD4 T cells from people without HIV and people with HIV prior to ART initiation. While transcriptional and chromatin accessibility changes were relatively limited in resting cells, we identified moderate changes in DNA methylation, suggesting early epigenetic reprogramming that may contribute to latent immune dysfunction.

Finally, to evaluate how ART timing shapes Mtb-specific CD4 T cell responses, we functionally profiled these cells in people without HIV and in individuals who started ART early or late after HIV acquisition. HIV infection and delayed ART initiation were associated with diminished frequencies of functional and polyfunctional Mtb-specific CD4 T cells, while early ART preserved effector functionality and subset diversity. Single-cell transcriptomics revealed that delayed ART initiation was linked to transcriptional silencing and skewing toward quiescent states, whereas early ART was associated with greater transcriptional activity and preservation of effector and regulatory subsets.

Together, these findings provide new insights into how HIV alters both the antigen-specific and global CD4 T cell landscape and underscore the critical role of early ART in preserving Mtb-specific immunity. This work offers molecular insights for the heightened risk of TB in people with HIV and informs future strategies for immune restoration in co-infected populations.

Impact of HIV infection and antiretroviral therapy on *Mycobacterium tuberculosis*-specific CD4
T cell responses

By

Rachel A. Pearson
B.S., Columbus State University, 2017
M.S. Columbus State University, 2019

Advisor: Cheryl L. Day, Ph.D.

A dissertation submitted to the Faculty of the
James T. Laney School of Graduate Studies of Emory University
in partial fulfillment of the requirements for the degree of
Doctor of Philosophy
in Graduate Division of Biological and Biomedical Science
Immunology and Molecular Pathogenesis
2025

Table of Contents

| | |
|--|----------|
| CHAPTER 1. INTRODUCTION | 1 |
| 1.1 OVERVIEW | 1 |
| 1.2 EPIDEMIOLOGY OF TUBERCULOSIS | 1 |
| 1.3 MTB PATHOGENESIS..... | 2 |
| 1.4 CLINICAL SPECTRUM OF MTB INFECTION | 4 |
| 1.5 DIAGNOSIS OF MTB | 5 |
| 1.6 RISK FACTORS FOR MTB INFECTION AND PROGRESSION..... | 7 |
| 1.7 MTB TREATMENT | 8 |
| 1.8 EPIDEMIOLOGY OF MTB AND HIV CO-INFECTION | 9 |
| 1.9 EFFECT OF HIV ON TB PROGRESSION..... | 10 |
| 1.10 IMMUNE RESPONSES TO MTB | 12 |
| 1.11 MTB-SPECIFIC CD4 ⁺ T CELL RESPONSES IN HIV | 14 |
| 1.12 EFFECT OF HIV TREATMENT ON MTB-SPECIFIC IMMUNE RESPONSES | 14 |
| 1.13 SUMMARY..... | 15 |
| CHAPTER 2: SINGLE-CELL TRANSCRIPTOMICS REVEALS DEPLETION AND DYSREGULATION OF MYCOBACTERIUM TUBERCULOSIS-SPECIFIC TH1 AND TH17 CELLS EARLY AFTER ACQUISITION OF HIV | 1 |
| 2.1 ABSTRACT..... | 2 |
| 2.2 INTRODUCTION | 1 |
| 2.3 MATERIALS AND METHODS..... | 4 |
| 2.3.1 <i>Study population and sample collection</i> | 4 |
| 2.3.2 <i>Ethics Statement</i> | 4 |
| 2.3.3 <i>T cell intracellular cytokine staining (ICS) assay and flow cytometry</i> | 5 |
| 2.3.4 <i>MIMOSA and COMPASS analysis of flow cytometry data</i> | 6 |
| 2.3.5 <i>Activation-induced marker assay and sorting Mtb-specific CD4 T cells</i> | 7 |
| 2.3.7 <i>ScRNA-seq data processing and analysis</i> | 8 |
| 2.3.8 <i>Statistical Analysis</i> | 9 |
| 2.4 RESULTS | 10 |
| 2.4.1 <i>Study Participants</i> | 10 |
| 2.4.2 <i>Mtb-specific CD4 T cells in PWH demonstrate impaired functionality and polyfunctionality</i> . | 10 |
| 2.4.3 <i>Single-cell transcriptomics identifies distinct subsets of Mtb-specific CD4 T cells</i> | 12 |
| 2.4.4 <i>Mtb-specific Th1 and Th17 cell numbers are diminished following HIV infection</i> | 13 |
| 2.4.5 <i>Average expression of effector genes declines after HIV infection</i> | 14 |
| 2.4.6 <i>Important pathways are downregulated in Mtb-specific CD4 T cells after HIV infection</i> | 14 |
| 2.5 DISCUSSION | 17 |
| 2.6 MAIN FIGURES | 25 |
| Table 2.1 | 25 |
| Figure 2.1..... | 26 |
| Figure 2.2..... | 28 |

| | |
|--------------------------------------|----|
| <i>Figure 2.3</i> | 30 |
| <i>Figure 2.4</i> | 32 |
| <i>Figure 2.5</i> | 34 |
| 2.7 SUPPLEMENTAL FIGURES | 36 |
| <i>Supplemental Figure 2.1</i> | 36 |
| <i>Supplemental Figure 2.2</i> | 38 |
| <i>Supplemental Figure 2.3</i> | 39 |

CHAPTER 3. EARLY ART INITIATION FOLLOWING HIV INFECTION PRESERVES THE DIVERSITY AND FUNCTION OF MTB-SPECIFIC CD4 T CELLS.....41

| | |
|--|----|
| 3.1 ABSTRACT..... | 42 |
| 3.2 INTRODUCTION | 43 |
| 3.3 METHODS..... | 46 |
| 3.3.1 <i>Study population and sample collection</i> | 46 |
| 3.3.2 <i>Ethics Statement</i> | 46 |
| 3.3.3 <i>Total CD4 T cell Sorting</i> | 47 |
| 3.3.4 <i>RNA Sequencing and Analysis</i> | 47 |
| 3.3.5 <i>ATAC-seq and Analysis</i> | 48 |
| 3.3.6 <i>Reduced-Representation Bisulfite Sequencing and Analysis</i> | 49 |
| 3.3.7 <i>T cell ICS assay and flow cytometry</i> | 50 |
| 3.3.8 <i>COMPASS analysis of flow cytometry data</i> | 50 |
| 3.3.9 <i>Activation-induced marker assay and sorting Mtb-specific CD4 T cells</i> | 51 |
| 3.3.10 <i>10x Genomics scRNA-seq library preparation</i> | 51 |
| 3.3.11 <i>ScRNA-seq data processing and analysis</i> | 51 |
| 3.3.12 <i>Statistical Analysis</i> | 52 |
| 3.4 RESULTS | 53 |
| 3.4.1 <i>Study Participants</i> | 53 |
| 3.4.2 <i>HIV infection induces moderate DNA methylation changes with minimal transcriptional or chromatin accessibility alterations in resting CD4 T cells</i> | 54 |
| 3.4.3 <i>HIV infection impairs polyfunctional Mtb-specific CD4 T cell responses, with greater dysfunction when ART is initiated more than 1 year after HIV infection</i> | 55 |
| 3.4.4 <i>Single cell transcriptional profiling indicates distinct clusters of Mtb-specific CD4 T cells</i> | 56 |
| 3.4.5 <i>HIV infection reshapes the transcriptional landscape and subset composition of Mtb-specific CD4 T cells, with early ART preserving effector diversity</i> | 57 |
| 3.4.6 <i>Early ART initiation preserves effector and regulatory gene expression in Mtb-specific CD4 T cells</i> | 59 |
| 3.4.7 <i>Reduced intensity of effector gene expression within conserved Mtb-specific CD4 T cell clusters</i> | 61 |
| 3.5 DISCUSSION | 62 |
| 3.6 MAIN FIGURES..... | 67 |
| <i>Table 3.1</i> | 67 |
| <i>Figure 3.1</i> | 68 |

| | |
|--------------------------------------|-----------|
| <i>Figure 3.2</i> | 70 |
| <i>Table 3.2</i> | 72 |
| <i>Figure 3.3</i> | 73 |
| <i>Figure 3.4</i> | 75 |
| <i>Figure 3.5</i> | 77 |
| <i>Figure 3.6</i> | 79 |
| 3.6 SUPPLEMENTAL FIGURES | 80 |
| <i>Supplemental Figure 3.1</i> | 80 |
| <i>Supplemental Figure 3.2</i> | 81 |
| <i>Supplemental Figure 3.3</i> | 82 |
| CHAPTER 4. DISCUSSION | 86 |
| 4.1 SUMMARY | 86 |
| 4.2 IMPLICATIONS..... | 88 |
| 4.3 FUTURE DIRECTIONS | 89 |
| CHAPTER 5. REFERENCES | 92 |

CHAPTER 1. Introduction

1.1 Overview

Tuberculosis (TB), caused by *Mycobacterium tuberculosis* (Mtb), remains one of the leading causes of all-cause mortality globally. The dual epidemics of TB and HIV have fueled each other in regions where both are prevalent, creating a ‘syndemic’ that exacerbates disease burden. Mtb infection is controlled largely by the immune system, with CD4 T cells playing a pivotal role in containing the bacteria. However, HIV infects CD4 T cells, thus undermining the immune response to Mtb and dramatically increasing the risk of TB disease. This chapter provides a comprehensive overview of (i) the epidemiology of TB, (ii) the epidemiology of Mtb/HIV co-infection, (iii) immune responses to Mtb and HIV, and (iv) the specific impact of HIV infection and treatment with antiretroviral therapy (ART) on Mtb-specific CD4 T cell responses. This chapter provides context and scientific rationale for studying the effect of HIV infection and treatment on Mtb-specific CD4 T cell responses.

1.2 Epidemiology of Tuberculosis

TB remains a formidable global health challenge. TB ranks as the 10th leading cause of death globally and—apart from the years 2020 to 2022, when the COVID-19 pandemic temporarily surpassed it¹—it remains the deadliest infectious disease caused by a single pathogen². TB continues to cause nearly twice as many deaths as HIV/AIDS (0.63 million)², despite being both preventable and curable. Latent TB infection (LTBI), defined by the presence of an immune response to Mtb antigens in the absence of symptoms and signs of clinical disease, affects about one-quarter of the global population—an estimated 1.7 to 2 billion people³. Among individuals

with LTBI, 5–10% will progress to active disease over their lifetime under normal immune conditions^{4,5}, with the highest risk occurring within the first two years following infection^{3,6,7}. While some individuals can naturally clear the infection⁸, many harbor dormant bacilli for decades⁵.

Approximately 90% of TB cases each year occur in adults, with men disproportionately affected. In 2023, adult men (aged ≥ 15 years) accounted for 55% (6.0 million cases) of total TB cases, compared to 33% (3.6 million cases) among adult women and 12% (1.3 million cases) among children aged 0–14 years². The disease burden is highest in low- and middle-income countries, which account for about 80% of cases². The highest regional burden in 2023 was observed in the World Health Organization (WHO)-defined South-East Asia Region (45%), followed by the African Region (24%) and the Western Pacific Region (17%)². Key high-burden countries include India, Indonesia, China, the Philippines, Pakistan, Nigeria, South Africa, and Bangladesh. Socioeconomic factors such as poverty, overcrowding, and undernutrition are major determinants of TB risk and perpetuate health disparities across regions^{9,10}.

1.3 Mtb Pathogenesis

While TB is predominantly a pulmonary disease, Mtb possesses the capacity to disseminate to virtually any organ system^{11,12}. Common sites of extrapulmonary TB include lymph nodes, the pleura, bones, joints, and the genitourinary system. Extrapulmonary TB comprises roughly 15% of global TB cases, disproportionately affecting children and immunocompromised individuals, such as those living with HIV. Despite this, the majority of TB cases remain pulmonary in nature. The pathogenesis of pulmonary TB is shaped by a complex interplay between bacterial virulence

mechanisms and host immune responses, commonly conceptualized as the "immunological life cycle" of Mtb, which unfolds through four distinct stages: transmission, infection, equilibrium, and reactivation¹³.

Mtb is transmitted primarily via airborne droplets expelled by individuals with pulmonary TB, particularly during coughing or sneezing¹⁴. After inhalation, Mtb bacilli reach the alveoli, where they are engulfed by resident alveolar macrophages^{15,16}. Normally, upon phagocytosis of a microbe, macrophages mature the phagosome and fuse it with lysosomes to kill the pathogen. Mtb, however, can arrest phagosome maturation. Virulent Mtb strains inhibit the acidification of the phagosome and the recruitment of proteolytic enzymes, enabling the bacilli to survive inside the macrophage's phagosomal compartment, using this cellular niche to survive and replicate^{17,18}. This triggers a broader inflammatory response that recruits monocytes and other immune cells, inadvertently expanding the population of cells Mtb can infect¹⁹. Despite early containment efforts, the adaptive immune response is characteristically delayed in TB. The priming of naïve T and B lymphocytes followed by their homing to pulmonary tissues may require approximately 4 to 6 weeks²⁰.

Following the activation of the adaptive immune response, successful immune containment leads to the formation of granulomas—complex structures composed of infected macrophages, including multinucleated giant cells and foamy macrophages, surrounded by CD4 and CD8 T lymphocytes and other immune cells²¹. These granulomas serve to restrict bacterial replication, localize infection, and mitigate tissue damage but also provide Mtb with a niche for persistence²². By this time, the bacilli may have already established a replicative stronghold. Adaptive immunity attempts to constrain the infection through the formation of granulomas¹⁸, which provide dynamic,

heterogeneous microenvironments where ongoing immune cell turnover and bacterial flux occur²³. When these responses are balanced, a clinically asymptomatic and non-infectious LTBI is established, during which granulomas function as immunological barriers that can contain *Mtb* bacilli over extended periods^{20,22}. However, when immune control is lost, typically due to immunosuppression or other risk factors, granulomas destabilize. This leads to necrosis, liquefaction, and eventual cavitation into airways, releasing bacilli and enabling person-to-person transmission^{20,23}.

1.4 Clinical Spectrum of *Mtb* Infection

Rather than following a strict binary between latent and active states, *Mtb* infection exists along a dynamic continuum (Figure 1.1)²⁰. Individuals may either eliminate the pathogen entirely, harbor a stable latent infection, or progress to subclinical or symptomatic disease. Subclinical TB, defined by a positive *Mtb* culture in the absence of symptoms²⁴, reflects an underrecognized yet epidemiologically significant phase that complicates case detection and public health control. When immune control fails—due to immunosuppressive conditions such as HIV, diabetes, malnutrition, or advancing age—latent bacilli may reactivate. This results in caseating granulomas, tissue necrosis, and clinical manifestations such as persistent cough, fever, night sweats, and weight loss. The biological basis of *Mtb* infection outcomes remains complex and multifaceted.

The clinical spectrum also encompasses several forms of TB disease. Primary TB typically occurs in children or immunocompromised individuals shortly after infection and is marked by non-cavitating pulmonary lesions or extrapulmonary manifestations^{20,21}. In contrast, post-primary TB—a reactivation of *Mtb*—arises months to years after the initial infection and is the predominant form

in adults¹¹. It is often characterized by upper lobe cavitation and high bacterial loads^{11,21}. Relapsing or recurrent TB refers to the reactivation of disease caused by the same Mtb strain, typically due to incomplete treatment, inadequate immune clearance, or bacterial persistence. In contrast, TB reinfection arises from a new exposure to a genetically distinct Mtb strain, a phenomenon particularly common in high-transmission settings. In some cases, individuals may harbor multiple strains simultaneously—called superinfections²⁵—which can complicate diagnosis, treatment, and disease resolution due to differential drug susceptibility and host immune responses²⁶. These phenomena are increasingly identifiable through molecular genotyping, which enables differentiation between new infections, reinfections, relapses, and superinfections, as well as discrimination between hospital- and community-acquired Mtb strains²⁷. This approach is particularly valuable in high-burden settings and among individuals with HIV, where immunosuppression significantly heightens the risk of reinfection^{20,27}. The spectrum of TB—from elimination to reactivation—underscores the need to better understand molecular mechanisms of Mtb control.

1.5 Diagnosis of Mtb

Diagnosing Mtb infection is inherently complex due to the diverse clinical spectrum spanning latent infection to active disease. Diagnostic tools are broadly categorized into two types: those that detect the host immune response to Mtb—primarily used for identifying LTBI—and those that directly detect the presence of Mtb, essential for confirming active TB disease¹⁴. It is important to note, however, that current immunologic tests cannot distinguish LTBI from active disease, highlighting a key limitation in TB diagnostics.

The main immunologic tests include the tuberculin skin test (TST) and interferon-gamma (IFN γ) release assays (IGRAs)²⁸. TST, or the Mantoux test, involves intradermal injection of purified protein derivative (PPD) and measures delayed hypersensitivity that presents as a measurable skin induration after 48–72 hours. Its limitations include the need for a follow-up visit and the potential for false-positive results due to prior *Bacillus Calmette-Guérin* (BCG) vaccination or exposure to non-tuberculous mycobacteria. IGRAs, including the FDA-approved QuantiFERON®-TB (QFT)²⁰ and T-SPOT® TB tests, overcome these challenges by detecting IFN γ release in response to *Mtb*-specific proteins, culture filtrate protein 10 (CFP-10) and early secreted antigenic target 6 (ESAT-6), which are absent from BCG²⁸. These assays require only a single patient visit and offer improved specificity, particularly in BCG-vaccinated individuals. QFT employs an enzyme-linked immunosorbent assay (ELISA), while T-SPOT uses an enzyme-linked immunospot (ELISPOT) technique²⁸. Despite their strengths in identifying *Mtb* infection, neither test can differentiate between LTBI and active TB.

For active TB, microbiological confirmation remains critical. Sputum samples are analyzed using liquid culture—considered the gold standard due to its high specificity and ability to detect viable bacilli—though it is time-intensive^{11,29}. Smear microscopy and fluorescent staining provide same-day results but have low sensitivity. Molecular diagnostics, such as Xpert MTB/RIF and Hain MTBDRplus, offer rapid, sensitive detection and the added advantage of identifying rifampicin and other drug resistance^{26,30}. Given its diagnostic accuracy and ease of use, the WHO recommends Xpert MTB/RIF as the first-line test for all suspected adult TB cases⁸. Nevertheless, diagnosing subclinical and incipient TB remains difficult, primarily due to low bacterial loads that fall below the detection thresholds of existing tools.

1.6 Risk Factors for Mtb Infection and Progression

While anyone exposed to Mtb can become infected, only a minority develop disease, and this progression is largely determined by host risk factors. The strongest risk factor for progressing from LTBI to TB is HIV co-infection. HIV-induced immunodeficiency massively elevates TB risk— on the order of 15–21 times higher risk of active TB compared to HIV-negative individuals^{9,31,32}. Other significant risk factors include: malnourishment and underweight status, which weaken immune defenses; diabetes mellitus, which approximately triples the risk of active TB due to immune dysregulation; cigarette smoking and chronic lung disease, which impair mucosal defenses; silicosis (from silica dust exposure), which damages lung macrophage function; and use of immunosuppressive therapies such as corticosteroids or tumor necrosis factor (TNF) inhibitors²⁹. Notably, the use of TNF blocking drugs for autoimmune diseases has been associated with greatly increased TB reactivation rates, underlining the importance of TNF in containing latent Mtb^{33,34}. Young children and the elderly are also more susceptible to TB disease due to immature or waning immunity. Socioeconomic and environmental factors – poverty, overcrowding, poor ventilation, and limited access to healthcare – facilitate ongoing Mtb transmission and hinder early diagnosis, thereby increasing community TB spread^{9,29}. Globally, as gross domestic product increases, TB incidence tends to decrease, whereas high prevalence of undernutrition correlates with higher TB incidence^{2,35,36}. These risk factors often synergize; for example, regions with high HIV prevalence may also have pervasive poverty and undernutrition, compounding TB risk³⁷.

1.7 Mtb Treatment

The WHO recommends several treatment options for LTBI, all of which aim to prevent progression to TB, particularly in high-risk populations such as PWH, close contacts of TB patients, and individuals on immunosuppressive therapies. The standard regimens include 6 or 9 months of daily isoniazid, which has long been the mainstay of LTBI treatment³. However, shorter rifamycin-based regimens are now strongly recommended due to improved adherence and reduced toxicity. These include 3 months of once-weekly rifapentine plus isoniazid (3HP)^{38,39}, 3 months of daily isoniazid plus rifampicin (3HR)⁴⁰, and 4 months of daily rifampicin alone (4R)^{3,41}. These regimens have demonstrated similar efficacy with better safety profiles compared to isoniazid monotherapy. The choice of regimen should consider factors such as patient age, comorbidities, potential drug interactions, and programmatic feasibility.

Despite its severity, TB is a curable disease in the vast majority of cases, provided effective treatment is given. Standard therapy for drug-susceptible TB consists of a combination of daily, fixed-dose administration of four first-line antibiotics: isoniazid, rifampicin (rifampin), pyrazinamide, and ethambutol, given for an intensive phase of 2 months, followed by a continuation phase of isoniazid and rifampicin for an additional 4 months (2HRZE/4HR)^{8,42}. This 6-month rifampicin-based regimen has been the backbone of TB treatment for decades⁴². The guidelines remain the same in people with HIV (PWH), with the added stipulation that people with newly diagnosed HIV should initiate anti-retroviral therapy (ART) within 2 weeks following the start of TB treatment, regardless of CD4 cell count⁸. Treatment success rates for drug-susceptible TB can exceed 85% under programmatically supervised therapy⁸. However, challenges remain due to adherence difficulties due to the long treatment duration and medication side effects and the

emergence of drug-resistant TB strains⁴³.

Multidrug-resistant Mtb (MDR-Mtb), defined as Mtb resistant to at least isoniazid and rifampicin, affected an estimated 410,000 new cases worldwide in 2023^{2,8}. Even more concerning is extensively drug-resistant TB (XDR-TB), which is resistant to first-line and several second-line drugs. Drug-resistant TB requires longer, more toxic, and far costlier treatment regimens, often with lower success rates. The global spread of MDR/XDR-TB threatens to reverse progress in TB control. Nonetheless, improvements in TB treatment continue; for example, novel all-oral regimens and shorter courses for drug-resistant TB are being implemented, and clinical trials have demonstrated that certain 4-month regimens may be effective in drug-susceptible TB⁴⁴⁻⁴⁷, which could shorten therapy in the future. Overall, timely diagnosis and proper treatment of active TB cases are cornerstone strategies – not only to cure individuals but also to halt transmission in the community.

1.8 Epidemiology of Mtb and HIV Co-infection

The intersection of the TB and HIV epidemics has had devastating consequences on global public health. Co-infection with Mtb and HIV is common in regions with high HIV prevalence, especially sub-Saharan Africa, and it has fundamentally altered the epidemiology and clinical management of TB. PWH are highly vulnerable to TB, and TB has become a leading cause of morbidity and mortality in this population³⁷. In 2023, TB caused approximately 25% of all AIDS-related deaths² with an estimated 161,000 deaths due to TB among PWH². These TB-associated deaths in PWH represented roughly 15% of the 1.09 million total TB deaths² in 2023, highlighting that co-infected patients bear a disproportionate share of TB mortality. Globally, about 8–9% of new TB cases

occur in PWH². In 2023, approximately 6.6% of all TB cases globally were HIV-associated, and about 74% of these HIV/TB co-infections occurred in the WHO African Region. Southern Africa in particular has been an epicenter of the TB/HIV co-epidemic – countries like South Africa, Eswatini, and Lesotho have extremely high TB incidence rates largely driven by HIV. In some high-burden African settings, over half of TB patients are living with HIV^{29,48}. Outside of Africa, hotspots of TB/HIV co-infection include parts of Eastern Europe and Russia– often linked to intravenous drug use and HIV– where TB incidence is high and multidrug resistance is also a problem²⁹. The convergent epidemics of TB and HIV have been described as an “emerging syndemic,”⁴⁹ in which each disease increases the transmission and severity of the other, resulting in worse health outcomes.

1.9 Effect of HIV on TB Progression

In the absence of effective ART, a person with HIV faces an annual TB reactivation risk of approximately 5–15%, in contrast to the 5–10% lifetime risk observed in individuals without HIV⁵⁰. Clinical data reflect this amplified risk: for example, in one cohort, PWH and latent TB had approximately a 20-fold greater likelihood of progressing to TB disease than those without HIV⁴⁹. Even PWH on ART remain at elevated risk; patients with well-controlled HIV on ART still have about a fourfold higher incidence of TB than people without HIV³¹. HIV not only increases the incidence of TB but also alters its clinical presentation. In advanced HIV infection, TB often presents atypically—more commonly as extrapulmonary manifestations such as lymphadenitis, disseminated (miliary) TB, or TB meningitis. Even when pulmonary TB occurs, it is more likely to present with negative sputum smears and a lack of typical cavitory lesions on chest X-rays, owing to impaired granuloma formation⁵¹. As a result, diagnosis can be more difficult. HIV-related

immunosuppression can convert what would have been a contained latent infection into a rapidly progressing, disseminated disease. Studies of pathology have shown that HIV co-infected patients have fewer well-formed granulomas in affected organs; instead, they often exhibit widespread distribution of bacilli with poorly organized inflammatory responses^{52,53}. The bacillary load in tissues is higher in co-infected individuals, especially as CD4 counts fall¹¹. Thus, HIV undermines the very immune mechanisms that keep *Mtb* in check, leading to faster progression and more severe TB disease.

The relationship between HIV and TB is bidirectional. Active TB can also worsen the course of HIV infection. TB causes chronic immune activation and inflammation, which can stimulate HIV replication. Clinical studies have observed that HIV viral loads tend to increase during active TB, and TB may accelerate CD4 T cell decline in PWH⁵⁴⁻⁵⁶. In co-infected patients who have not yet started ART, active TB is associated with higher HIV viral load and a greater likelihood of progressing to AIDS⁵⁷. *Mtb* infection upregulates expression of pro-inflammatory cytokines, such as TNF and IL-1 β , and chemokines that recruit activated CD4 T cells to the site of infection⁵⁸. These CD4 T cells, many of which express the HIV co-receptor CCR5, serve as target cells for HIV. Consequently, an active TB granuloma can become a locale fostering active HIV replication⁵⁹. The enhanced HIV replication can in turn further deplete CD4 cells locally, undermining *Mtb* control and creating a vicious cycle⁵³. There is also evidence that TB can expand the HIV reservoir by providing long-lived infected macrophages or other cells in granulomas as “safe havens” for HIV⁶⁰. HIV’s immunosuppressive effects allow *Mtb* to flourish, while *Mtb*-induced immune activation boosts HIV replication and disease progression.

1.10 Immune Responses to Mtb

The immune response to Mtb is complex and involves a coordinated interplay between the innate and adaptive arms of immunity. Following aerosol exposure and phagocytosis by alveolar macrophages, dendritic cells in the lung also internalize Mtb bacilli or their antigens and migrate to regional lymph nodes, where they initiate T cell priming. Innate pattern recognition receptors (PRRs), such as Toll-like receptors (TLRs) and cGAS-STING⁶¹, recognize mycobacterial components and trigger pro-inflammatory signaling. Macrophages and dendritic cells produce cytokines like interleukin-12 (IL-12) and IL-18, which promote differentiation of naïve CD4 T cells into T helper 1 (Th1) cells⁶². Natural killer (NK) cells and $\gamma\delta$ T cells also participate in early responses, secreting IFN γ and lysing infected cells, although they are not as specific as the adaptive response that follows⁶¹.

The adaptive immune response, manifesting a few weeks after infection, is crucial for long-term containment of Mtb. CD4 T cells are the central players in anti-Mtb immunity, but not always sufficient. Th1-polarized CD4 T cells recognize Mtb peptide antigens presented on macrophage MHC-II molecules and respond by producing IFN γ ⁶³ and TNF, the two cytokines most essential for controlling Mtb^{22,64,65}. IFN γ further activates macrophages to augment phagocytosis and bacterial killing— it upregulates inducible nitric oxide synthase and reactive oxygen intermediates, and enhances phagolysosomal fusion, thereby helping to kill ingested mycobacteria^{22,65,66}. The importance of IFN γ is evidenced by the extreme susceptibility to disseminated mycobacterial infections in people with rare genetic defects in the IL-12/IFN γ axis⁶⁷. TNF is another critical cytokine that facilitates structural integrity of granulomas and activates macrophages to produce nitric oxide. Individuals with LTBI on TNF blocking therapy, for conditions like rheumatoid

arthritis⁶⁸ and psoriasis⁶⁹, are at increased risk of TB reactivation, illustrating the importance of TNF in Mtb control. Th17 cells, producing IL-17 and IL-22, have been implicated in driving neutrophil recruitment to sites of infection and enhancing mucosal immunity, which might be particularly important in the early containment of infection or in the lung airway defense⁶⁵.

IFN γ ⁷⁰ and TNF⁷¹ released by activated CD4 T cells in the granuloma periphery diffuse to the infected macrophages in the core and “license” them to control bacterial growth⁷¹. In this way, the granuloma physically and immunologically walls off the infection, limiting bacterial spread but not eradication of bacteria. Importantly, granulomas also concentrate immune effectors; they act as niche sites for cell–cell interaction, and in some cases can function as ectopic lymphoid structures where local priming of T cells occurs⁷². If the immune response is effective, granulomas remain solid and non-necrotic but if immune control wanes, the center of the granuloma can undergo caseation necrosis – a necrotic, cheese-like cell debris that forms due to intense immune-mediated tissue destruction⁷³. Caseation necrosis can lead to cavitation in pulmonary TB, which is associated with high infectiousness as cavities allow bacteria to proliferate extracellularly and be expelled. Thus, the immune response to Mtb requires a delicate balance for containment without excessive inflammation that contributes to tissue damage and disease.

CD8 T cells also contribute to immunity by recognizing Mtb antigens on MHC-I through cross-presentation and killing infected cells or releasing cytotoxic granules that may directly lyse bacilli in the phagosome⁷⁴. B cells and antibodies have traditionally been considered to play a limited role in TB immunity, as antibodies by themselves do not appear sufficient to clear an intracellular pathogen like Mtb. However, emerging evidence suggests some antibody functions like opsonization and B cell activity in granulomas may modulate the immune response⁷⁵.

1.11 Mtb-Specific CD4⁺ T Cell Responses in HIV

HIV preferentially targets memory CD4 T cells⁷⁶, including Mtb-specific subsets, making them particularly vulnerable to depletion in PWH. As HIV progresses, the absolute count of CD4 T cells in the blood and lymphoid organs falls, often dramatically. Once the CD4 count drops below critical thresholds (<200 cells/ μ L), the risk of opportunistic infections such as TB rises markedly. However, these cells are vulnerable to HIV-mediated depletion even before overall CD4 T cell counts decline, and their loss is more pronounced than for other antigen-specific cells, such as those targeting cytomegalovirus^{77,78}. Mtb-specific CD4 T cell subsets such as Th1^{77,79}, TH17⁷⁹, and Th22⁸⁰ cells are notably diminished in PWH. Beyond depletion, Mtb-specific CD4 T cells also exhibit functional impairments^{79,81} including reduced production of key cytokines such as IFN- γ ⁸², TNF⁸¹, IL-2^{83,84}, and IL-17⁷⁹. Defining the factors that modulate Mtb-specific CD4 T cell immunity in PWH is crucial for identifying immune correlates of protection against TB progression.

1.12 Effect of HIV Treatment on Mtb-specific Immune Responses

Although chronic HIV infection has a detrimental impact on Mtb-specific immune responses, this is at least partially mitigated by the advent of effective ART. Suppression of HIV replication by ART results in immune reconstitution⁸⁵. Over months on ART, many patients experience increases in peripheral CD4 T cell counts and improved T cell function and this effect extends to PWH that naturally control viral replication independent of ART⁸⁶. In the context of TB, starting ART in PWH can reduce the incidence of TB by about 50% or more over the long term, as immune function rebounds². The timing of ART initiation during TB in PWH is crucial. If ART is started

early, within 2 weeks of TB treatment, especially in those with very low CD4 counts, it provides earlier immune recovery and survival benefit, but it also carries a higher risk of TB-associated immune reconstitution inflammatory syndrome (TB-IRIS)⁸⁷. Delaying ART reduces IRIS risk but leaves the patient longer in an immunosuppressed state where Mtb and other infections can progress or new infections may occur³⁴. Initiating ART gradually restores Mtb-specific CD4 T cell responses, as patients on therapy develop stronger IFN γ responses to Mtb antigens and regain some degree of T cell polyfunctionality⁸⁸. ART also reduces the chronic immune activation and exhaustion markers on T cells⁸⁶. However, if there is already profound CD4 loss before ART, some specific immune responses may not fully reconstitute^{89,90}. There is evidence that certain Mtb-specific T cell populations, especially central memory cells, might be irrevocably lost if they were depleted during uncontrolled HIV infection⁹¹⁻⁹³. Early ART, by preserving higher nadir CD4 counts—the lowest level of CD4 T cells recorded at any point during the course of HIV infection—likely maintains a broader repertoire of Mtb-specific T cells^{94,95}. Thus, the timing of ART can influence the quality of immune reconstitution.

1.13 Summary

Despite significant advancements in our understanding of TB and HIV, the precise molecular mechanisms governing Mtb control remain elusive. While CD4 T cells are recognized as pivotal in containing Mtb infection, the specific correlates of protection and progression are not fully defined. HIV infection exacerbates this uncertainty by depleting and impairing Mtb-specific CD4 T cell responses, thereby increasing susceptibility to Mtb. Although ART can partially restore these immune responses, the extent and quality of reconstitution are influenced by factors such as the timing of ART initiation. This dissertation aims to bridge the knowledge gap by providing

molecular insights into how HIV infection and ART affect the transcriptomic landscape of Mtb-specific CD4 T cells, enhancing our understanding of TB pathogenesis in the context of HIV co-infection. The work outlined in remainder of this dissertation carry important implications—not only for aiding identification of reliable immune correlates of protection against Mtb in PWH, but also for informing the design of vaccines and immunotherapies. Moreover, by uncovering specific transcriptomic pathways disrupted by HIV, this research highlights potential molecular targets that may be amenable to therapeutic modulation—paving the way for strategies to restore effective immunity and reduce TB susceptibility in this vulnerable population.

**CHAPTER 2: Single-cell transcriptomics reveals depletion and dysregulation of
Mycobacterium tuberculosis-specific Th1 and Th17 cells early after acquisition of HIV**

Rachel A. Pearson^{1,2}, Krista N. Krish^{1,2}, Wendy E. Whatney^{1,2}, Walter Jaoko³, Kishor Mandaliya⁴,
Julie Overbaugh⁵, Susan M. Graham^{6,7,8}, R. Scott McClelland^{6,7,8}, Sakeenah L. Hicks¹, Jeffrey
Maurer¹, Christopher D. Scharer¹, Cheryl L. Day^{1,2*}

¹Department of Microbiology & Immunology, Emory University School of Medicine, Atlanta, GA

²Emory Vaccine Center, Emory University, Atlanta, GA

³Department of Medical Microbiology & Immunology, University of Nairobi, Nairobi, Kenya

⁴PathCare Laboratories, Mombasa, Kenya

⁵Division of Human Biology, Fred Hutch Cancer Center, Seattle, WA, USA

⁶Department of Epidemiology, University of Washington, Seattle, WA, USA

⁷Department of Global Health, University of Washington, Seattle, WA, USA

⁸Department of Medicine, University of Washington, Seattle, WA, USA

***Corresponding Author:**

Cheryl L. Day, PhD

954 Gatewood Rd NE

Emory Vaccine Center, Room 1024

Atlanta, GA 30329

Email: cday@emory.edu

Phone: 404-727-4374

2.1 Abstract

HIV significantly increases the risk of developing tuberculosis (TB) and is associated with impaired CD4 T cell responses to *Mycobacterium tuberculosis* (Mtb). We evaluated the frequency and functional capacity of Mtb-specific CD4 T cells in individuals with and without HIV using flow cytometry and performed single-cell RNA sequencing on these cells longitudinally in a subset of individuals before and after acquisition of HIV. Our findings reveal preferential depletion and functional impairment of Mtb-specific CD4 T cells early after acquisition of HIV, characterized by reduced cytokine production, loss of effector functions, and transcriptional dysregulation. Mtb-specific Th1 and Th17 cells decreased, whereas *TCF7*⁺ stem-like cells were enriched following acquisition of HIV. Pathway analysis revealed upregulation of hypoxia and WNT signaling, and downregulation of cell adhesion, migration, antigen processing, and cytokine signaling pathways. These findings provide novel insights into HIV-mediated dysregulation of CD4 T cell responses to Mtb.

2.2 Introduction

Tuberculosis (TB), caused by *Mycobacterium tuberculosis* (Mtb), continues to pose a significant global health challenge, with approximately 10.8 million cases and 1.25 million deaths reported in 2023². Infection with Mtb can result in a spectrum of clinical outcomes, ranging from bacterial clearance to latent tuberculosis infection (LTBI) to subclinical and symptomatic TB disease⁹⁶. While the vast majority of individuals remain asymptomatic, 5-10% do not control Mtb replication and develop to active TB disease⁴. This progression is influenced by complex and not fully understood factors, although animal and human studies have demonstrated the critical role of CD4 T cells in controlling Mtb infection^{65,97}. Effective Mtb-specific immune responses require T cells capable of producing key cytokines, such as IFN- γ , TNF, and IL-17, associated with T-helper 1 (Th1) and T-helper 17 (Th17) responses^{65,97}. These cytokines are essential for granuloma formation and the containment of Mtb⁹⁷. However, CD4 T cell-mediated correlates of protection against Mtb infection and TB disease progression have not been fully defined.

Co-infections, such as with HIV, and comorbidities, such as diabetes and malnutrition, are known to influence Mtb infection outcomes⁹. HIV infection markedly increases the risk of progression from LTBI to TB⁹. Incidence rates of TB in people with HIV (PWH) are elevated as early as one year after HIV infection and prior to severe immunosuppression, suggesting that HIV compromises Mtb immunity early following infection irrespective of decreasing CD4 T cell count⁷. This elevated risk persists even in PWH who achieve viral suppression through long-term antiretroviral therapy (ART) and immune reconstitution³¹. The complex interplay between HIV

and Mtb drives a dual epidemic in regions with high TB prevalence and significant HIV burden, exacerbating disease outcomes and complicating public health interventions.

HIV preferentially targets memory CD4 T cells⁷⁶, including Mtb-specific subsets, making them particularly vulnerable to depletion in PWH. While HIV-induced immune dysregulation extends beyond CD4 T cell dysfunction, these cells play a crucial role in understanding the heightened susceptibility to TB in PWH. Evidence suggests that Mtb-specific CD4 T cells are depleted in PWH, even before overall decline in absolute number of CD4 T cells⁷⁷, with a preferential decline in frequency when compared with cytomegalovirus-specific CD4 T cells in PWH⁷⁸. Mtb-specific CD4 T cell subsets such as Th1^{77,79}, Th17⁷⁹, and Th22 cells are notably diminished in PWH. Beyond depletion, Mtb-specific CD4 T cells also exhibit functional impairments^{79,81} including reduced production of key cytokines such as IFN- γ ⁸², TNF⁸¹, IL-2^{83,84}, and IL-17⁷⁹.

Defining the factors that modulate Mtb-specific CD4 T cell immunity in PWH is crucial for identifying immune correlates of protection against TB progression. A previous study reported depletion of Mtb-specific IFN- γ ⁺ T cells early after HIV infection in a longitudinal study of five women in Tanzania evaluated before and after HIV infection⁷⁷, although the cellular signaling pathways and mechanisms underlying this decline were not evaluated and remain unclear. We hypothesized that HIV infection modifies signaling pathways and downstream effector functions of CD4 T cells responding to Mtb, thus leading to functional impairment and depletion, and ultimately compromising Mtb control. To investigate this, we leveraged a unique cohort from Mombasa, Kenya, examining the impact of HIV on Mtb-specific CD4 T cell responses. Using

high-dimensional flow cytometry, we assessed the frequency and functional capacity of Mtb-specific CD4 T cells in individuals with and without HIV. Additionally, we performed longitudinal single-cell RNA sequencing (scRNA-seq) of Mtb-specific CD4 T cells from the same individuals before and after acquisition of HIV infection to better understand how HIV modifies gene expression and signaling pathways that may contribute to depletion and functional impairment of these cells. This study provides critical insights into how HIV disrupts immune control of Mtb early after HIV infection, before initiation of ART, with implications for developing targeted therapies and enhancing immune control of Mtb in PWH.

2.3 Materials and Methods

2.3.1 Study population and sample collection

Participants were recruited from the Mombasa Cohort, a prospective open cohort study established in 1993 assessing the risks for HIV acquisition and transmission⁹⁸. Participants were considered eligible if aged 16 and older, residing within 1-day commuting distance to the study clinic, self-identifying as exchanging sex for payment in cash or in kind, and able to provide informed consent. Screening for HIV was performed following Kenyan national guidelines; for PWH, antiretroviral therapy (ART) was provided according to World Health Organization and Kenyan national guidelines. HIV-1 viral loads and CD4 cell counts were measured for all PWH. For the present study, samples were available for analysis from 17 individuals without HIV and from 10 individuals with HIV; 5 individuals had samples collected before and after acquisition of HIV. The samples evaluated in the present study were collected between 2014 and 2017; samples from PWH were evaluated prior to initiation of ART.

Whole blood from participants was collected in vacutainer EDTA tubes and peripheral blood mononuclear cells (PBMCs) were isolated from whole blood by density gradient centrifugation. PBMCs were cryopreserved in liquid nitrogen in Mombasa, Kenya and shipped in a cryogenic dry shipper to Emory University in Atlanta, Georgia, USA for analysis.

2.3.2 Ethics Statement

All participants provided written, informed consent for participation in the study. The Mombasa Cohort Study was approved by ethics committees at the University of Washington and the

Kenyatta National Hospital. The specific study reported here was approved by the Institutional Review Board at Emory University.

2.3.3 T cell intracellular cytokine staining (ICS) assay and flow cytometry

Cryopreserved PBMCs were thawed and washed with RPMI and 10 μ g/mL DNase I (Millipore Sigma), resuspended in R10 (RPMI 1640 (Corning) with 10% heat-inactivated fetal calf serum (FCS), 100 μ g/mL penicillin (Cellgro), 100 μ g/mL streptomycin (Cellgro), and 2mM L-glutamine (Cellgro)) media, and rested at 37°C with 5% CO₂ for 3-6 hours. Pure functional grade anti-CD40 (0.5 μ g/mL; Miltenyi Biotec) was added for 15 min at 37°C and anti-CD107a BUV395 (BD Horizon) was added to each condition. Cells were stimulated with the following antigens: 1 μ g/mL each of Mtb peptide pools ESAT-6 and CFP-10 (NR-34824 and NR-34825, obtained through BEI Resources, NIAID, NIH), 10 μ g/mL Mtb H37Rv whole cell lysate (WCL; NR-13648, obtained through BEI Resources, NIAID, NIH), or 1 μ g/mL of staphylococcus enterotoxin B (SEB; Toxin Technology, Inc.); cells incubated in media alone served as a negative control. After 1 hour at 37°C, monensin (1x; BioLegend) and brefeldin A (10 μ g/mL; Acros Organics) were added and the cells incubated overnight at 37°C with 5% CO₂. Cells were washed, stained with Zombie NearIR Live/Dead stain (BioLegend) at room temperature (RT) for 15 min and then stained with surface antibodies against CD3-Alexa Fluor 700 (Clone UCHT1, BioLegend), CD4-BUV563 (Clone SK3, BD Horizon), CD8-BB700 (Clone, RPA-T8, BD Horizon), and incubated at RT for 30 min in the dark. Cells were washed, fixed with Cytotfix solution (BD Biosciences) for 20 min, and permeabilized by washing the cells with 1X Perm Wash Buffer (BD Biosciences). Cells were stained with antibodies for intracellular features: CD40L-BV421 (Clone 24-31, BioLegend),

CD69-BV650 (Clone FN50, BioLegend), IL2-BUV737 (Clone MQ1-17H12, BD Biosciences), IFN γ -BV480 (Clone B27, BD Biosciences), TNF-BV750 (Clone MAb11, BD Biosciences), and IL-17A-BV785 (Clone BL168, BioLegend) in Brilliant Stain Buffer Plus (BD Biosciences) and 1X PBS for 30 min at RT in the dark. Cells were washed with 1X Perm Wash Buffer and suspended in 1X PBS + 1% FCS and acquired on a FACSymphony (BD) using FACSDiva software (v9.0). FCS files were analyzed in FlowJo (BD v10.9.1) and frequency and count data were exported for further analysis.

2.3.4 MIMOSA and COMPASS analysis of flow cytometry data

Antigen-specific CD4 T cell responses were assessed using the Mixture Models for Single-Cell Assays (MIMOSA) method⁹⁹, which uses a computational approach called Markov Chain Monte Carlo (MCMC) to estimate the likelihood that a given cell is responding to a stimulus. Samples with a response probability of $\geq 70\%$ and a false discovery rate (FDR) of $\leq 3\%$ were classified as a positive response for each stimulation.

Cell counts in the T cell ICS assay were analyzed using the COMbinatorial Polyfunctionality Analysis of Antigen-Specific T cell Subsets (COMPASS) algorithm, as previously described¹⁰⁰. COMPASS employs a Bayesian computational approach to detect antigen-specific changes in all observable functional T cell subsets, without restricting the analysis to specific cytokine combinations and calculates a functionality score and a polyfunctionality score. The functionality score reflects the breadth of the cytokine response, accounting for both the magnitude and diversity of the antigen-specific cytokine subsets. It is defined as the proportion of detected antigen-specific

cytokine subsets relative to all potential subsets. The polyfunctionality score quantifies the diversity of the cytokine response by considering the number of cytokines present in each subset.

2.3.5 Activation-induced marker assay and sorting Mtb-specific CD4 T cells

Frozen PBMCs were thawed, counted, and incubated with pure functional grade anti-CD40 (0.5µg/mL; Miltenyi Biotec) for 15 min at 37°C with 5% CO₂. Cells were stimulated with Mtb WCL overnight at 37°C with 5% CO₂ in an activation-induced marker (AIM) assay. PBMCs were washed in PBS, stained with Zombie NearIR Live/Dead (BioLegend) for 15 min in the dark. Cells were washed with Cell Staining Buffer (BioLegend) and stained with the following antibodies: CD3-AF700 (Clone UCHT1, BioLegend), CD4-BV480 (Clone L200, BD Horizon), CD8-BB700 (Clone RPA-T8, BD Horizon), CD69-BV650 (Clone FN50, BioLegend), and CD40L-BV421 (Clone 24-31, BioLegend). TotalSeqTM-C anti-human Hashtag oligonucleotide antibodies (HTO; 0.5µg/10⁶ cells; BioLegend) were added to specified donor samples and cells were incubated for 30 min at 4°C in the dark. Cells were washed with Cell Staining Buffer and suspended in 1X PBS + 1% FCS and live CD3⁺CD8⁻CD4⁺CD40L⁺CD69⁺ Mtb-specific CD4 T cells were sorted into R10 media using a FACSAria II Cell Sorter (BD); samples were combined and stored on ice for 10X Genomics scRNA-seq protocol. Samples were demultiplexed in downstream scRNA-seq analysis, detailed below.

2.3.6 10x Genomics scRNA-seq library preparation

Single cell RNA sequencing (scRNA-seq) was performed following the protocol from Chromium Single Cell 5' Reagent Kits User Guide (v2 Chemistry Dual Index), Document Number CG000330

Rev A, 10x Genomics (August 2020). For each sample, an estimated 8,523-43,946 cells were used as input for GEM generation. 50ng or 20 μ L volume equivalents of cDNA transcripts were amplified for 12 cycles to generate size-selected GEX sequencing libraries. 5 μ L of volume of the purified DNA for the protein Feature input was used to generate the Cell Surface Protein (CSP) sequencing libraries containing the HTOs. Final sequencing libraries were quantitated by QuBit (Life Technologies, Q33231), size distributions determined by bioanalyzer (Agilent 2100), pooled at a 5:1 GEX:CSP molar ratio, and sequenced at the Emory Nonhuman Primate Genomics Core on a NovaSeq6000 using a PE26:90 run.

2.3.7 ScRNA-seq data processing and analysis

Demultiplexed FASTQ files were processed using Cell Ranger v6-multi¹⁰¹ option using the GRCh38-2020-A reference transcriptome, Seurat function HTODemux, and with custom code. Further data analyses were performed using Seurat (v.4.0)¹⁰². Cells with greater than 8% mitochondrial genes were excluded from analysis. Cells with more than 6,000 or less than 500 detected genes were considered outliers and excluded from downstream analyses. Any cells expressing immunoglobulin genes, $\gamma\delta$ TCR, CD8 β , and any cells labeled as non-T cells by the algorithm in the celldex¹⁰³ package using the Human Primary Cell Atlas¹⁰⁴ were removed. TCR genes were ignored for downstream differential gene expression analysis. Raw unique molecular identifier (UMI) counts were transformed using Seurat's SCTransform (v2)¹⁰⁵ function which normalizes to unique molecular identifier counts per million total counts before being log-transformed and scaled. Principle component analysis (PCA) was performed, and the 22 most statistically significant principal components were used for uniform manifold approximation and

projection (UMAP) algorithm. Clusters were identified using the nearest neighbor algorithm in Seurat and UMAP plots were generated based on selected PCA dimensions at a resolution of 0.35. The Seurat function FindAllMarkers was used to identify marker genes between clusters. Clusters were annotated based on canonical helper T cell markers that were differentially expressed genes between clusters or highly expressed genes within the cluster. Log-normalized data are shown. For differential gene expression in Mtb-specific CD4 T cells from individuals before and after HIV infection, Seurat function FindMarkers MAST¹⁰⁶ test was used with a latent variable set as donor for paired data. Single-cell pathway analysis (SCPA)¹⁰⁷ was used to determine significantly downregulated and upregulated pathways using Hallmark, Reactome, and GO biological process gene sets.

2.3.8 Statistical analysis and supplemental files

Data was visualized using GraphPad Prism (v.10.0.3), Seurat, ggplot2, ggmaplot, and EnhancedVolcano packages in R. Differences between cell frequencies in two groups for flow cytometry experiments were analyzed using the Mann Whitney U test. All other statistical analysis was performed with Seurat functions or SCPA as described above. All Supplemental Tables 2.1-2.4 are available on github here: <https://github.com/rachel7p/dissertation.git>.

2.4 Results

2.4.1 Study Participants

Participants were evaluated from the ongoing Mombasa Cohort, an open cohort study in Mombasa, Kenya investigating risk factors for HIV acquisition among female sex workers. We evaluated PWH and without HIV. The median age of participants in both groups was 30 years. PWH were evaluated early after HIV infection (median 2 months post-seroconversion) and prior to initiation of ART. The median absolute CD4 count was 519 cells/ μ L and median HIV plasma viral load was 59,253 copies/mL plasma (Table 2.1).

2.4.2 Mtb-specific CD4 T cells in PWH demonstrate impaired functionality and polyfunctionality

To investigate the impact of HIV on CD4 T cell functional capacity, we utilized high-dimensional flow cytometry to measure cytokine production and the proportion of cytokine-producing and AIM-expressing CD4 T cells in PWH and people without HIV in response to Mtb antigens (ESAT-6 and CFP-10 peptide pools and Mtb WCL), and SEB (Figure 2.1A, B and Supplemental Figure 2.1A). First, we determined the frequency of positive responses to each stimulation using Mixture Models for Single-Cell Assays (MIMOSA) analysis, which utilizes a Bayesian statistical method to calculate the probability of a positive responses to antigen stimulation⁹⁹. A response was considered positive if any cytokine (IFN γ , TNF, IL-2, or IL-17A) was detected above threshold or if both AIM markers (CD40L and CD69), were expressed above threshold. All participants had positive responses to Mtb WCL and SEB stimulations; 85% (16 out of 17 people without HIV and

7 out of 10 PWH) of individuals exhibited positive responses to ESAT-6 and CFP-10 (Supplemental Figure 2.1B), indicating prior sensitization to Mtb.

Next, we measured the frequency of cytokine⁺ and AIM⁺ CD4 T cells to each antigen and then assessed frequencies of distinct functional subsets of CD4 T cells in people with or without HIV (Figure 2.1C). CD4 T cells from PWH stimulated with Mtb WCL and ESAT-6/CFP-10 exhibited significantly reduced frequencies of cytokine⁺ and AIM⁺ populations compared to people without HIV, both in polyfunctional subsets (Figure 2.1C) and total frequencies of cytokine⁺ cells (Supplemental Figure 2.1C). While all antigen-specific polyfunctional CD4 T cell frequencies were blunted in PWH in response to Mtb stimuli compared to those without HIV, statistically significant declines in frequencies were observed in AIM⁺IFN γ ⁺TNF⁺ and AIM⁺TNF⁺ CD4 T cell populations in response to Mtb WCL and AIM⁺IFN γ ⁺ CD4 T cells in response to ESAT-6 and CFP-10. Importantly, this reduction was specific to Mtb antigens and was not observed in SEB-stimulated CD4 T cells, indicating an antigen-specific effect (Figure 2.1C, Supplemental Figure 1C). We next evaluated the quality of responses using the combinatorial polyfunctionality analysis of antigen-specific T-cell subsets (COMPASS) algorithm, which assesses CD4 T cell cytokine production capacity and AIM expression to (functionality) or multiple cytokines/activation markers simultaneously (polyfunctionality) and generates a score¹⁰⁸. PWH exhibited diminished functional and polyfunctional responses to Mtb stimuli, whereas responses to SEB stimulation remained consistent across HIV status (Figure 2.1D). These results indicate that HIV infection disproportionately impacts Mtb-specific CD4 T cells, leading to a reduction in the frequency and functional capacity.

2.4.3 Single-cell transcriptomics identifies distinct subsets of Mtb-specific CD4 T cells

To further investigate the impact of HIV infection on Mtb-specific CD4 T cells, we performed scRNA-seq to characterize the transcriptome of these cells in the same individuals before and after HIV acquisition. Live CD40L⁺CD69⁺ CD4 T cells were sorted from five participants following overnight stimulation with WCL. Samples were evaluated from the same participants before and after acquisition of HIV (Figure 2.2A-B, Supplemental Figure 2.2A).

We identified seven distinct clusters of Mtb-specific CD4 T cells using unsupervised hierarchical clustering of differential gene expression between clusters (Figure 2.2C and Supplemental Table 2.1). The clusters were annotated according to the expression of canonical helper T cell markers. The Th1 cluster was identified by the expression of one or more of these genes: *CXCR3*, *IFNG*, *IL2*, or *TBX21*. The Th2 cluster was characterized by *CCR4*, *GATA3*, *IL4*, *IL5*, or *IL13*, while the Th17 cluster expressed *CCR6*, *RORC*, *IL17A*, or *IL17F*. The Th1/17 cluster exhibited a combination of Th1 and Th17 markers. The Th22 cluster expressed *IL22* in the absence of other lineage-specific cytokines. Lastly, the Th1 cytotoxic cluster was marked by the expression of *CXCR3*, *GZMA*, *GZMB*, *GZMH*, and *GNLY* (Figure 2.2D-F, Supplemental Figure 2.2B). The most abundant cluster expressed high levels of stemness-associated genes, including *TCF7*, *LEF1*, and *KLF2*, while lacking expression of canonical Th lineage markers or effector cytokines. These data indicate that CD4 T cell responses to Mtb are comprised of heterogeneous subsets of memory CD4 T cells and establish a framework of mRNA expression to compare changes in the Mtb-specific CD4 T cell transcriptome before and after HIV infection.

2.4.4 Mtb-specific Th1 and Th17 cell numbers are diminished following HIV infection

To understand the effect of HIV on the transcriptome of Mtb-specific CD4 T cells and the distribution of CD4 T cell lineages, we analyzed transcriptomic data from Mtb-specific CD4 T cells obtained from five individuals both before (pre-HIV) and after (post-HIV) HIV seroconversion. Samples after acquisition of HIV were collected between 1-5 months after HIV seroconversion, providing a detailed evaluation of the early transcriptomic changes early after HIV infection. We utilized the previously defined transcriptomic profiles and cluster annotations to examine changes in CD4 T cell subset distribution and associated gene expression patterns (Figure 2.3A). Our analysis revealed a significant decline in the number of Th1 and Th17 cells, both critical for effective immune responses against Mtb, and a concurrent expansion of *TCF7+* CD4 T cells following HIV infection (Figure 2.3B-C). This shift was evident in the reduction of the total percentage of cells in the Th1 and Th17 clusters pre-HIV compared to post-HIV and an increase in the percentage of cells within the *TCF7+* cluster after HIV infection (Figure 2.3B).

These findings were further supported by the observation that, prior to acquisition of HIV, cells predominantly clustered within the Th1 and Th17 populations. In contrast, the majority of cells after HIV infection shifted to the *TCF7+* population, indicating a transition from an effector-like T cell state to a stem-like T cell state (Figure 2.3C). Additionally, a total of 701 differentially expressed genes (DEGs) were identified, characterized by a log₂ fold change greater than 0.25 or less than -0.25 and an adjusted p-value of <0.05, when comparing the transcriptomes of Mtb-specific CD4 T cells before and after HIV infection (Figure 2.3D and Supplemental Figure 2.3). Among these DEGs, 366 were upregulated, while 335 were downregulated following HIV

infection. Taken together, these data suggest that HIV infection induces significant alterations in the transcriptomic landscape and subset distribution of Mtb-specific CD4 T cells.

2.4.5 Average expression of effector genes declines after HIV infection

To further investigate whether HIV impacts the average expression of effector and functional genes in Mtb-specific CD4 T cells, we analyzed DEGs between cells obtained pre- and post-HIV infection (Supplemental Table 2.2). This analysis revealed distinct patterns of gene expression, with a marked decline in key effector genes and an increase in the expression of stemness-associated markers following HIV acquisition (Figure 2.4A).

Specifically, the expansion of the *TCF7*⁺ cluster was associated with an upregulation of stemness genes, including *TCF7*, *LEF1*, and *KLF2*, indicative of a shift toward a less differentiated, stem-like phenotype. By contrast, critical effector genes such as *IFNG*, *TNF*, *IL2RA*, *IL17F*, *IL22*, *LTA*, *LTB*, *GZMA*, *GZMB*, and *GZMY* exhibited both a reduction in the number of cells expressing these genes and a decrease in RNA transcript levels within individual cells (Figure 2.4B-C). This dual reduction suggests that HIV compromises not only the abundance of Mtb-specific CD4 T cells capable of effector functions but also the intensity of those functions at the single-cell level. These changes in gene expression within individual cells suggest that HIV not only affects cell lineage distribution but also impacts the transcriptional activity of remaining effector cells.

2.4.6 Important pathways are downregulated in Mtb-specific CD4 T cells after HIV infection

To gain a deeper understanding of the broader pathways that may be dysregulated following HIV infection, we performed Single Cell Pathway Analysis (SCPA). SCPA offers a more sensitive and

nuanced detection of pathway changes at the single-cell level compared to traditional gene set enrichment analysis methods¹⁰⁹. This approach enables the identification of cell-specific alterations that might otherwise be masked in bulk pathway analyses. Using hallmark, gene ontology biological processes (GOBP), and reactome gene sets with SCPA, we identified 429 pathways that were enriched within specified cutoffs (see Methods) between Mtb-specific CD4 T cells from before and after HIV infection (Supplemental Table 3). The majority of DEGs fall within pathways related to RNA and protein processing, cytokine signaling, cell death, and activation and proliferation (Figure 2.5A and Supplemental Table 2.4).

Specific pathways associated with signaling and cytokine production, adhesion and migration, antigen processing and presentation, cellular activation and proliferation, inflammation, cytotoxicity, and apoptosis were all significantly downregulated in Mtb-specific CD4 T cells following HIV infection (Figure 2.5B). Pathways involved in cytokine signaling—including IL-2/STAT5 signaling, apoptotic signaling, and TCR signaling—were among the most significantly downregulated following HIV infection. This downregulation was corroborated by significantly lower expression of genes central to IL2-STAT5 signaling, including *LTB*, *CSF2*, *CISH*, and *CXCL10*; genes central to regulation of apoptosis, including *CFLAR*, *BCL2A1*, and *DNAJ1A*; and genes central to TCR signaling, including *NFKB1A*, *NFKB1*, *PSMB2*, *CD5*, and *CD6* (Figure 2.5C). Conversely, pathways involved in hypoxia response, RNA processing, translation, and canonical WNT signaling were significantly upregulated in Mtb-specific CD4 T cells following HIV infection. Underscoring the upregulation of these pathways are concomitant upregulation of genes central to the pathways like genes involved in hypoxia, including *BTG1*, *DDIT4*, and *MXII*; genes central to RNA processing, including *IL4R*, *ZFP36*, and *PABPC1*, and genes central in WNT

signaling, including *TCF7* and *LEF1* (Figure 2.5C). Collectively, these findings reveal that HIV profoundly impacts the functional capacity and transcriptional landscape of Mtb-specific CD4 T cells.

2.5 Discussion

HIV co-infection significantly increases the risk of development of TB⁷, likely associated with disruptions in CD4 T cell-mediated immunity, particularly the Th1 and Th17 responses critical for controlling Mtb^{77-79,81,82}. To better understand the impact of HIV on CD4 T cell responses to Mtb, we utilized high-dimensional flow cytometry to analyze the frequency and functional capacity of these cells in people with and without HIV. Additionally, we performed scRNA-seq and pathway analysis on Mtb-specific CD4 T cells longitudinally from the same individuals, both before and after acquisition of HIV. Our data indicate that HIV infection is associated with preferential dysfunction of Mtb-specific CD4 T cells, characterized by reduced cytokine production, diminished AIM expression, and loss of both functional and polyfunctional capacity in PWH. ScRNA-seq of Mtb-specific CD4 T cells revealed a decline in Th1 and Th17 subsets, expansion of *TCF7*⁺ stem-like cells, and an overall reduction in cytokine and effector gene expression following acute HIV infection. Additionally, pathways related to translation, RNA processing, and WNT signaling were upregulated following acquisition of HIV, coincident with downregulation of adhesion, migration, cytokine production, and proliferation pathways in Mtb-specific CD4 T cells. Together, these data reveal widespread dysregulation of the functional capacity and transcriptome of CD4 T cell responses to Mtb after HIV infection.

The identification of antigen-specific CD4 T cells by upregulation of activation induced markers (AIMs) such as CD40L and CD69 is a well-established, cytokine-independent approach for examining Mtb-specific CD4 T cells, facilitating the capture of a broad spectrum of antigen-responsive cells without reliance on production of specific cytokines^{110,111}. By combining evaluation of AIM and cytokine expression, we show that Mtb-specific CD4 T cell populations in

PWH exhibit both reduced frequencies and diminished functional capacity. Specifically, in response to the Mtb peptides ESAT-6 and CFP-10, the frequencies of CD40L⁺CD69⁺IFN γ ⁺ subsets and IFN γ ⁺ CD4 T cells are significantly reduced. Similarly, in response to Mtb WCL, there are reduced frequencies of CD40L⁺CD69⁺IFN γ ⁺TNF⁺ and CD40L⁺CD69⁺TNF⁺ polyfunctional subsets, along with a decline in total IFN γ ⁺, TNF⁺, and IL-2⁺ CD4 T cells in PWH. Additionally, both functional and polyfunctionality scores in response to Mtb peptides and Mtb WCL are significantly lower in PWH, compared with people without HIV. Notably, these impairments are observed only in response to Mtb-specific stimuli and not to SEB, indicating that the reduced frequency and diminished quality of CD4 T cell responses are specific to Mtb rather than a generalized immune deficiency. This aligns with previous studies from our group⁸¹ and others that show functional impairment in Mtb-specific CD4 T cells^{79,81,82} and preferential depletion of Mtb-specific CD4 T cells^{77,78,81}. The overall decline in CD4 T cell immune quality may impair the ability to maintain an effective and coordinated response to Mtb.

Next, we established a transcriptional framework of Mtb-specific CD4 T cells in PBMCs collected longitudinally from five individuals before and after acquisition of HIV. We identified seven distinct clusters of Mtb-specific CD4 T cell subsets based on canonical helper T cell markers¹¹². Three clusters comprised more than 75% of the cells, a large *TCF7*⁺ cluster, a Th1 cluster, and a Th17 cluster; the remaining cells were dispersed in a Th1/17 cluster, a Th22 cluster, a Th2 cluster, and a cytotoxic Th1 cluster. Our findings revealed a marked decline in Th1 and Th17 cell populations, which are critical for protective immunity against Mtb⁹⁷. These subsets produce cytokines such as IFN γ , TNF, and IL-17A/F, essential for macrophage activation, immune cell recruitment, granuloma formation, and Mtb containment^{64,113-115}. A recent study in Mauritian

cynomolgus macaques found that while the overall frequency of total Mtb-specific tetramer⁺ CD4 T cells in lung granulomas were associated with higher bacterial burden, tetramer⁺ Th1 (T-bet⁺) and Th17 (RORγT⁺) responses were linked to lower bacterial burden¹¹⁶. Similarly, in mouse models of Mtb infection, Th17 cells are crucial for limiting bacterial growth¹¹⁷ in the lungs and are essential for granuloma formation¹¹⁸. These findings underscore the role of Th1 and Th17 polarized Mtb-specific CD4 T cells in controlling Mtb infection. Previous studies have indicated that functional stem-like and naïve-like CD4 T cells are generated following Mtb exposure¹¹⁹⁻¹²¹ and that stem-like CD4 T cells expressing *TCF7*/*TCF-1* have heterogenous expression of stemness markers¹²², corroborating our findings of an antigen-experienced *TCF7*⁺ population. The observed reduction in Mtb-specific Th1 and Th17 cells, together with an expansion of *TCF7*⁺ stem-like CD4 T cells and reduced cytokine production and effector function, signifies a shift in the immune landscape following HIV infection. This antigen-specific dysfunction aligns with findings from previous studies assessing Mtb-specific CD4 T cells in PWH which report diminished numbers, impaired effector functions, and preferential depletion of Mtb-specific CD4 T cells^{78,81}, further underscoring the vulnerability of Mtb-specific T cell responses in the context of HIV. Although cells expressing *TCF7* generally maintain proliferative capacity and immune potential^{123,124}, their reduced differentiation and effector functionality may impair the immune response to Mtb, increasing the risk of progression to active TB.

SCPA revealed significant upregulation of the WNT signaling pathway in Mtb-specific CD4 T cells after HIV infection, with corresponding increased expression of key pathway genes such as *TCF7*, *LEF1*, *CCDC88C*, *USP34*, and *UBE2B*. WNT signaling is well-documented in the tumor microenvironment for promoting stemness and immune evasion by suppressing T cell activation

and effector differentiation, hindering anti-tumor responses¹²⁵. In PWH, WNT activation likely reinforces the stem-like properties of *TCF7*⁺ cells, preserving their resilience while undermining the effector responses needed to control *Mtb*¹²⁶. This pathway may also contribute to immune suppression by inducing inhibitory molecules and altering cellular metabolism¹²⁴. Studies of *Mtb*-specific CD4 T cell responses in people who remain IGRA-negative and TST-negative despite high levels of exposure to people with infectious TB have found that these individuals exhibit clonally expanded *Mtb*-specific Th17 and regulatory T cell-like functional programs, which were also associated with a lack of TB progression in publicly available data from a South African adolescent cohort of TB progressors and non-progressors. These highly exposed, IGRA⁻TST⁻ individuals also displayed a stem-like CD4 T cell profile with higher *TCF7* and *LEF1* expression, suggesting a more protective response from the stem-like state of CD4 T cells⁹². However, the stem-like state of CD4 T cells was not significantly different between TB progressors and non-progressors in a cohort of adolescents in South Africa⁹². Other studies indicate that polarization of antigen-experienced stem-like CD4 T cells may be dysregulated due to the lack of polarizing signals in the microenvironment, particularly due to suppression from Tregs^{127,128} or dysfunctional cytokine responses¹²⁸. The decline in transcription factor *TBX21* expression—critical for Th1 differentiation¹¹²—along with a reduction of cytokine-producing CD4 T cells after HIV infection may create an environment in which the stem-like cells do not receive necessary signals to differentiate and expand^{121,129}, thus persisting in a stem-like state with less functional capabilities. Moreover, the autocrine function of CD4 T cell-derived cytokines¹³⁰, which help polarize stem- and naïve-like T cells, may be impaired after HIV infection. Together, these findings suggest that targeting *TCF7* and the WNT pathway could help restore immune balance in PWH, enhancing

Mtb-specific effector functions while maintaining T cell resilience. Whether the remaining stem-like CD4 T cells retain their ability to differentiate after HIV infection remains an open question for exploration.

Our data also indicated that pathways associated with hypoxia response, translation, and RNA processing were upregulated in Mtb-specific CD4 T cells following HIV infection. Hypoxia related pathways play a vital role in Th17 differentiation¹³¹, protection against oxidative stress¹³², and granuloma stabilization through HIF-1 α signaling¹³². Although SCPA revealed we upregulation of hypoxia pathways in Mtb-specific CD4 T cells following HIV infection, the individual genes central to hypoxia, including *HMOX1* and *HIF1A* (HIF-1 α), which are linked to protective responses in Mtb infection, are downregulated following HIV infection. This could indicate dysregulation of hypoxia-induced protection in the oxidative stress response. This response likely reflects an adaptive mechanism to HIV-induced hypoxia or altered metabolic states rather than an effective compensatory mechanism¹³³. The upregulation of RNA processing and translation pathways suggests an active cellular response to stimuli^{134,135}. However, when combined with the impaired effector function of these T cells, this may weaken the protective immune response, potentially contributing to loss of Mtb control.

The downregulation of adhesion and migration pathways in Mtb-specific CD4 T cells after HIV infection highlights a critical mechanism by which HIV may further impair control of Mtb replication. Adhesion molecules and migration-related signaling are crucial for the effective trafficking of immune cells to infection sites, such as granulomas in the lungs¹³⁶. Our findings show a significant downregulation of genes involved in cell migration and chemotaxis, including *CCL3* (MIP-1 α), *CCL4* (MIP-1 β), *CXCL10*, *DPP4*, *TBX21*, *SLAMF1*, *PLAUR*, *CCL5*, and

SI00A9, which are essential for immune cell homing to sites of infection. Additionally, genes involved in integrin-mediated adhesion, such as *HSPD1*, *ITGB2*, *CDC42*, *RAC1*, *PTK2B*, *ITPKB*, and *RELA*, were also downregulated, indicating a disruption in the signaling pathways and cytoskeletal dynamics necessary for immune cell adhesion and migration. The reduced expression of chemokine receptors (e.g., *CCL3*, *CCL4*, *CCL5*, *CXCL10*) and the upregulation of *CXCL8*, a chemokine involved in neutrophil trafficking, as well as *CXCR4*, a co-receptor for HIV, further disrupt the recruitment of Th1 and Th17 cells to the lung and favor a more inflammatory environment. These changes likely compromise localized immunity against Mtb and may impair tissue-resident T cells and their ability to mediate control of Mtb replication.

SCPA also indicated downregulation of pathways related to cytokine production and signaling, antigen processing, cellular activation, proliferation, cytotoxicity, and apoptosis. This suggests that HIV infection disrupts critical signaling pathways essential for the activation and function of Mtb-specific CD4 T cells. Impairment of NF- κ B¹³⁷⁻¹³⁹ and IL2-STAT5 signaling¹⁴⁰ compromises cytokine production and effector gene expression, while downregulation of proliferation-associated genes like *IL2RA* (CD25) limits the expansion of Mtb-specific CD4 T cells^{141,142} and subsequent control of Mtb¹⁴³. Cytotoxicity, essential for eliminating Mtb-infected macrophages¹⁴⁴ and direct killing of Mtb¹⁴⁵⁻¹⁴⁷, is also diminished following HIV infection. Mtb-specific CD4 T cells have been shown to directly lyse Mtb via granulysin and granzyme-mediated killing¹⁴⁵. Simultaneously, suppression of apoptosis pathways hinders the elimination of infected cells and contributes to prolonged immune activation or exhaustion, exacerbating immune dysfunction¹⁴⁸. These findings highlight the multifaceted disruptions in signaling, proliferation, cytotoxicity, and

apoptosis responses that collectively impair Mtb-specific immunity and increase susceptibility to TB in PWH.

While this study provides significant insights into HIV-induced dysregulation of CD4 T cells responding to Mtb, several limitations should be noted. First, we evaluated Mtb-specific CD4 T cells in PBMCs and were not able to evaluate responses at the site of Mtb infection in the lung. Studies have shown differential CD4 T cell profiles between the lung and blood¹⁴⁹, further underscoring potential differences between tissue-resident and circulating CD4 T cells. Second, our approach to sorting Mtb-specific CD4 T cells for scRNA-seq was based on upregulation of CD69 and CD40L, thus Mtb-specific cells that did not express these markers, such as dysfunctional or exhausted T cells that may be particularly prevalent in people with HIV, were not included in our transcriptome analysis. Third, the use of Mtb WCL stimulation, while eliciting a broad mycobacteria-reactive T cell response, may have included T cells cross-reactive to conserved elements of other mycobacterial species. Despite this potential cross-reactivity, CD4 T cells responding to this stimulation are likely to contribute to the immune response to Mtb exposure and infection and thus remain relevant for understanding the overall Mtb-specific CD4 T cell dynamics. Finally, we evaluated the transcriptome of Mtb-specific CD4 T cells and did not assess other CD4 T cell populations within these individuals, thus we cannot determine if the transcriptional changes that we observed after acquisition of HIV are unique to Mtb-specific CD4 T cells or reflect broader HIV-associated dysregulation of CD4 T cell responses regardless of antigen specificity.

One of the major strengths of this study is our use of scRNA-seq to analyze Mtb-specific CD4 T cells longitudinally in the same individuals before and after acquisition of HIV. The documentation

of the timing of HIV seroconversion in the Mombasa Cohort offers a unique opportunity to study immune alterations that occur early after HIV infection. The ability to evaluate both the quantity, quality, and transcriptome of Mtb-specific CD4 T cells before and after HIV infection in the same individuals mitigates confounding introduced by individual-level heterogeneity in cross-sectional studies comparing different groups of people with and without HIV, and thus represents a significant advancement in providing novel insights into how HIV impacts CD4 T cell responses to Mtb.

In summary, this study provides a comprehensive analysis of the impact of HIV infection on Mtb-specific CD4 T cell function, revealing widespread CD4 T cell dysregulation that may contribute to ineffective control of Mtb and thus increase the risk of developing TB. Our data indicate that HIV infection leads to a significant decline in Th1 and Th17 subsets, reduced cytokine production, and loss of polyfunctional T cell responses. Additionally, there is an expansion of *TCF7*⁺ stem-like cells, accompanied by upregulation of WNT signaling and downregulation of adhesion, migration, and effector pathways, impairing immune cell trafficking and containment of Mtb. These findings have broad implications, including identifying pathways that may be amenable to therapeutic intervention to enhance or preserve CD4 T cell functional capacity, and further underscore the importance of early diagnosis and timely ART initiation to mitigate depletion and impairment of Mtb-specific CD4 T cell subsets. Initiation of ART early after HIV infection may help to maintain a more robust immune response, potentially reducing the risk of TB progression in people with HIV.

2.6 Main Figures

Table 2.1

Table 1. Characteristics of study participants.

| | Without HIV N = 17 | With HIV N = 10 |
|--|-------------------------------|----------------------------|
| Age (years) ^a (IQR) | 30 (27-34) | 30 (28-35) |
| Sex (%F) | 100 | 100 |
| CD4 count (cells/ μ L) ^a (IQR) | ND ^b | 519 (454-648) |
| Viral Load (HIV-1 RNA copies/mL) ^a (IQR) | ND ^b | 59253 (5178-126747) |
| Time since HIV seroconversion (months) ^a (IQR) | ND ^b | 2 (1-5) |

^a Value denotes median.

^b Not done.

IQR, Interquartile range.

Figure 2.1

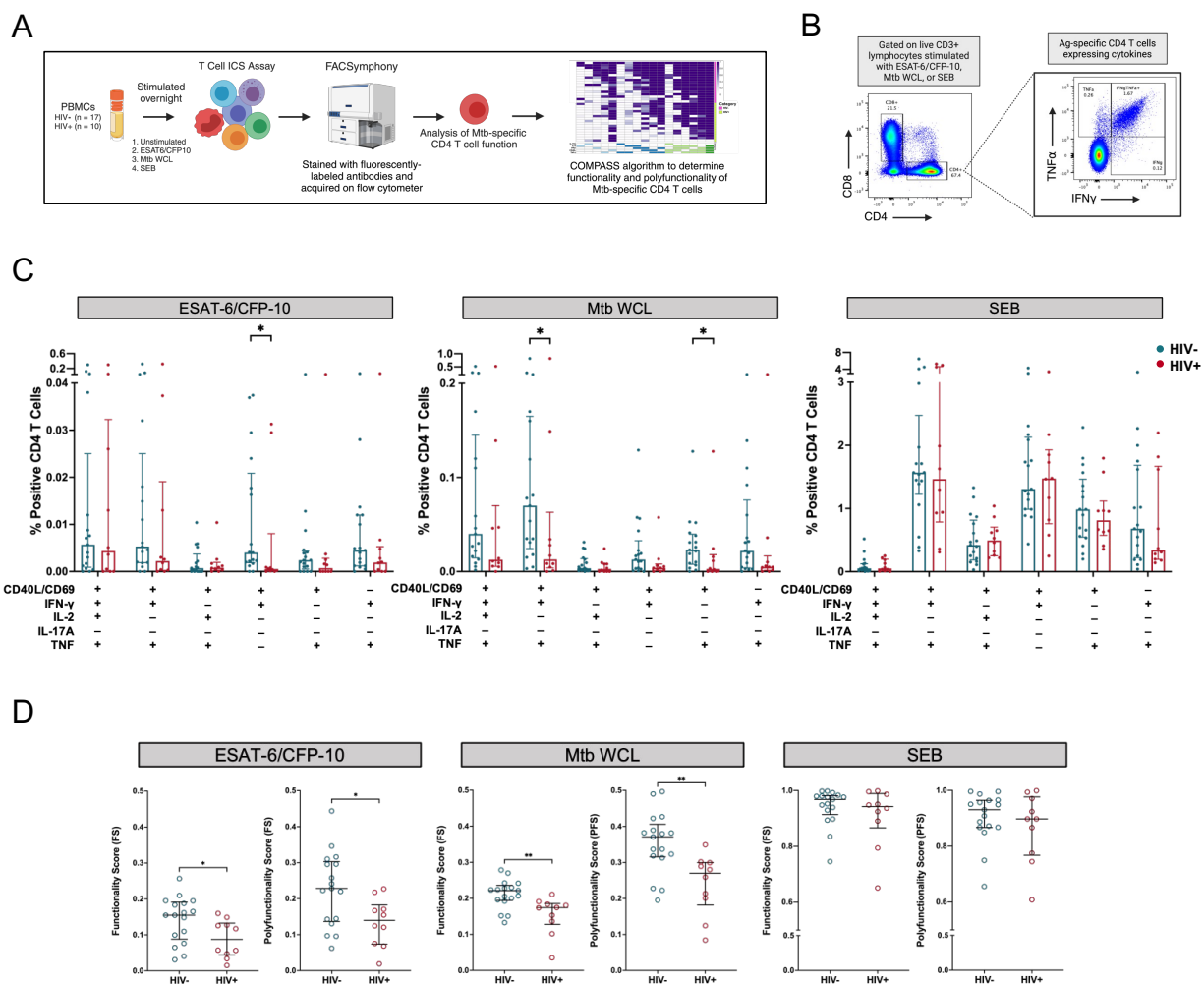


Figure 2.1. Reduced functional capacity of Mtb-specific CD4 T cells in people with HIV. A)

Overview of the experimental approach. PBMCs from PWH (HIV+; n=10) and people without HIV (HIV-; n=17) were stimulated overnight with ESAT-6 and CFP-10 peptide pools, Mtb whole cell lysate (WCL), or SEB in an intracellular cytokine staining (ICS) assay. **B)** Representative flow cytometry plots of Mtb-specific CD4 T cells expressing TNF and IFN- γ following overnight stimulation with Mtb WCL. **C)** Frequencies of polyfunctional subsets expressing distinct combinations of CD40L, CD69, IFN- γ , IL-2, IL-17A, and TNF. Frequencies of each subset are shown after subtraction of background levels of each marker in the unstimulated (media) control; bars represent the median and whiskers represent the interquartile range (IQR). **D)** ICS data were analyzed using COMPASS (see Materials and Methods) and the summarized results were aggregated by group (HIV+ or HIV-) and displayed as functionality (FS) and polyfunctionality scores (PFS). The middle line represents the median and the whiskers represent the IQR. Differences in frequencies of polyfunctional populations and FS and PFS of Mtb-specific CD4 T cells were analyzed using a Mann-Whitney U test (* $p < 0.05$, ** $p \leq 0.01$).

Figure 2.2

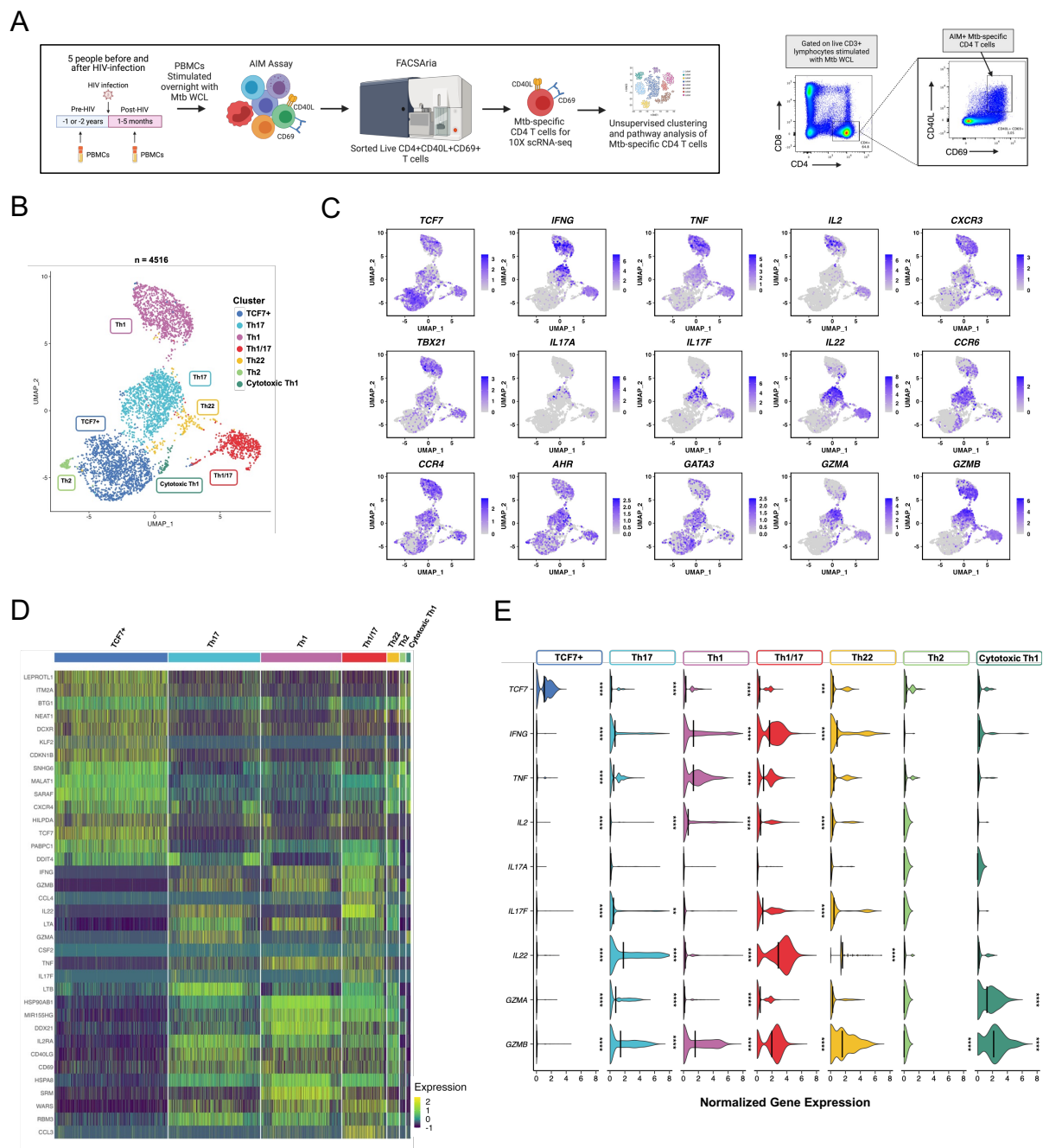


Figure 2.2. Unsupervised clustering of Mtb-specific CD4 T cell single-cell RNA sequencing data identifies distinct populations of CD4 T cells characterized by canonical helper T cell markers. **A)** Schematic of the experimental approach. PBMCs from five individuals before and after acquisition of HIV were stimulated overnight with Mtb WCL in an activation-induced marker (AIM) assay. Live CD3⁺CD8⁻CD4⁺CD40L⁺CD69⁺ T cells were sorted and used for scRNA-seq. Sc-RNA-seq data was analyzed using Seurat, PCA, DEG analysis, dimensionality reduction, and unsupervised clustering. Cluster identity was determined using standard markers for CD4 T cell populations and DEG analysis across clusters. **B)** Representative flow cytometry plots of Mtb-specific CD40L⁺CD69⁺ Mtb-specific CD4 T cells sorted for scRNA-seq. **C)** UMAP plot determined by dimensional reduction of scRNA-seq data from 4,516 Mtb-specific CD4 T cells aggregated from two timepoints from five individuals before and after acquisition of HIV. **D)** UMAPs overlaid with gene expression of selected genes used for cluster identity of CD4 T cell subsets. The purple scale in the legends represent the normalized expression levels of the gene displayed in the corresponding plot. **E)** Heatmap of single-cell normalized expression values organized by cluster. Each column represents a single cell, with gene expression in each row; colors represent the degree of expression. Column headings are the annotated clusters. **F)** Violin pots of normalized gene expression of cells within each cluster for each marker. DEGs in individual clusters compared to all other clusters were identified using Seurat's FindAllMarkers function with the MAST test for paired samples. Asterisks denote adjusted p-values (** ≤ 0.01 , *** ≤ 0.001 , **** ≤ 0.0001).

Figure 2.3

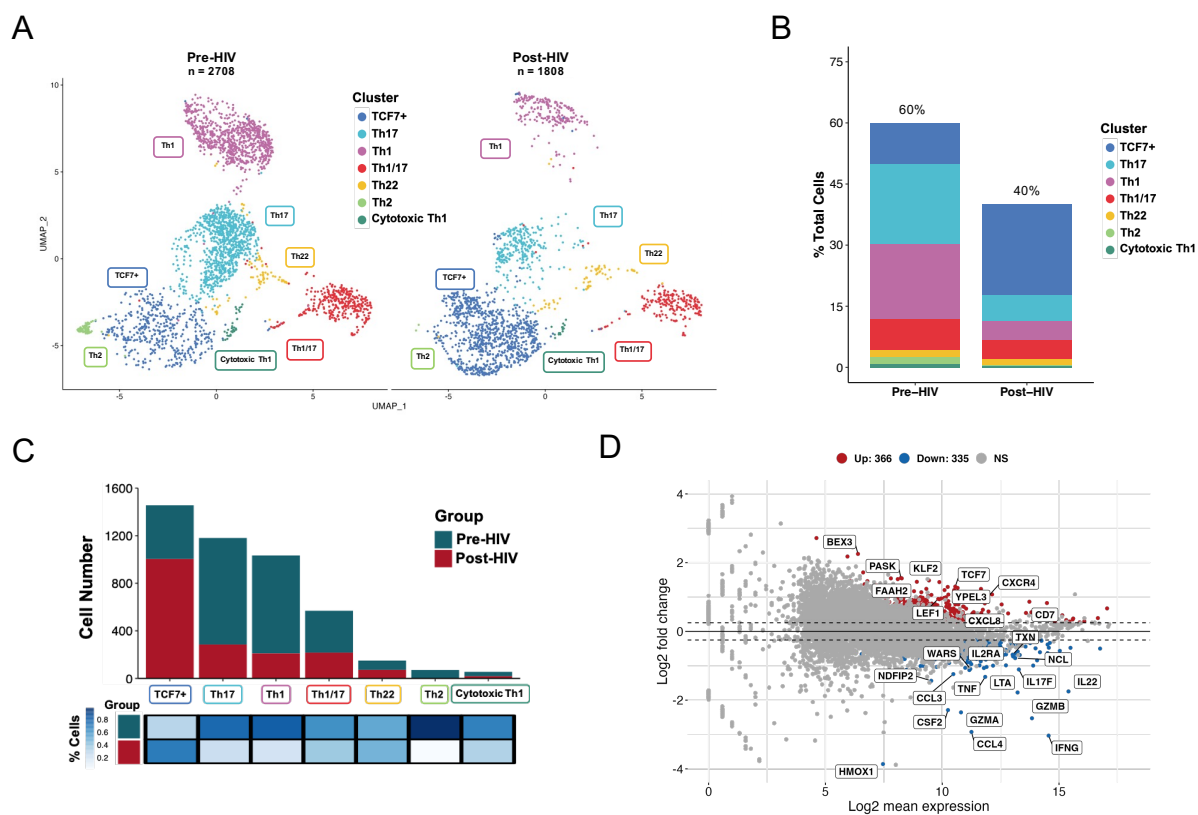


Figure 2.3. Mtb-specific Th1 and Th17 cells are significantly reduced following HIV infection. ScRNA-seq was conducted on Mtb-specific CD4 T cells before and after acquisition of HIV infection as described in Figure 2.2. **A)** UMAP of scRNA-seq of Mtb-specific CD4 T cells from 5 individuals before (Pre-HIV) and after HIV infection (Post-HIV). **B)** Fraction of total Mtb-specific CD4 T cells split by cluster and HIV status. **C)** Bar plots showing the total number of cells in each cluster, stratified by group, and a heatmap showing the percentage distribution of cells within each cluster. **D)** MA plot displaying the log₂ fold change (FC) of DEGs versus the log₂ average gene expression in Mtb-specific CD4 T cells. Genes that are significantly upregulated after HIV infection are indicated in red; genes downregulated after HIV infection are indicated in blue; non-significant genes (NS) are colored in grey. The dotted line represents a log₂ FC above 0.25 or below -0.25. DEGs were found using the Seurat FindMarkers and were considered significantly differentiated at an adjusted p-value ≤ 0.05 .

Figure 2.4

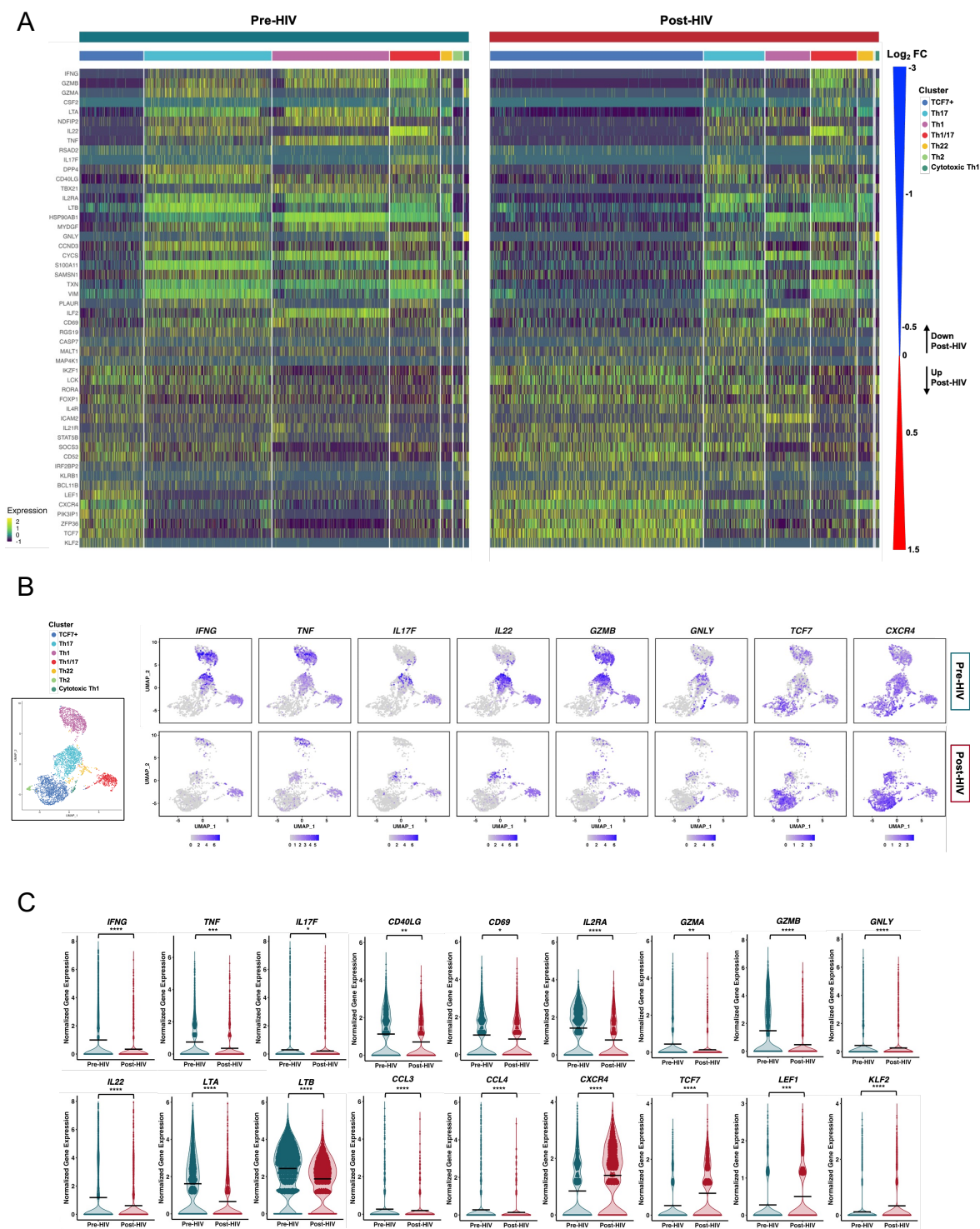


Figure 2.4. HIV infection is associated with diminished expression of key effector genes and elevated expression of stemness makers in Mtb-specific CD4 T cells. **A)** Heatmap of select effector DEGs by cluster and split by HIV status and ordered by FC. The blue wedge indicates genes downregulated after HIV infection and the red wedge indicates genes upregulated after HIV infection; FC magnitude increases outward from 0. **B)** UMAP projections overlaid with gene expression before and after HIV, aligned with Figure 2.3A for cluster comparison. The purple scale indicates the degree of gene expression in the corresponding plots before and after HIV. **C)** Violin plots of average normalized gene expression of select effector DEGs with a high magnitude of FC. DEGs comparing post-HIV and pre-HIV were determined by Seurat FindMarkers using the MAST paired test (* $p < 0.05$, ** $p \leq 0.01$, *** $p \leq 0.001$, **** $p \leq 0.0001$).

Figure 2.5

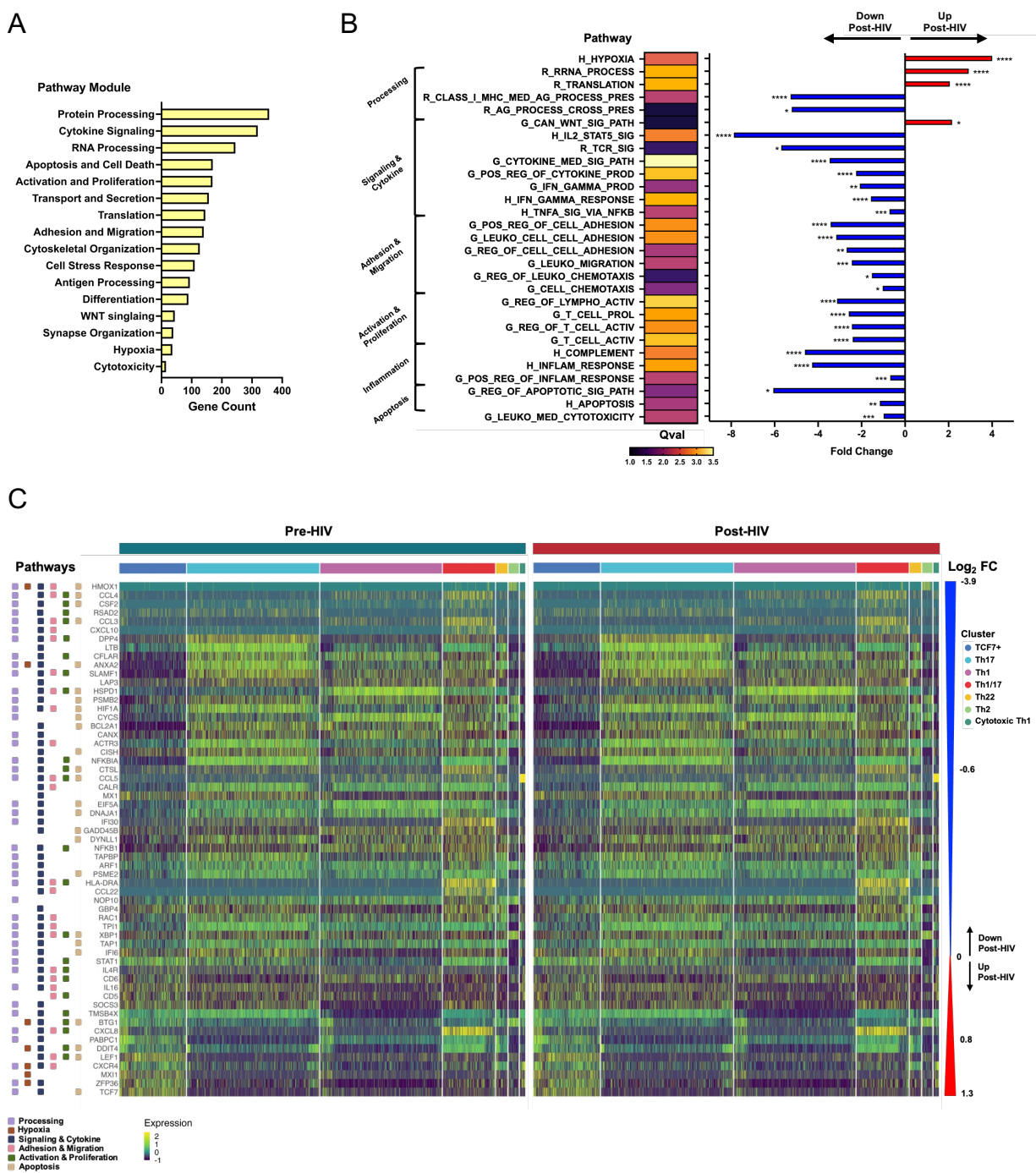
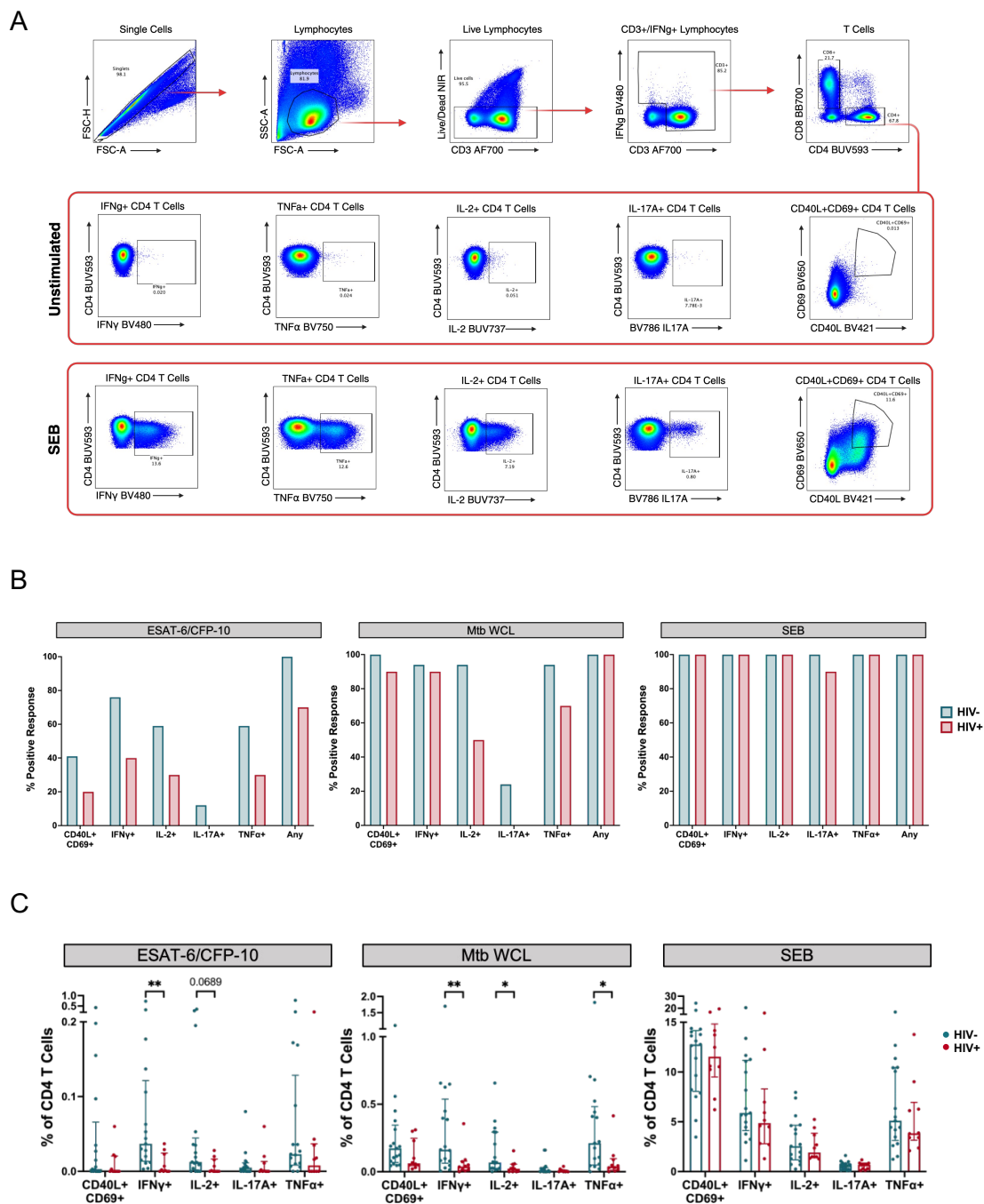


Figure 2.5. Functional and migratory pathways are dysregulated in Mtb-specific CD4 T cells following HIV. **A)** The number of DEGs with an adjusted p-value ≤ 0.05 within significantly enriched pathways (adjusted p-value ≤ 0.05) following HIV infection, grouped into modules. These modules were defined based on the relatedness of pathways derived from Hallmark, GO Biological Process, and Reactome gene sets. **B)** Single-cell pathway analysis of Mtb-specific CD4 T cells in people with HIV, relative to pre-HIV infection. The Q-values represent the fraction of cells in which each pathway is significantly enriched (FDR ≤ 0.05), highlighting the cell-level prevalence of pathway enrichment associated with HIV acquisition. Pathways with strong biological relevance and high Q-values are shown. Red indicates pathways that were upregulated and blue represents pathways that were downregulated following HIV infection. Left brackets indicate the grouped pathway categories. Asterisks represent the adjusted p-value (* ≤ 0.05 , ** ≤ 0.011 , *** ≤ 0.001 , **** ≤ 0.0001 .) **C)** Heatmap of DEGs within highlighted pathways selected from significant (FDR ≤ 0.05) DEGs by highest fold change of biologically relevant genes. The timepoint and clusters are represented by colored bars above the heatmap. The colored squares next to each row of the heatmap represent the pathway category associated with the corresponding gene. FC magnitude increases outwards from zero with red indicating upregulation and blue indicating downregulation following HIV infection. Color in the heatmap represents the cell-level magnitude of gene expression. Q-values, adjusted p-values, and fold changes of each pathway were determined using the SCPA package.

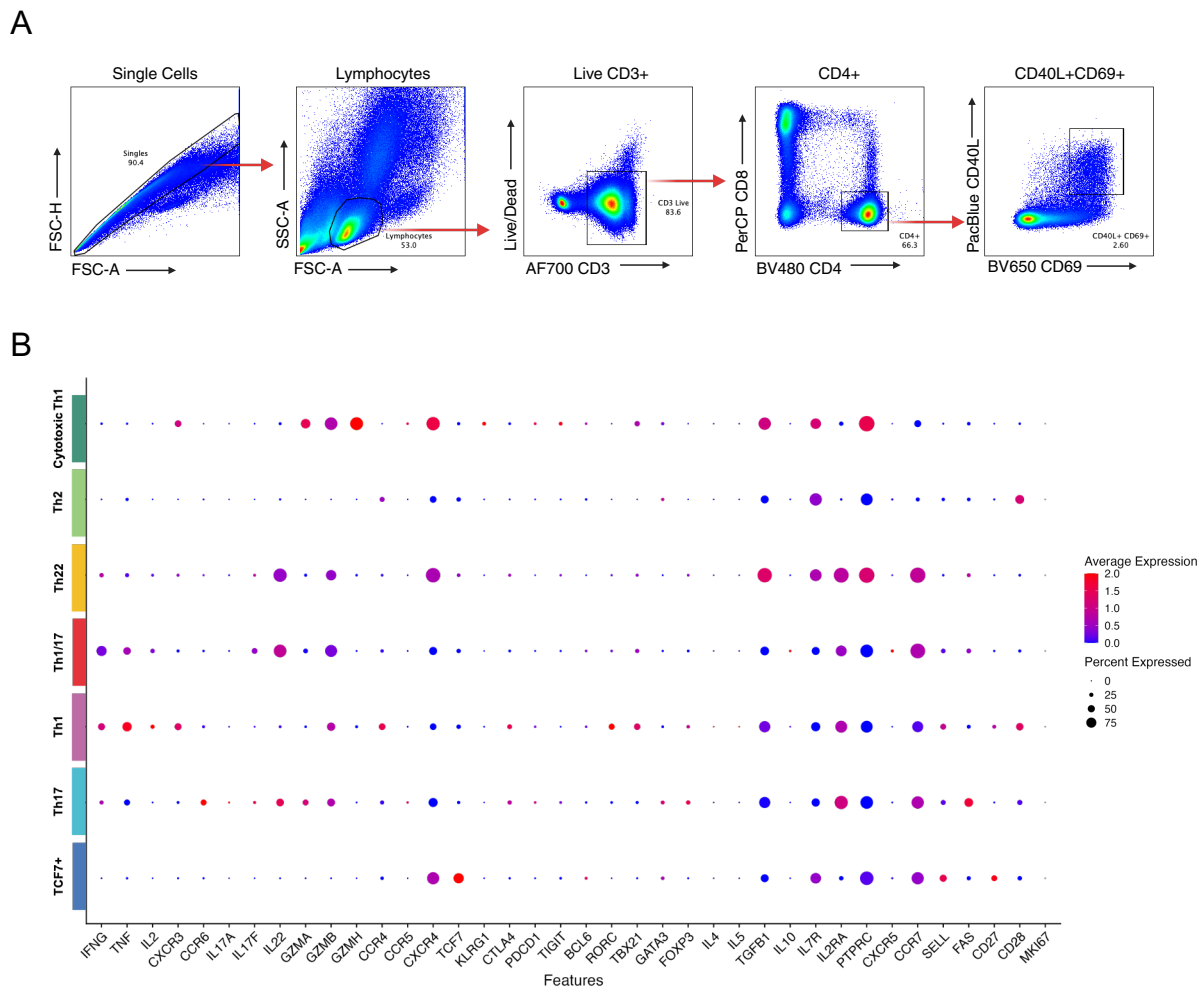
2.7 Supplemental Figures

Supplemental Figure 2.1



Supplemental Figure 2.1. Identification of antigen-specific CD4 T cell responses and flow cytometry gating strategy. **A)** Representative gating strategy of the T cell ICS assay from an individual without HIV. Gating for unstimulated (media alone) sample and a sample stimulated with SEB (positive control) from the same individual is shown for comparison. **B)** Proportion of individuals with positive responses to stimulation conditions determined using MIMOSA (see Materials and Methods) with a posterior probability $\geq 70\%$ and FDR $\leq 3\%$. **C)** Frequencies of AIM⁺ and cytokine⁺ CD4 T cells following stimulation. The top middle line represents the median and the whiskers represent the IQR. Differences in frequencies of populations of Mtb-specific CD4 T cells were analyzed using a Mann-Whitney U test (* $p < 0.05$, ** $p \leq 0.01$).

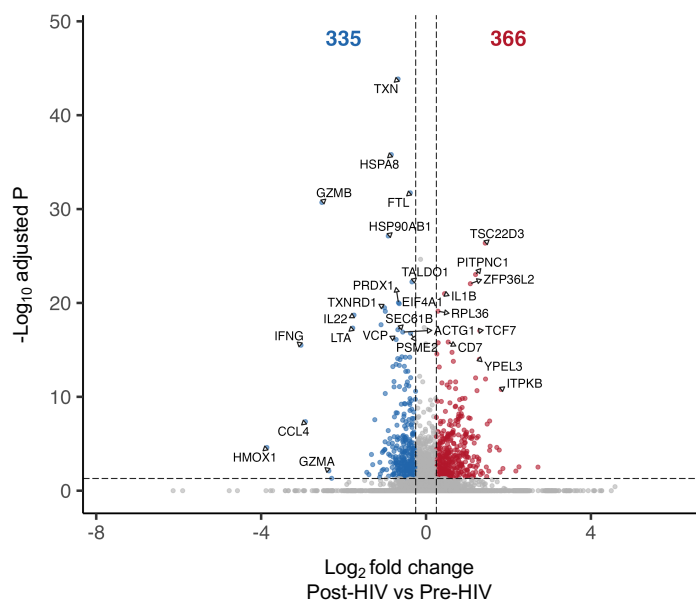
Supplemental Figure 2.2



Supplemental Figure 2.2. FACS gating strategy and average expression of lineage genes. A)

Representative gating used to sort live $CD3^+CD8^-CD4^+CD40L^+CD69^+$ Mtb-specific CD4 T cells for scRNA-seq. B) Dot plot showing normalized average gene expression of canonical helper T cell markers and differentiation makers from each cluster. The dot color reflects the average expression level of each marker within every cluster and the dot size indicates the percentage of cells within the cluster expressing the marker.

Supplemental Figure 2.3



Supplemental Figure 2.3. Differentially-expressed genes from scRNA-seq of Mtb-specific CD4 T cells before and after HIV acquisition. Volcano plot of all genes from Mtb-specific CD4 T cells before and after HIV infection. The dotted lines represent the FC cutoff above 0.25 or below -0.25 and any colored dots represent DEGs with an adjusted p value ≤ 0.05 ; red indicates genes upregulated (positive FC) following HIV infection and blue indicates genes downregulated (negative FC) after HIV infection.

Acknowledgements: We thank the study participants, without whom this study would not have been possible. We also thank M. Elliot Williams and Prashant Bajpai for their assistance with scRNA-seq data analysis and visualization.

Author Contributions: Concept and study design: RAP, SMG, RSM, CDS, CLD. Data collection, experimental optimization, and acquisition: RAP, KNK, WEW, SLH, JM, CDS. Provision of study materials and reagents: JO, WJ, KM, SMG, RSM. Analysis and interpretation of data: RAP, JM, CDS, CLD. Writing the original draft of the manuscript: RAP, CLD. Reviewing of manuscript draft: all authors.

Funding: This study was supported by grants from the National Institute of Allergy and Infectious Diseases (NIAID) at the National Institutes of Health (NIH) under grant number R21AI155221 (CLD). CLD is supported in part by the Emory/Georgia TB Research Advancement Center (TRAC; P30AI168386). RAP was supported in part by an NIAID T32 Training Program fellowship (T32AI138952). The study was supported by funding from NIH to the Emory National Primate Research Center (P51OD11132). The funders had no role in the study design, data collection and analysis, decision to publish, or preparation of the manuscript.

Potential conflicts of interest: All authors declare that they have no conflict of interest.

CHAPTER 3. Early ART Initiation Following HIV Infection Preserves the Diversity and Function of Mtb-Specific CD4 T Cells

Rachel A. Pearson^{1,2}, Krista N. Krish^{1,2}, Wendy E. Whatney^{1,2}, Walter Jaoko³, Kishor Mandaliya⁴, Julie Overbaugh⁵, Susan M. Graham^{6,7,8}, R. Scott McClelland^{6,7,8}, Sakeenah L. Hicks¹, Jeffrey Maurer¹, Christopher D. Scharer¹, Cheryl L. Day^{1,2*}

¹Department of Microbiology & Immunology, Emory University School of Medicine, Atlanta, GA

²Emory Vaccine Center, Emory University, Atlanta, GA

³Department of Medical Microbiology & Immunology, University of Nairobi, Nairobi, Kenya

⁴PathCare Laboratories, Mombasa, Kenya

⁵Division of Human Biology, Fred Hutch Cancer Center, Seattle, WA, USA

⁶Department of Epidemiology, University of Washington, Seattle, WA, USA

⁷Department of Global Health, University of Washington, Seattle, WA, USA

⁸Department of Medicine, University of Washington, Seattle, WA, USA

***Corresponding Author:**

Cheryl L. Day, PhD

954 Gatewood Rd NE

Emory Vaccine Center, Room 1024

Atlanta, GA 30329

Email: cday@emory.edu

Phone: 404-727-4374

3.1 Abstract

HIV infection disrupts immune regulation, yet its effects on the epigenetic and transcriptional programming of resting CD4 T cells during chronic infection remain incompletely understood. In this chapter, we applied a multi-omic approach—including RNA sequencing, ATAC-seq, and reduced representation bisulfite sequencing (RRBS)—to total peripheral CD4 T cells from individuals without HIV and from people with HIV (PWH) prior to antiretroviral therapy (ART). While gene expression and chromatin accessibility differences were limited, we observed broader but modest shifts in DNA methylation, suggesting that chronic HIV infection may induce early epigenetic priming independent of major transcriptional changes. These alterations may not immediately translate into functional differences in resting cells but could influence recall responses upon activation.

To evaluate how HIV and ART timing affect antigen-specific immunity, we profiled Mtb-specific CD4 T cell responses in PWH before starting treatment, PWH who initiated ART early or late, and in HIV-negative individuals. Functional assays revealed a significant loss of polyfunctional Mtb-specific CD4 T cells in PWH, particularly among those initiating ART later after infection. This impairment was antigen-specific and not observed with polyclonal stimulation, suggesting selective dysfunction in the Mtb-specific compartment. In contrast, individuals who initiated ART early retained polyfunctionality comparable to HIV-negative controls.

Single-cell RNA sequencing of Mtb-specific CD4 T cells identified conserved transcriptional subsets across groups—including stem-like, effector, regulatory, and cytotoxic populations—but revealed diminished effector gene expression and skewing toward quiescent states in untreated and late-treated PWH. Early ART preserved subset diversity and transcriptional activity, supporting a role for timely viral suppression in maintaining Mtb-specific immune competence.

Together, these findings demonstrate that chronic HIV infection subtly reprograms the regulatory landscape of CD4 T cells and impairs Mtb-specific immunity in an ART timing-dependent manner. The results underscore the importance of early ART not only in controlling viral replication but also in preserving the transcriptional and functional integrity of pathogen-specific CD4 T cell responses.

3.2 Introduction

HIV infection continues to be a major global health challenge, not only for its direct immunodeficiency effects but also due to the increased susceptibility it confers to opportunistic infections such as *Mycobacterium tuberculosis* (Mtb). Tuberculosis (TB) remains the leading cause of death among people with HIV (PWH)², and the interplay between HIV and TB is complex and multifaceted. A key element of protective immunity against Mtb is the activity of Mtb-specific CD4 T cells, which are critical for the containment and control of Mtb¹⁵⁰ through their ability to produce cytokines such as IFN γ , TNF, and IL-2 in a coordinated, polyfunctional manner^{81,88,97,111}. However, HIV infection is known to impair both the quantity^{76,81} and functional quality^{79,151} of these T cells¹²⁹, contributing to the elevated risk of TB even in individuals receiving antiretroviral therapy (ART). Although ART mitigates some of the immune dysfunction caused by HIV, the extent to which it preserves or restores Mtb-specific CD4 T cell responses^{94,129}—particularly depending on when it is initiated—remains inadequately understood^{82,87,95,152}.

Recent studies have suggested that the timing of ART initiation is a critical determinant of immune recovery, with earlier initiation conferring better preservation of CD4 T cell function and reduced TB risk^{90,153}. Despite these findings, gaps remain in our understanding of how HIV and ART timing influence both the functional and transcriptional profiles of antigen-specific CD4 T cells, particularly at a single-cell resolution. Moreover, while previous work has described global T cell perturbations in PWH^{154,155}, the antigen-specific landscape—particularly the transcriptomic regulation of Mtb-specific CD4 T cells in HIV—has not been thoroughly investigated. This knowledge is essential to decipher the mechanistic underpinnings of HIV-related immune impairment and to identify correlates of protection that may inform more effective therapeutic and

vaccine strategies.

In this study, we hypothesized that HIV infection alters both the functional and transcriptional programming of Mtb-specific CD4 T cells, and that early ART initiation mitigates these detrimental effects. To test effects of HIV on CD4 T cells, we conducted a multi-omic analysis of peripheral CD4 T cells in people with and without HIV in a well-characterized study population from the Mombasa Cohort. We examined resting CD4 T cells to identify changes in the transcriptional landscape, chromatin accessibility, and DNA methylation profile in PWH. Next, we evaluated the functional capacity of Mtb-specific CD4 T cells using intracellular cytokine staining (ICS) after overnight stimulation with staphylococcus enterotoxin B (SEB) and Mtb whole cell lysate (WCL) in people without HIV, PWH prior to the start of ART, and PWH following viral suppression on ART. To assess changes in the transcriptional profile of these cells, we used single-cell RNA sequencing (scRNA-seq) to study Mtb-specific CD4 T cells after overnight stimulation with WCL across HIV infection status and different timing of ART. Importantly, we stratified individuals based on ART timing—early versus late initiation—providing a unique opportunity to assess how treatment timing impacts immune preservation.

By using functional assays with single-cell transcriptomics and epigenetic profiling, our study provides novel insights into how HIV disrupts Mtb-specific CD4 T cell responses. We show that HIV skews these cells toward less differentiated, transcriptionally quiescent states, impairs polyfunctionality, and disrupts effector subset diversity. Importantly, our results indicate that early ART initiation was associated with preserved transcriptional diversity and functional integrity, highlighting the importance of early initiation of ART to mitigate the effects of prolonged HIV viremia on Mtb-specific CD4 T cell dysfunction. These findings fill critical gaps in our

understanding of antigen-specific immune dysregulation in HIV and offer a mechanistic basis for improving TB prevention strategies in PWH.

3.3 Methods

3.3.1 Study population and sample collection

Participants were recruited from the Mombasa Cohort⁹⁸ as described in the Methods of Chapter 2.2.1. Screening for HIV was performed following Kenyan national guidelines; for PWH, antiretroviral therapy (ART) was provided according to WHO and Kenyan national guidelines. HIV-1 viral loads and CD4 cell counts were measured for all PWH. Participants demographics in each group are described for total CD4 T cell assays in Table 3.1 and antigen-specific single-cell assays in Table 3.2. The samples evaluated in the present study were collected between 2014 and 2017; samples from PWH were evaluated prior to initiation of ART, after ART initiation early (<6 months) after HIV infection, or after ART initiation late (1-4 years) after HIV infection.

Whole blood from participants was collected in vacutainer EDTA tubes and peripheral blood mononuclear cells (PBMCs) were isolated from whole blood by density gradient centrifugation. PBMCs were cryopreserved in liquid nitrogen in Mombasa, Kenya and shipped in a cryogenic dry shipper to Emory University in Atlanta, Georgia, USA for analysis.

3.3.2 Ethics Statement

All participants provided written, informed consent for participation in the study. The Mombasa Cohort Study was approved by ethics committees at the University of Washington and the Kenyatta National Hospital. The specific study reported here was approved by the Institutional Review Board at Emory University.

3.3.3 Total CD4 T cell Sorting

Frozen PBMCs were thawed, counted, resuspended in R10 media, and stained with Zombie NearIR Live/Dead (BioLegend) for 15 min in the dark. Cells were washed with 1X PBS and stained 30 min in the dark at room temperature (RT) with the following antibodies: CD3-AF700 (Clone UCHT1, BioLegend), CD4-BV480 (Clone L200, BD Horizon), CD8-BB700 (Clone RPA-T8, BD Horizon), CD14-BV650 (Clone 3G8, BioLegend), and CD19-BV421 (Clone HIB19, BioLegend). Cells were washed suspended in 1X PBS and live CD3⁺CD8⁻CD19⁻CD14⁻CD4⁺ CD4 T cells and sorted on a FACS Aria II Cell Sorter (BD). Each sample was sorted into 3 separate tubes for downstream bulk analysis. For RNA-seq, 1,000 cells were sorted into RNase-free collection tubes (MedSupply Partners #62-1008-1) with RLT Buffer (Qiagen 79216) + 1% 2-Mercaptoethanol/BME (Sigma M6250). Cells were snap frozen in a 200-proof ethanol dry ice bath and stored at -80°C until sequencing. For ATAC-seq, 5,000-10,000 cells were sorted into R10 media, stored on ice, and transferred for sequencing. For RRBS, 2,000 cells were sorted into R10 media, stored on ice, and cells were centrifuged at 300 x g for 10 min. at 4°C to pellet them. All media was removed except for 20-50 µL and immediately stored at -80°C until sequencing.

3.3.4 RNA Sequencing and Analysis

RNA was extracted from sorted cell populations using the AllPrep DNA/RNA Mini Kit (Qiagen) following the manufacturer's protocol. Fifty picograms of total RNA were used for cDNA synthesis with the SMART-seq v3 kit (Takara) and amplified through ten cycles of PCR. Subsequently, 1 ng of cDNA was used as input for library preparation with the Nextera XT DNA Library Prep Kit (Illumina), using nine cycles of PCR. Libraries were quantified via qPCR,

assessed for fragment size distribution using a Bioanalyzer, pooled, and sequenced on an Illumina HiSeq 2500 with 50-bp paired-end reads.

Sequencing reads were aligned to the human genome (hg19) using TopHat2 v2.0.13¹⁵⁶ with the UCSC KnownGene¹⁵⁷ annotation. Duplicate reads were removed using PICARD v1.127 (<http://broadinstitute.github.io/picard/>). Gene-level expression was quantified as RPKM using GenomicRanges v1.22.4¹⁵⁸ and custom R scripts. Genes were included for downstream analysis if there were >3 reads per million in all samples for at least one group. Differential expression was analyzed using edgeR v3.18.1¹⁵⁹ with a generalized linear model; covariates included patient identity and HIV/ART status, depending on the comparison. Genes with log₂ fold change ≥ 0.25 and FDR < 0.05 were considered significant. Heat maps were generated from quantile-normalized reads per kilobase per million (RPKM) values, with plotted genes further normalized using z-scores.

3.3.5 ATAC-seq and Analysis

ATAC-seq was conducted on flow-sorted CD4 T cells, which were lysed in 50 μ L of nuclei lysis buffer (10 mM Tris pH 7.4, 10 mM NaCl, 3 mM MgCl₂ and 0.1% IGEPAL CA-630), subjected to tagmentation (25 μ L of 300 mM NaCl, 100 mM EDTA, 0.6% SDS and 1.6 μ g proteinase-K) and placed in a thermocycler at 37°C for 1 h. High molecular weight DNA was removed using a 0.6x SPRI negative bead selection protocol, low molecular weight fragments purified by 1.2xSPRI-bead positive selection, and PCR amplified using Nextera indexing primers (Illumina) and 2xHiFi HotStart Ready Mix (Roche). Libraries were purified, quantified by qPCR, assessed for fragment

patterning via Bioanalyzer, and sequenced on an Illumina HiSeq 2500 using 50-bp paired-end reads.

Reads were aligned to hg19 using Bowtie v1.1.1, with duplicates removed by PICARD. MACS2 v2.1¹⁶⁰ was used for peak calling. A unified peak set was created using HOMER's mergePeaks.pl¹⁶¹ function, and peak counts were annotated and normalized to RPPM using GenomicRanges. Differential accessibility analysis was performed with edgeR, and peaks with $\geq 0.25 \log_2$ fold change and FDR < 0.05 were deemed significant.

3.3.6 Reduced-Representation Bisulfite Sequencing and Analysis

Genomic DNA was digested with MspI or TaqI enzymes for RRBS. Digestion efficiency was validated by qPCR. Methylated and unmethylated control phage DNAs were fragmented and spiked into samples as bisulfite conversion controls. Adapters were ligated using the HyperPrep Kit (KAPA Biosystems), followed by bisulfite conversion using the EpiTect Bisulfite Kit with an extended denaturation step. Final libraries were PCR-amplified with custom primers, quality-checked, and sequenced on a HiSeq 2500.

Raw reads were mapped to a combined reference genome (hg19, Φ X174, lambda phage) using Bismark v0.16.3. CpG methylation levels were extracted and analyzed using Rsamtools and custom R scripts. Differential methylation was assessed using DSS v2.10.0 with CpGs showing $\geq 20\%$ change and FDR < 0.05 considered significant.

3.3.7 T cell ICS assay and flow cytometry

A more detailed description of this assay and antibody information can be found in Chapter 2.3.3 Methods. Cryopreserved PBMCs were thawed and incubated for 1 hour at 37°C under the following conditions: 10µg/mL Mtb H37Rv whole cell lysate (WCL; NR-13648, obtained through BEI Resources, NIAID, NIH), or 1µg/mL of staphylococcus enterotoxin B (SEB; Toxin Technology, Inc.), or media alone as a negative control. Cells were treated with Golgi block (monensin and brefeldin A) and stimulated overnight 37°C. Cells were washed, stained with Zombie NearIR Live/Dead stain and then stained with surface antibodies against CD3, CD4, and CD8 fixed, and permeabilized. Cells were then stained with antibodies for intracellular features: CD40L, CD69, IL2, IFN γ , TNF, and IL-17A. Cells were acquired on a FACSymphony (BD) using FACSDiva software (v9.0) and FCS files were analyzed in FlowJo (BD v10.9.1).

3.3.8 COMPASS analysis of flow cytometry data

Cell counts in the T cell ICS assay were analyzed using the COMPASS algorithm¹⁰⁰, described in Chapter 2.3.4 Methods. Briefly, COMPASS identifies antigen-specific cytokine-producing subsets by calculating the posterior probability of a positive response, considering subsets with a probability >70% and a false discovery rate (FDR) <0.03 as significant. The algorithm then assigns each participant a functionality score (FS) and polyfunctionality score (PFS), reflecting the breadth and quality of their antigen-specific T cell responses.

3.3.9 Activation-induced marker assay and sorting Mtb-specific CD4 T cells

A more detailed description of this assay can be found in Chapter 2.3.5 Methods. Frozen PBMCs were thawed, counted, and incubated with anti-CD40 and stimulated with Mtb WCL overnight. PBMCs stained with Zombie NearIR Live/Dead, then stained with CD3, CD4, CD8, CD69, and CD40L. Hashtag oligonucleotide antibodies for donor and timepoint demultiplexing in analysis. FCS and live CD3⁺CD8⁻CD4⁺CD40L⁺CD69⁺ Mtb-specific CD4 T cells were sorted with FACS Aria II Cell Sorter (BD) and samples were combined and stored on ice for 10X Genomics scRNA-seq protocol.

3.3.10 10x Genomics scRNA-seq library preparation

Live Mtb-specific CD4 T cells were prepared for scRNA-seq and sequenced using the protocol described in Chapter 2.3.6 Methods.

3.3.11 ScRNA-seq data processing and analysis

Data was processed and analyzed according to the protocol described in Chapter 2.3.7 Methods with the following changes. Cells with greater than 9% mitochondrial genes and >35,000 or <500 detected genes were considered outliers and excluded from downstream analyses. Raw unique molecular identifier (UMI) counts for each batch were individually transformed using Seurat's SCTransform (v2)¹⁰⁵ function and the SCT assays were integrated by batch using Seurat's standard integration pipeline and to normalize to UMI counts per million total counts and log-transform and scale them. PCA was performed with the top 30 most statistically significant principal components. UMAP plots were generated based on selected PCA dimensions at a resolution of 0.4. The Seurat

function FindAllMarkers was used to identify marker genes between clusters and DEGs across all clusters within comparison groups (1vAll). Differentially expressed genes (DEGs) between comparison groups were identified using the Seurat function FindMarkers with the MAST¹⁰⁶ test, incorporating a group-specific latent variable. For pairwise (1v1) analyses, groups were compared in a predefined order of reference group preference: HIV-negative, Pre-ART, Post-ART Early, and Post-ART Late, with HIV-negative always treated as the reference group.

3.3.12 Statistical Analysis

Data was visualized using GraphPad Prism (v.10.0.3), Seurat v4, ggplot2, ggmaplot, and EnhancedVolcano packages in R. Differences between cell frequencies in across groups for flow cytometry experiments were analyzed using the Kruskal–Wallis test with Dunn’s post hoc test for multiple comparisons. All other statistical analysis was performed with Seurat functions as **3.3**

3.4 Results

3.4.1 Study Participants

Participants were evaluated from the ongoing Mombasa Cohort, an open cohort study in Mombasa, Kenya investigating risk factors for HIV acquisition among female sex workers. We evaluated people without HIV (HIV-), PWH before ART initiation (pre-ART), PWH starting ART early (0-8 months) after HIV infection (post-ART early), and PWH starting ART late (12-45 months) after HIV infection (post-ART late). The median age of HIV- participants was 30 years old, pre-ART participants was 32 years old, post-ART early was 35 years old, and post-ART late was 38 years old. PWH pre-ART were evaluated 3-44 months after HIV infection (median 5.5 months post-seroconversion).

For the bulk CD4 T cell analysis, the median age of HIV- participants was 30 years old, but the median aged differed slightly based on the assay: median age for RNA-seq was 32 years old and 33.5 years old for both ATAC-seq and RRBS. The median absolute CD4 count in PWH group was 519 cells/ μ L across all assays. The median HIV plasma viral load was in the pre-ART group differed depending on the assay, with 88,658 copies/mL as the median for RNA-seq, 52,554 copies/mL as the median for ATAC-seq, and 44,925 copies/mL as the median for RRBS (Table 3.1).

For scRNA-seq analysis, the median absolute CD4 count in each HIV⁺ group was 519 cells/ μ L in pre-ART, 471 cells/ μ L in post-ART early, and 677 cells/ μ L in post-ART late. However, the CD4 count was not significantly different across groups (Supplemental Figure 3.1). The median HIV plasma viral load was 52,554 copies/mL in the pre-ART group, undetectable-125 copies/mL in the

post-ART early group, and all participants had undetectable viral loads in the post-ART late group (Table 3.2).

3.4.2 HIV infection induces moderate DNA methylation changes with minimal transcriptional or chromatin accessibility alterations in resting CD4 T cells

To examine how early HIV infection impacts the epigenetic and transcriptional landscape of resting CD4 T cells, we performed RNA-seq, ATAC-seq, and RRBS on sorted resting, live CD4 T cells from people without HIV (HIV⁻) and PWH prior to initiation of ART (Figure 3.1A). Across both RNA-seq and ATAC-seq datasets, comparative analyses revealed minimal differences between groups. Only a small number of differentially expressed genes (DEGs) were identified meeting the threshold cutoff of an FDR of 0.05 and an absolute log₂ fold change ≥ 0.5 – 4 downregulated and 6 upregulated in individuals with HIV relative to those without HIV. Similarly, there were minimal differences in chromatin accessibility, with only 7 downregulated and 4 upregulated differentially accessible regions (DARs) in distinct gene loci that met the threshold (Figure 3.1B). While a larger number of DARs achieved statistical significance (1484 up and 1506 down), most did not surpass the required percent methylation change of cutoff ($|\log_2FC| \geq 0.25$), suggesting that HIV infection does not broadly modify chromatin accessibility in peripheral blood CD4 T cells (Figure 3.1C). In contrast, RRBS analysis revealed a markedly different pattern, with a large number of differentially methylated loci (DMLs) between HIV⁺ and HIV⁻ groups, indicating remodeling of DNA methylation. These DNA methylation alterations were not accompanied by widespread shifts in transcription or chromatin accessibility, pointing to a unique regulatory disconnect or potential latency in downstream transcriptional consequences. Heatmap visualization of selected features confirmed this disparity, showing sparse but specific alterations

in gene expression and accessibility, contrasted by broad methylation changes (Figure 3.11D). The modest transcriptional and chromatin-level changes likely reflect the predominance of naïve CD4 T cells within the sorted population, potentially diluting signals from more functionally dynamic subsets. Given this, we next focused on antigen-specific CD4 T cells to better resolve HIV-induced immune remodeling at a functional level.

3.4.3 HIV infection impairs polyfunctional Mtb-specific CD4 T cell responses, with greater dysfunction when ART is initiated more than 1 year after HIV infection

To assess the impact of HIV infection and ART timing on Mtb-specific CD4 T cell functionality, we stimulated PBMCs from HIV⁻ individuals and PWH prior to starting ART (pre-ART), after starting ART within 8 months after HIV infection (post-ART early), or after starting ART 1-4 years after HIV infection (post-ART late) with Mtb WCL and evaluated cytokine production and activation marker expression using intracellular cytokine staining (ICS) to assess the AIMs CD40L and CD69 and combinatorial analysis (Figure 3.2A–B). Boolean gating revealed a significant reduction in the frequency of polyfunctional AIM⁺IFN γ ⁺IL-2⁺TNF⁺ CD4 T cells between PWH and pre-ART, PWH post-ART Early and post-ART Late, with people who initiated ART later showing a further decrease compared with PWH pre-ART. Similarly, frequencies of AIM⁺IFN γ ⁺TNF⁺ CD4 T cells were diminished in both pre-ART and late-treated individuals compared to HIV⁻ individuals. These reductions were specific to Mtb WCL stimulation and not observed following SEB stimulation, indicating an antigen-specific impairment (Figure 3.2C, Supplemental Figure 2.1).

To further quantify the functional breadth of the antigen-specific CD4 T cell response, we applied the COMPASS algorithm to calculate functionality scores (FS) and polyfunctionality scores (PFS) across groups (Figure 3.2D). FS and PFS were significantly reduced in PWH before ART and late-treated individuals compared to HIV⁻ controls, with no significant difference observed between PWH before ART and early-treated individuals, probably due to limited statistical power with the low number of participants in the post-ART group. These findings suggest that delaying ART may exacerbate Mtb-specific T cell dysfunction beyond that seen in untreated infection. In contrast, responses to SEB stimulation remained consistent across all groups, reinforcing the antigen specificity of the observed dysfunction. These findings demonstrate that HIV infection impairs the polyfunctional capacity of Mtb-specific CD4 T cells and that early ART initiation may help preserve this critical component of immune defense.

3.4.4 Single cell transcriptional profiling indicates distinct clusters of Mtb-specific CD4 T cells

To characterize the transcriptional heterogeneity of Mtb-specific CD4 T cells, we performed scRNA-seq on live CD40L⁺CD69⁺ CD4 T cells sorted after overnight stimulation with Mtb WCL from people without HIV and PWH before starting ART and starting ART at different times after HIV infection (Figure 3.3A–B). After correcting for donor-specific and batch-specific effects, unsupervised clustering based on differential gene expression identified nine transcriptionally distinct clusters shared across all participants, regardless of HIV or ART status (Figure 3.3C and Supplemental Figure 3.2). Annotation of these clusters was based on canonical lineage-defining transcription factors, cytokines, and genes associated with activation or stemness (Figure 3.3D–E). Two clusters were defined by high expression of *TCF7*, *LEF1*, and *KLF2* and lacked effector

cytokines, consistent with a stem-like or memory precursor phenotype. One of these *TCF7*⁺ clusters additionally expressed *CD38*, *STAT1*, *STAT2*, *STAT3*, *STAT4*, and *STAT6*, suggesting an activated stem-like state, while the other lacked these features and exhibited a more quiescent profile (Supplemental Figure 3.3A–B). A Th1 cluster was identified by expression of *CXCR3*, *IFNG*, *IL2*, and *TBX21*, while a Th17-like Treg cluster co-expressed *FOXP3*, *IL2RA*, *TGFB1*, *CCR6*, and did not express *IL7RA*. Distinct Th17 and Th22 clusters were defined by expression of canonical lineage markers. The Th17 cluster expressed *CCR6*, *RORC*, *IL17A*, and *IL17F*, while the Th22 cluster was characterized by *IL22* and *AHR* in the absence of *IL17A*, *IL17F*, or *IFNG*. A separate Th1/Th22 hybrid cluster co-expressed *IFNG* and *IL22*, indicating a transitional or mixed-effector phenotype. Additional subsets included a cytotoxic Th1 cluster enriched for granzymes, *GNLY*, and *CXCR3*, and another cluster enriched for pro-apoptotic transcripts such as *BAX*, *BBC3 (PUMA)*, and *PMAIP1 (NOXA)*. Together, the two *TCF7*⁺ clusters accounted for the majority of all Mtb-specific CD4 T cells profiled, underscoring the predominance of precursor-like states within the circulating antigen-specific pool. The presence of these transcriptionally defined clusters across all individuals provides a foundational framework for interrogating the influence of HIV infection and timing of ART initiation on the transcriptome of Mtb-specific CD4 T cells.

3.4.5 HIV infection reshapes the transcriptional landscape and subset composition of Mtb-specific CD4 T cells, with early ART preserving effector diversity

To assess how HIV infection and the timing of ART initiation influence the composition and transcriptional states of Mtb-specific CD4 T cells, we analyzed scRNA-seq data across clinical groups. Hierarchical unsupervised clustering and comparative analyses of cluster distributions

revealed marked shifts in subset representation in PWH (Figure 3.4A–C). In people without HIV and PWH who initiated ART early, Mtb-specific CD4 T cells were broadly distributed across multiple effector subsets, including Th17-like Tregs, Th1, and Th1/Th22 populations. In contrast, cells from PWH prior to initiation of ART or those who initiated ART late were disproportionately concentrated in activated and quiescent *TCF7*⁺ clusters, which are defined by high expression of *TCF7* and represent stem-like phenotypes. Notably, 61.7% of cells from untreated individuals and 76.8% of cells from those who initiated ART late localized to these clusters, compared to 33.4% and 44.4% in people without HIV and early ART initiators, respectively. Although a modest expansion of *TCF7*⁺ cells was also observed in individuals who initiated ART early, this population exhibited a more activated transcriptional profile, including elevated expression of *STAT* family genes distinguishing them from the quiescent *TCF7*⁺ cells predominant in people with HIV pre-ART or late-treated individuals. Differential gene expression analyses reinforced these findings, with MA and volcano plots highlighting the most extensive transcriptional disruptions in comparisons between late ART initiators and people without HIV (Figure 3.4D–E; Supplemental Figure 3.4). Collectively, these results indicate that HIV infection drives early changes in Mtb-specific CD4 T cell diversity and effector differentiation, skewing the repertoire toward less functional, precursor-like states. However, early ART initiation preserves a broader array of effector subsets and maintains a transcriptional landscape more closely aligned with people without HIV, underscoring the critical role of early intervention in preserving pathogen-specific immunity.

3.4.6 Early ART initiation preserves effector and regulatory gene expression in Mtb-specific CD4 T cells

To dissect the functional consequences of HIV infection and the timing of ART initiation on Mtb-specific CD4 T cells, we evaluated the expression of highly significant effector and regulatory genes across clinical groups. Violin plots revealed widespread transcriptional disruption in cells from people with HIV pre-ART or initiated ART late, characterized by marked reductions in key effector cytokines (*IFNG*, *TNF*, *IL17A*, *IL17F*, *IL22*), cytotoxic mediators (*GZMA*, *GZMB*), lineage-defining transcription factors (*TBX21*, *RORC*, *BATF*), and chemokine receptors (*CXCR3*, *CCR4*, *CCR5*, *CCR6*) (Figure 3.5). In contrast, individuals who initiated ART early largely preserved or enhanced the expression of these genes, with levels comparable to those without HIV or surpassing those in untreated or late-treated individuals. Expression of *CCR7* was notably elevated in the early ART group above all other groups, indicating preserved central memory features, while *SELL* was consistently upregulated across all groups with HIV compared to people without HIV.

Markers of activation and exhaustion, including *CD40LG*, *CD69*, *PDCD1*, *TIGIT*, and *CTLA4*, were variably expressed across groups. Expression of *CD40LG* and *CD69* was diminished in late-treated individuals but preserved in those who started ART early after HIV infection. *CTLA4* was significantly upregulated in individuals treated early compared with pre-ART and late-treated groups, while *TIGIT* showed increased expression in early-treated individuals that exceeded levels in people without HIV. In contrast, *BTLA* was downregulated only in the untreated group, with levels preserved in the early and late ART groups. Interestingly, *KLRG1*, a marker of terminal differentiation, was downregulated in early ART individuals compared to HIV-negative controls,

suggesting a less exhausted phenotype. Stem-like transcription factors *TCF7* and *LEF1* were elevated across all groups of people with HIV, consistent with a skewing toward precursor-like states irrespective of treatment timing. Homeostatic markers displayed variable regulation: both *CD27* and *IL7R* were reduced in PWH prior to ART initiation, with *IL7R* expression notably lower than in both people without HIV and PWH pre-ART, while *CD27* levels dropped below those observed in PWH with late start of ART but remained higher than in people without HIV. *CCR7* expression, by contrast, was highest in early ART, consistent with retention of central memory potential.

Apoptosis-regulating genes also reflected ART-associated shifts. *BCL2* and *CASP4* were upregulated in early ART recipients, while pro-apoptotic *BAX* and *BTG1* were downregulated, suggesting enhanced survival potential in this group. *FAS* expression was downregulated in both pre-ART and late-treated individuals compared to but people without HIV and early ART groups, aligning with a more regulated apoptotic profile. Finally, we observed significant downregulation of Treg-associated genes *FOXP3*, *TGFB1*, and *IL2RA* in both pre-ART and post-ART late groups, indicating depletion or destabilization of Th17-like regulatory subsets. Taken together, these data demonstrate that individuals who initiated ART early most closely resembled the transcriptional profile of people without HIV across effector, regulatory, activation, survival, and trafficking gene programs.

3.4.7 Reduced intensity of effector gene expression within conserved Mtb-specific CD4 T cell clusters

To determine whether the loss of effector function in Mtb-specific CD4 T cells was also due to reduction in transcriptional output within individual cells, we examined gene expression intensity within defined clusters using a heatmap of single-cell expression values (Figure 3.6). Across the Th1 cluster, which was present at similar frequencies in all groups, the magnitude of *TNF* expression per cell was markedly reduced in individuals before ART or initiated ART late compared to people without HIV and those who initiated ART early. In people without HIV and early ART recipients, a larger proportion of Th1 cells expressed high levels of *TNF*, indicating robust effector activity. By contrast, in pre-ART and late-treated individuals, *TNF* expression was not only diminished in intensity but was also detected in fewer cells within the cluster. This pattern was mirrored for other effector genes across additional functional clusters. Importantly, this transcriptional impairment persisted in individuals who initiated ART late, whereas early treatment effectively restored per-cell expression to levels comparable to those seen in people without HIV. These findings suggest that HIV-induced dysfunction in Mtb-specific CD4 T cells is driven also by suppression of their transcriptional activity, and that early ART initiation is critical for preserving the intrinsic functional capacity of these cells.

3.5 Discussion

HIV infection is known to disrupt immune homeostasis, yet its early impact on resting CD4 T cell epigenetic programming remains incompletely understood. Our multi-omic profiling approach reveals that while transcriptional and chromatin accessibility changes in these cells are relatively limited during HIV infection, there is some shift in DNA methylation patterns. This suggests that epigenetic remodeling may precede or occur independently of broader transcriptional activation or repression, potentially laying a foundation for long-term immune dysfunction. The dissociation between methylation and gene expression also raises the possibility that regulatory changes in resting CD4 T cells may not immediately translate into altered function but instead reflect priming or silencing states that manifest upon activation. It could also be due to the presence of naïve CD4 T cells that mask the changes in memory CD4 populations. These findings underscore the complexity of CD4 T cell reprogramming during HIV infection.

To investigate how HIV infection shapes the broader immune regulatory environment, we characterized the transcriptional, chromatin accessibility, and DNA methylation landscapes of total peripheral CD4 T cells using RNA-seq, ATAC-seq, and RRBS. Across all three modalities, including gene expression, chromatin accessibility, and DNA methylation, we observed modest differences between HIV-negative individuals and PWH prior to ART initiation. While there were limited differentially expressed genes and accessible chromatin regions, RRBS analysis identified a larger number of differentially methylated loci, though the overall magnitude of methylation differences was also modest. This parallel pattern of restrained changes across transcriptional, chromatin, and epigenetic layers suggests that early HIV infection may subtly influence CD4 T cell regulatory states without inducing overt functional remodeling. These modest shifts could

represent early or context-dependent alterations that may become more pronounced upon cellular activation or disease progression. The predominance of naïve CD4 T cells in our sorted population may also dilute signals from more transcriptionally dynamic memory or antigen-experienced subsets. Together, these findings highlight the subtlety of early immune perturbations following HIV infection and underscore the importance of studying antigen-specific or tissue-resident cells, which may better reflect the functional consequences of these regulatory changes.

To assess the impact of HIV infection and ART timing on Mtb-specific CD4 T cell function, we stimulated PBMCs from people without HIV and PWH—prior to ART and after early or late ART initiation—with Mtb WCL or SEB and measured cytokine production and activation markers using ICS. This approach enabled the evaluation of polyfunctional profiles and the identification of shifts in the immune response associated with infection and treatment. Functional profiling revealed a substantial reduction in the frequencies of functional and polyfunctional Mtb-specific CD4 T cells, including diminished frequencies of polyfunctional IFN γ +TNF+IL-2+AIM+ populations in PWH and in those who started ART later after infection. Notably, PWH that were untreated and started ART later after HIV infection showed reduction functionality and polyfunctionality to Mtb stimulation compared with individuals without HIV. Likewise, functionality and polyfunctionality scores were diminished in untreated PWH and treated late. Conversely, PWH that started ART early after HIV infection had functionality and polyfunctionality scores comparable to individuals without HIV. The observed reductions were specific to Mtb WCL stimulation and not observed following SEB stimulation, indicating an antigen-specific impairment which is consistent with other studies^{78,79}. These insights suggest that HIV selectively reshapes CD4 T cell responses in a way that compromises the immune

system's ability to respond to Mtb, and that later ART initiation may further impair this aspect of host defense.

The ability of CD4 T cells to mount polyfunctional responses to Mtb is essential for protective immunity^{83,162}, though it is not solely sufficient for complete Mtb control, and this functionality is substantially impaired by HIV infection^{50,53,81,88,91,151,163,164}. To characterize the transcriptional heterogeneity of Mtb-specific CD4 T cells, we performed scRNA-seq on live CD40L⁺CD69⁺ CD4 T cells sorted after overnight stimulation with Mtb WCL from people without HIV and PWH pre-ART and those who started ART at different times after HIV. Unsupervised clustering revealed a conserved transcriptional architecture composed of multiple distinct clusters across groups, reflecting diverse functional phenotypes including stem-like, effector, regulatory, and cytotoxic subsets. This conserved organization provides a crucial framework for interpreting how HIV and ART timing modulate Mtb-specific CD4 T cell differentiation and function. To assess changes in the transcriptional landscape of Mtb-specific CD4 T cells after HIV infection and between groups starting ART at different time, we used this framework to perform differential gene expression between groups and characterized the population and gene expression shifts. Our findings suggest a model in which the composition and functional output of Mtb-specific CD4 T cells are diminished in HIV by favoring less differentiated, quiescent states over effector and regulatory subsets and reducing transcriptional activity within effector subsets. This shift likely undermines the immune system's ability to effectively respond to Mtb and contributes to the heightened risk of tuberculosis among people with HIV. Our results indicated that early initiation of ART was associated with preservation of effector diversity, including the maintenance of Th1, Th17, and Treg subsets, and by promoting a pool of more transcriptionally active stem-like CD4

T cells with greater potential for functional differentiation. These data further underscore the importance of ART timing in maintaining immune competence and suggest that transcriptional resilience within Mtb-specific CD4 T cells may serve as a mechanistic correlate of protection in the setting of HIV co-infection.

While this study provides significant insights into HIV-induced dysregulation of CD4 T cells responding to Mtb, several limitations must be acknowledged. First, the median time on ART was higher in those that started ART late than those that started ART early, 13 months and 21 months, respectively and the range of time on ART was wider in the late ART groups as well (Table 3.2). Second, the timing of ART initiation is inherently linked to the duration of HIV infection, introducing a potential confounder, as individuals who started ART later had been infected for a longer period. Third, post-ART samples were chosen based on time on ART and viral suppression (<200 HIV-1 RNA copies/ μ L of blood) however, some individuals oscillated between detectable viral loads above and below the threshold over the time of follow-up. Thus, ART adherence was not monitored by test and only relied on verbal accounts from participants. This is a limitation because differences in ART adherence could be a confounder as well.

Despite these limitations, the study presents several notable strengths. The ability to isolate sufficient numbers of Mtb-specific CD4 T cells enabled robust and statistically meaningful comparative analyses between groups. Precise documentation of HIV seroconversion and ART initiation allowed for clear stratification based on ART timing—an advantage unique to this prospective cohort, as the duration of HIV infection and timing of ART initiation relative to duration of HIV infection is rarely known in other study designs. Furthermore, the combined use of functional interrogation through flow cytometry and transcriptional profiling of Mtb-specific

CD4 T cells, alongside independent epigenetic and transcriptional analyses of total CD4 T cells, offered a comprehensive and multidimensional perspective on HIV-associated immune perturbations. Collectively, this unique design offers valuable insights into how HIV infection and the timing of ART initiation shape Mtb-specific immune responses.

These findings offer key insights into the mechanisms by which HIV impairs immune defenses against Mtb. The observed skewing toward stem-like, less differentiated states in Mtb-specific CD4 T cells, particularly in pre-ART and late-ART-treated individuals, suggests longer exposure to HIV viremia limits the diversity of Mtb-specific effector cells that likely compromises protective immunity. Importantly, individuals who initiated ART early exhibited preserved subset diversity and more robust effector gene expression, suggesting ART-mediated suppression of viremia early after HIV infection may facilitate preservation of Mtb-specific CD4 T cell responses. Altogether, our data emphasize the importance of early ART not only in suppressing HIV viral load but also in maintaining the functional integrity of Mtb-specific immune responses, particularly in the context of co-infections like Mtb. In the future, studies should focus on elucidating the mechanisms underlying the epigenetic priming of CD4 T cells during early HIV infection, determining whether these alterations are reversible with ART, and exploring how tissue-resident immune responses compare to peripheral profiles to better inform strategies for preserving or restoring protective immunity against Mtb and other opportunistic pathogens.

3.6 Main Figures

Table 3.1

Table 3.1 Characteristics of study participants.

| | Assay | HIV- | Pre-ART |
|---|--------------|-----------------------------------|--|
| Age (years) (Range) | RNA-seq | N = 24 30 ^a (23-48) | N = 13 32 ^a (22-51) |
| | ATAC-seq | N = 22 30 ^a (23-48) | N = 12 33.5 ^a (22-51) |
| | RRBS | N = 23 30 ^a (23-48) | N = 11 33.5 ^a (22-46) |
| Sex (%F) | All | 100 | 100 |
| CD4 count (cells/μL) (Range) | All | ND | 519 ^a (454-648) |
| Viral Load (HIV-1 RNA copies/mL) (Range) | RNA-seq | ND | 88658.00 ^a (4560- 1794912) |
| | ATAC-seq | ND | 52554 ^a (4560- 1794912) |
| | RRBS | ND | 44925 ^a (4560-1151927) |
| Time since HIV seroconversion (months) (Range) | All | ND | 5 ^a (1-44) |

^a Value denotes median.

^b Not done.

Figure 3.1

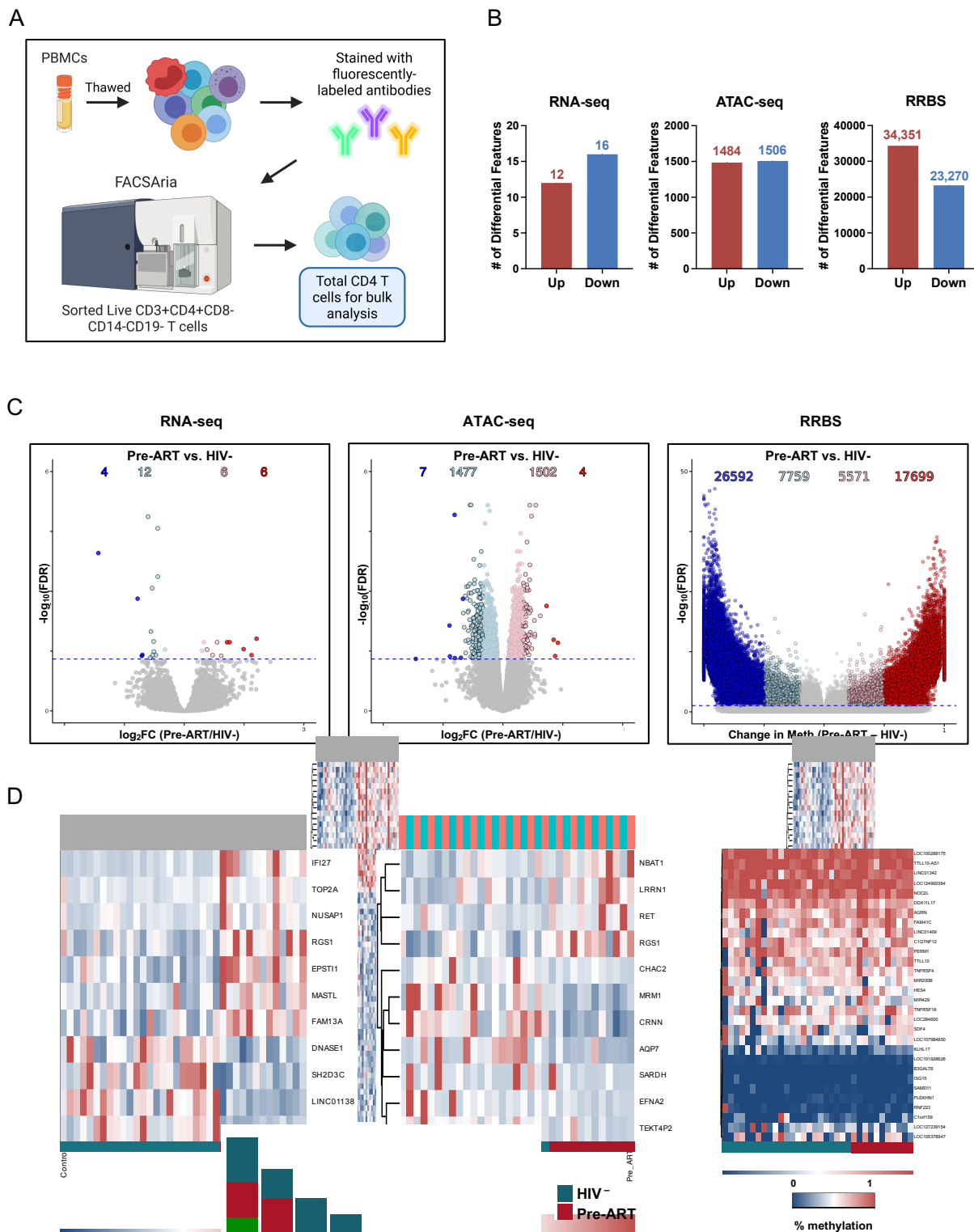


Figure 3.1. Multi-omic profiling of resting CD4 T cells reveals differential gene regulation in people with HIV. (A) Schematic overview of the experimental workflow for sorting total resting, live CD4 T cells from peripheral blood mononuclear cells (PBMCs) and performing bulk RNA-seq, ATAC-seq, and reduced representation bisulfite sequencing (RRBS) from participants with HIV prior to initiation of ART (Pre-ART) and without HIV (HIV⁻). (B) Barplots of the number of significant genes with an FDR <0.05 for each assay. (C) Volcano plots depicting differentially expressed genes (DEGs, left), differentially accessible regions (DARs, middle), and differentially methylated loci (DMLs, right) between HIV⁺ and HIV⁻ individuals. Differential features are defined as follows: DEGs and DARs with absolute log₂ fold change ($|\log_2FC| \geq 0.25$) and false discovery rate (FDR) < 0.05 (edgeR), and DMLs with $\geq 20\%$ methylation change and FDR < 0.01 (DSS). Red indicates a positive change (HIV⁺ > HIV⁻) and blue indicates a negative change (HIV⁺ < HIV⁻), with lighter shades representing features below log₂FC or methylation change thresholds but still statistically significant. (D) Heatmaps of z-score normalized expression and accessibility values for selected genes meeting significance thresholds in RNA-seq and ATAC-seq. The RRBS heatmap shows the percentage of methylation change between HIV⁻ and Pre-ART.

Figure 3.2

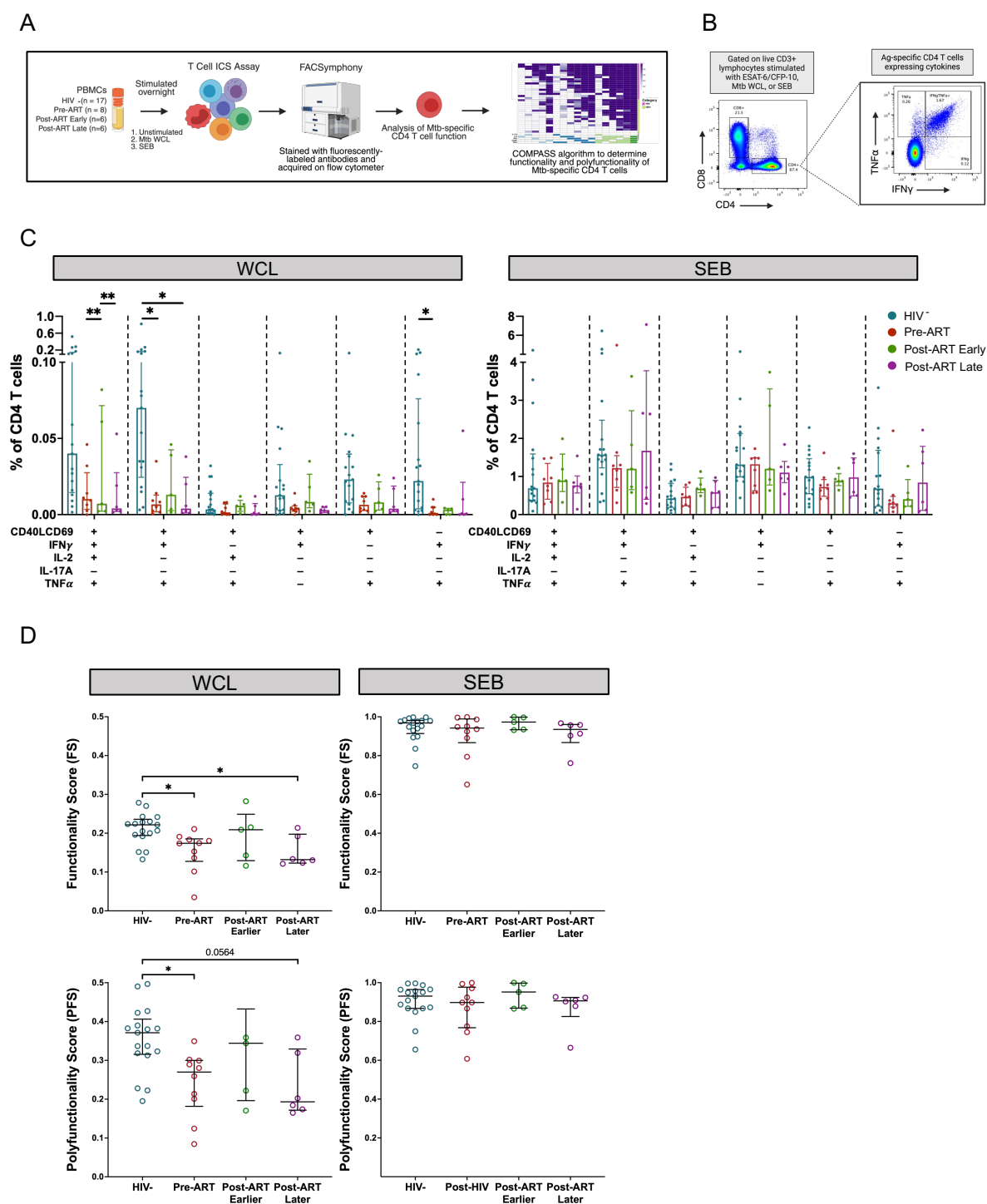


Figure 3.2. HIV infection impairs polyfunctional capacity of Mtb-specific CD4 T cell responses. (A) Experimental design outlining stimulation of PBMCs from people without (HIV⁻; $n = 17$), people with HIV (PWH) prior to initiation of antiretroviral therapy (Pre-ART; $n = 8$), and PWH following early (Post-ART Early; $n = 6$) or late (Post-ART Late; $n = 6$) initiation of ART with *Mycobacterium tuberculosis* (Mtb) whole cell lysate (WCL) or staphylococcal enterotoxin B (SEB), followed by intracellular cytokine staining (ICS). (B) Representative flow cytometry plots showing Mtb-specific CD4 T cells producing TNF and IFN- γ following overnight stimulation with Mtb WCL. (C) Frequencies of polyfunctional CD4 T cell subsets expressing various combinations of CD40L, CD69, IFN- γ , IL-2, IL-17A, and TNF, after background subtraction from unstimulated controls. Data are shown as medians with interquartile ranges (IQR). (D) Functional profiling of Mtb-specific CD4 T cell responses using COMPASS analysis, summarized as functionality scores (FS) and polyfunctionality scores (PFS) for each group. Lines represent the median and IQRs. Statistical significance for group comparisons was assessed using the Mann-Whitney U test (* $p < 0.05$, ** $p \leq 0.01$).

Table 3.2

Table 3.2 Characteristics of study participants.

| | HIV- N = 19 | Pre-ART N = 8 | Post-ART Early N = 6 | Post-ART Late N = 7 |
|---|-----------------|-------------------------------------|-------------------------|------------------------|
| Age (years)^a (Range) | 30 (23-48) | 32 (25-46) | 35 (29-39) | 38 (26-52) |
| Sex (%F) | 100 | 100 | 100 | 100 |
| CD4 count (cells/μL)^a (Range) | ND ^b | 519 (333-991) | 471 (355-895) | 677 (295-1051) |
| Viral Load (HIV-1 RNA copies/mL)^a (Range) | ND ^b | 52554 ^a (5384-149048) | Undetectable-125 | Undetectable |
| Time since HIV seroconversion (months)^a (Range) | ND ^b | 5.5 (3-44) | 23.5 (13-24) | 53 (23-80) |
| Time on ART (months)^a (Range) | ND ^b | ND ^b | 13 (10-22) | 21 (8-49) |

^a Value denotes median.

^b Not done.

Figure 3.3

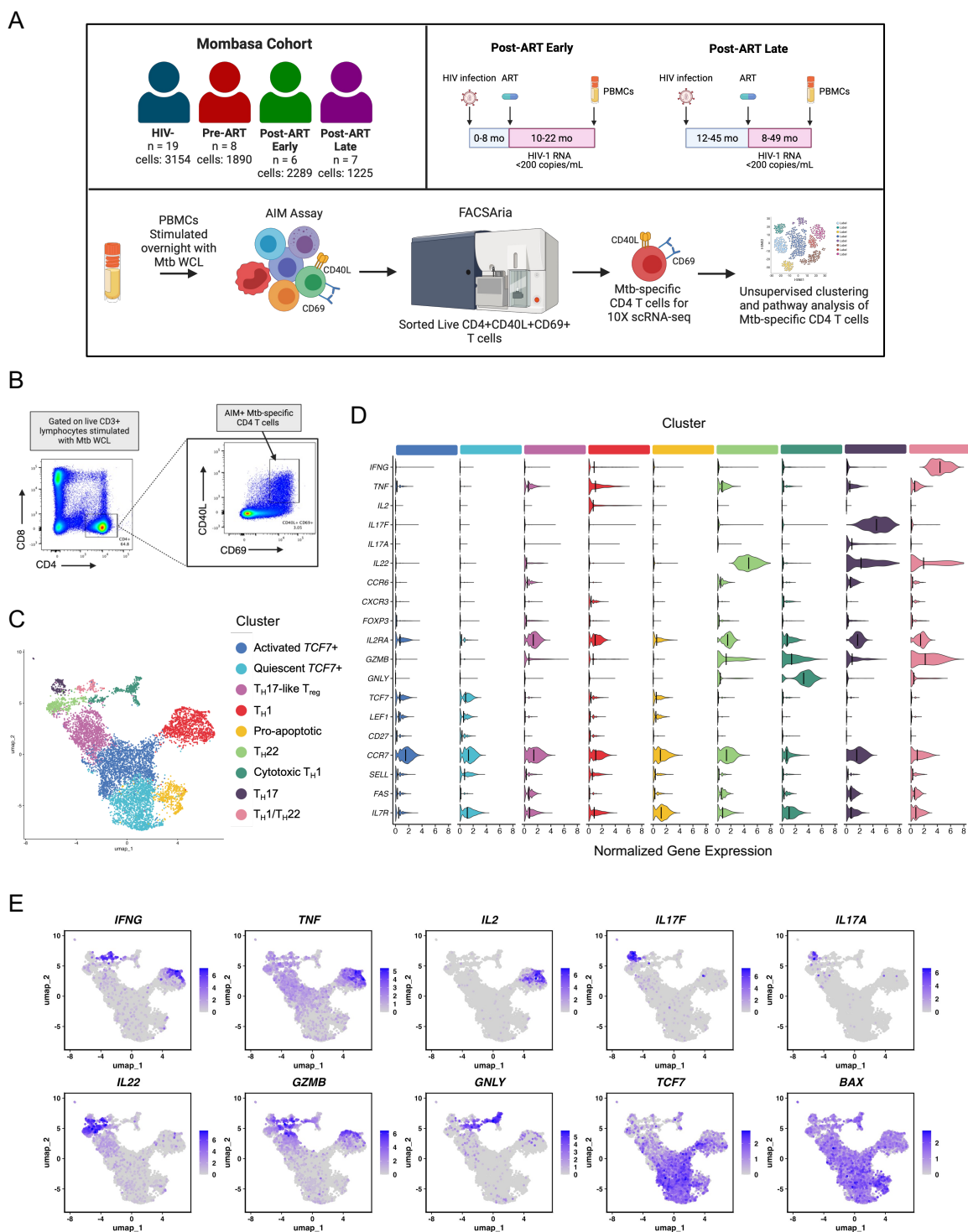


Figure 3.3. ScRNA-seq reveals transcriptionally distinct subsets of Mtb-specific CD4 T cells across HIV and ART status.

(A) Schematic of participant groups: Post-ART Early indicates ART initiation within 6 months of HIV infection; Post-ART Late indicates ART initiation >1 year after infection. PBMCs from people without HIV (HIV⁻), people with HIV (Pre-ART), and those Post-ART Early or Late were stimulated overnight with Mtb WCL in an AIM assay. Live CD3⁺CD8⁻CD4⁺CD40L⁺CD69⁺ T cells were sorted and analyzed by scRNA-seq. Data were processed using Seurat for PCA, DEG analysis, dimensionality reduction, and unsupervised clustering. Cluster identities were assigned using canonical CD4 T cell markers and cluster-specific DEGs. B) Representative FACS plots showing Mtb-specific CD40L⁺CD69⁺ CD4 T cells sorted for scRNA-seq. (C) UMAP projection of 8,558 Mtb-specific CD4 T cells aggregated across all groups. (D) Violin plots displaying normalized gene expression within each cluster for selected markers that were used for cluster annotation. DEGs between clusters were identified using Seurat's FindAllMarkers with the MAST test. (E) UMAP overlays of gene expression used for cluster identification, with purple intensity indicating expression levels.

Figure 3.4

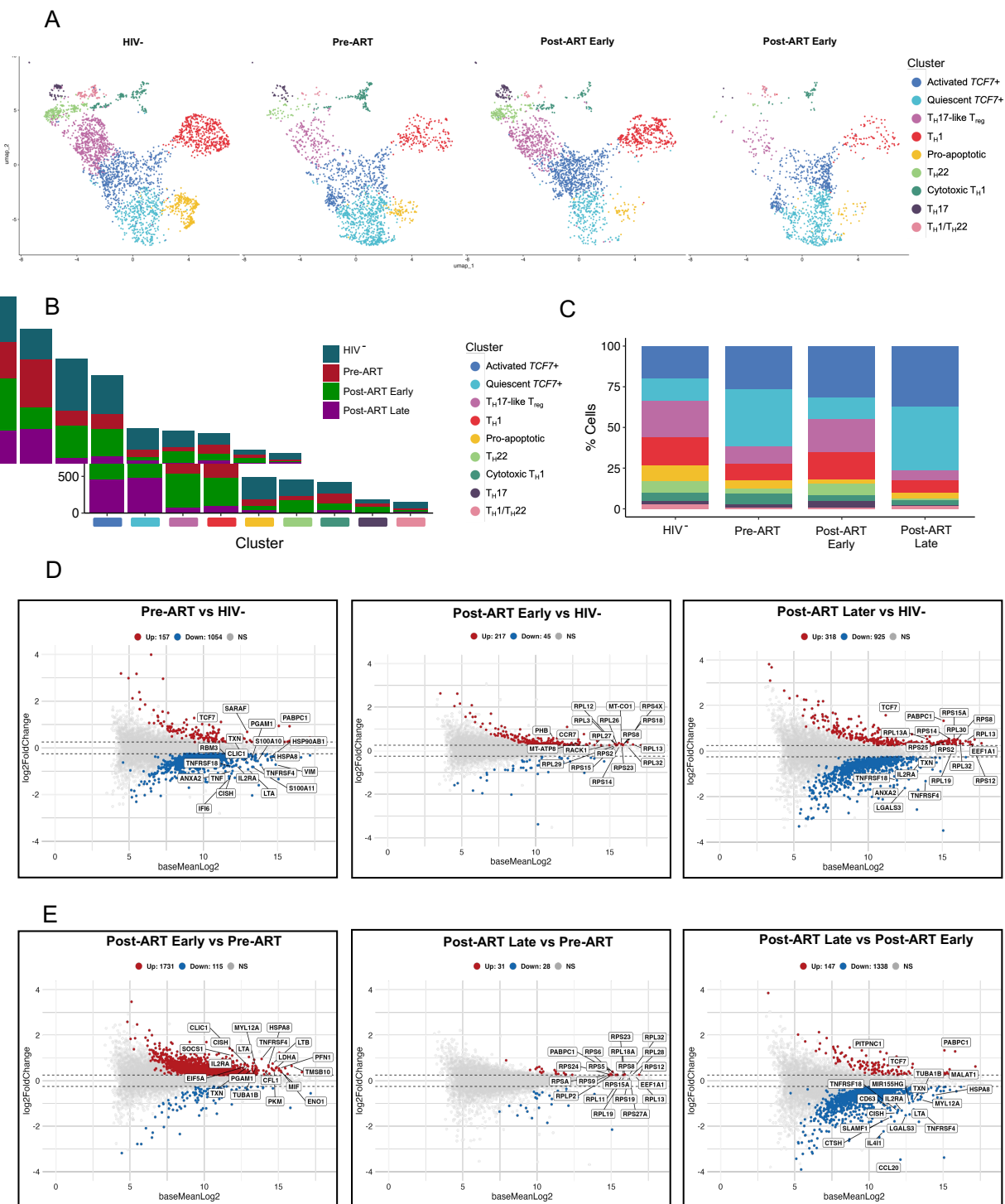


Figure 3.4. HIV infection reshapes the distribution of Mtb-specific CD4 T cell subsets, with early ART initiation preserving functional populations. (A) UMAP projection of scRNA-seq data from Mtb-specific CD4 T cells isolated from people without HIV (HIV⁻) and people with HIV (Pre-ART, Post-ART Early, and Post-ART Late), as described in Figure 3. (B) Proportional distribution of transcriptionally defined CD4 T cell clusters across participant groups, highlighting HIV-associated shifts in subset composition. (C) Total number of cells per cluster stratified by group, demonstrating loss of Th17-like Tregs, Th1, and Th22 subsets and expansion of a quiescent *TCF7*⁺ population following HIV acquisition. (D) MA plot showing log₂FC versus average gene expression of DEGs for each group comparison to HIV⁻ individuals. (E) Additional MA plots comparing Post-ART Early and Post-ART Late to Pre-ART and to each other. Genes significantly upregulated are indicated in red, downregulated in blue, and non-significant (NS) in grey. DEGs were identified using Seurat's FindMarkers function with adjusted $p \leq 0.05$ and $|\log_2FC| > 0.25$.

Figure 3.5

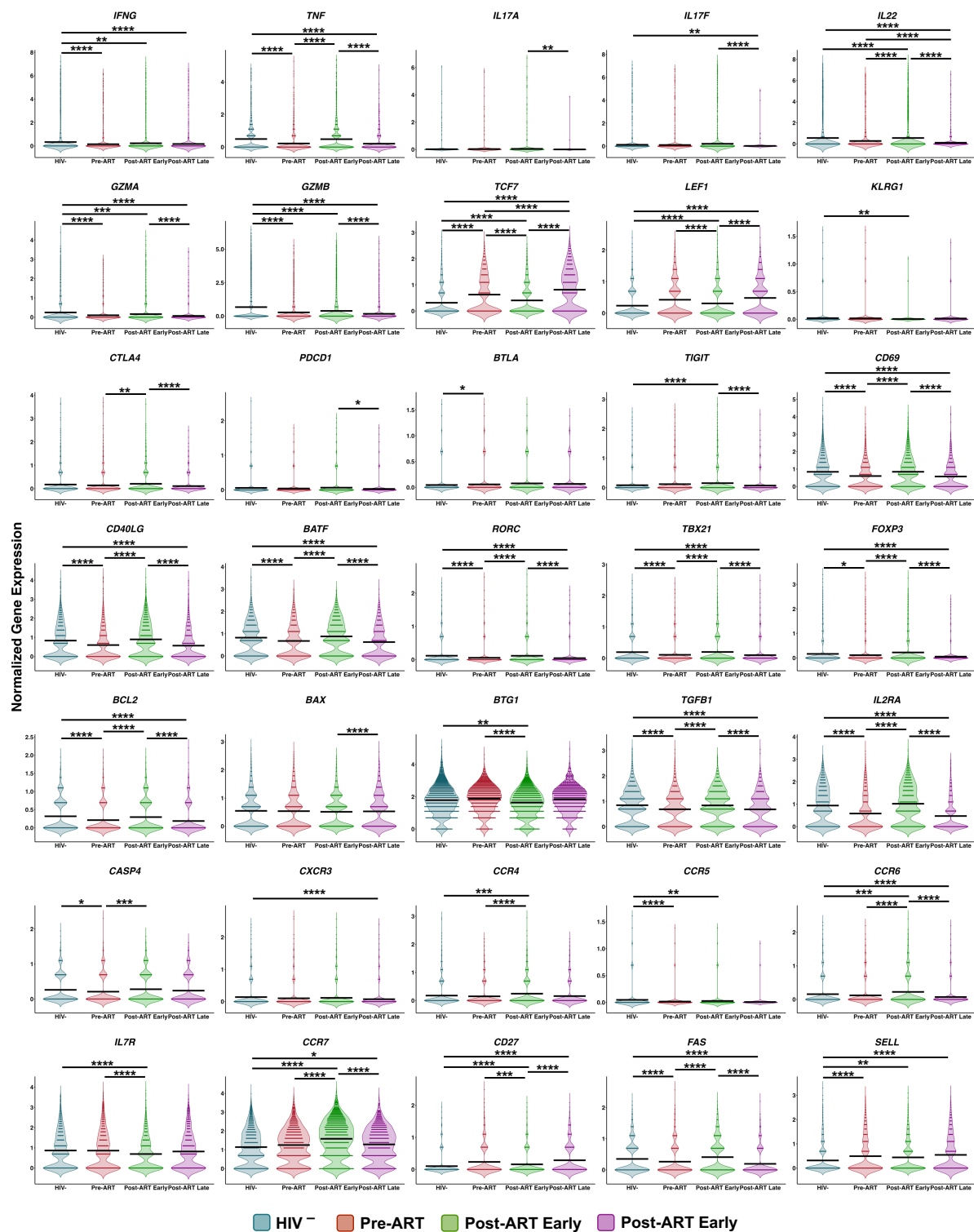


Figure 3.5. Early ART initiation is associated with preservation of effector gene expression in Mtb-specific CD4 T cells. Violin plots illustrating normalized expression levels of select effector DEGs with high fold change and established functional relevance, comparing Mtb-specific CD4 T cells across participant groups. DEGs were identified using Seurat's FindMarkers function with the MAST test (* $p < 0.05$, ** $p \leq 0.01$, *** $p \leq 0.001$, **** $p \leq 0.0001$).

Figure 3.6

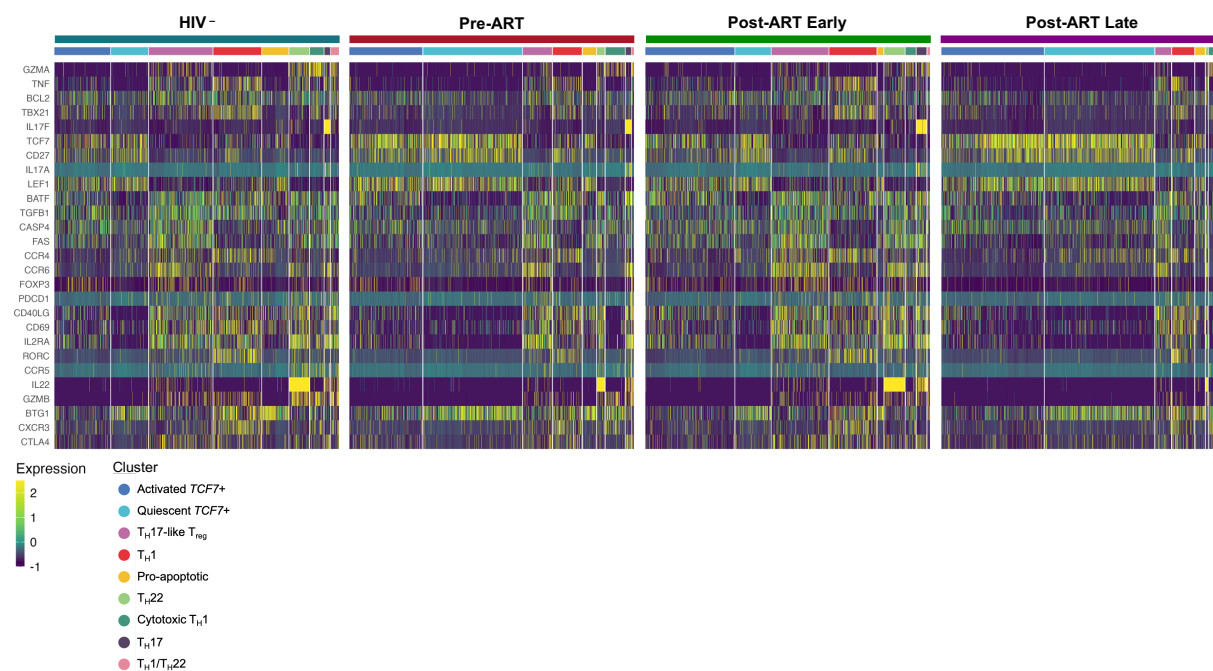
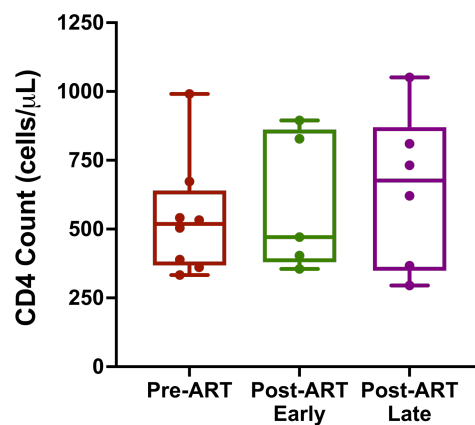


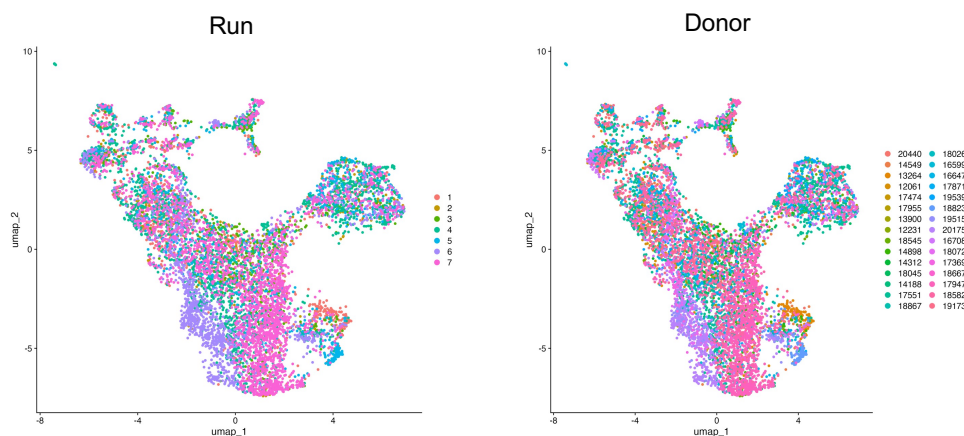
Figure 3.6. Early ART initiation is associated with preservation of unique cluster-specific effector gene expression that is otherwise decreased in people with HIV. Heatmap showing normalized single-cell expression of key effector DEGs across annotated clusters of Mtb-specific CD4 T cells, stratified by HIV status and timing of ART initiation. Each column represents a single cell and each row a gene, with color intensity reflecting gene expression levels. Columns are grouped by cluster and subdivided by participant group (HIV⁻, Pre-ART, Post-ART Early, Post-ART Late), ordered by increasing fold change (FC) from top to bottom. DEGs were identified using Seurat's FindMarkers function with thresholds of adjusted $p \leq 0.05$ and $|\log_2FC| > 0.25$.

3.6 Supplemental Figures

Supplemental Figure 3.1

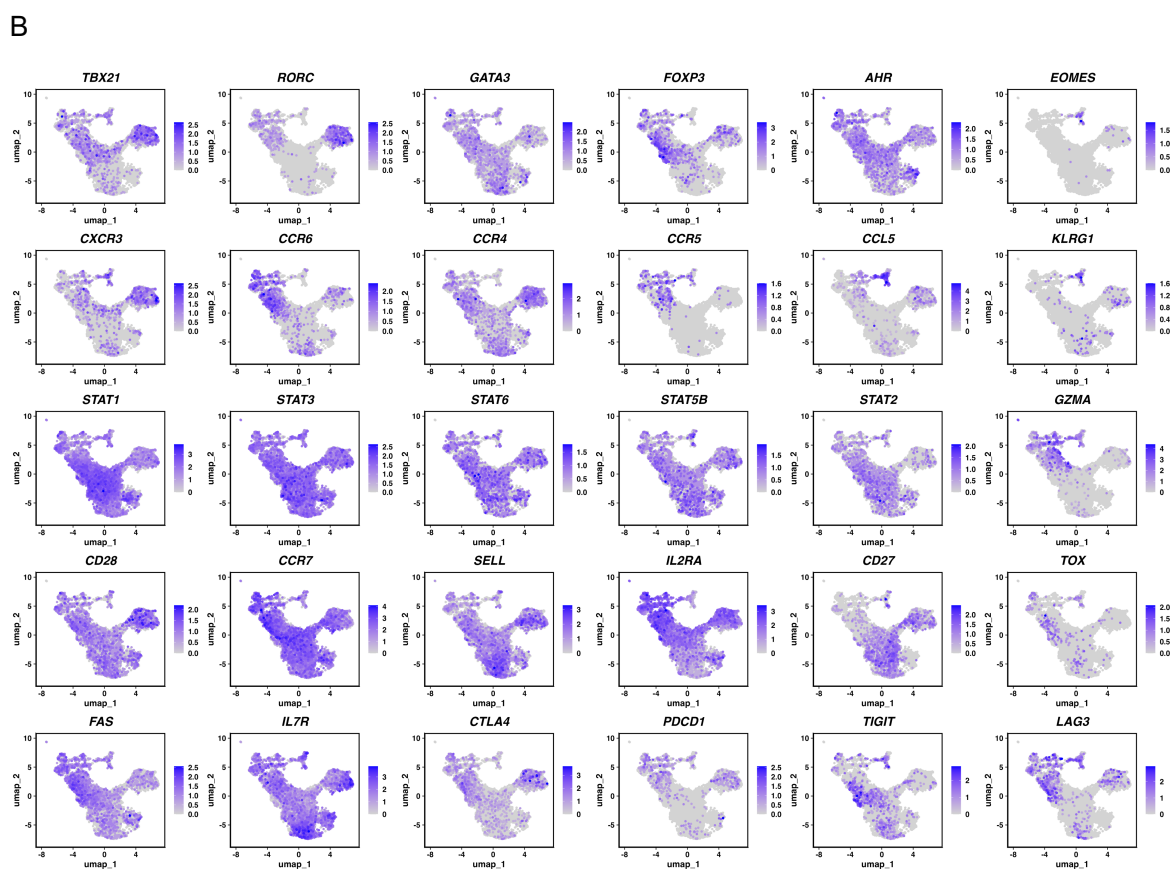
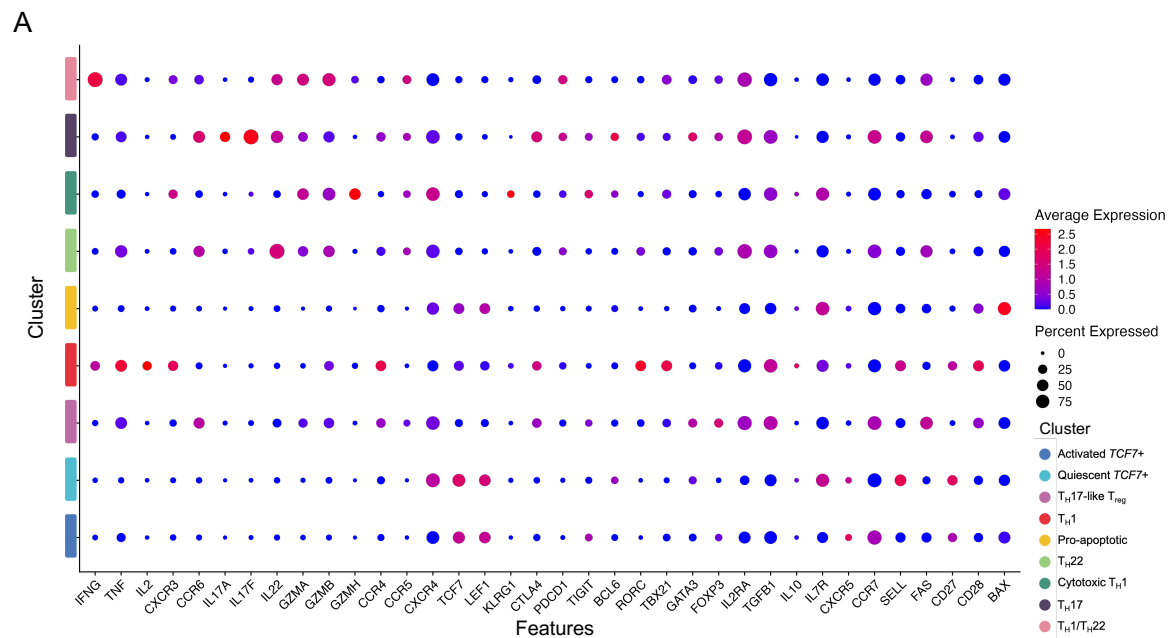


Supplemental Figure 3.1. CD4 T cell counts are consistent across participant groups. Barplots of PWH Pre-HIV (n = 8), Post-ART Early (n = 6), and Post-ART Late (n = 7). Boxes represent the interquartile range, the bar represents the median, and the whiskers represent the range.

Supplemental Figure 3.2

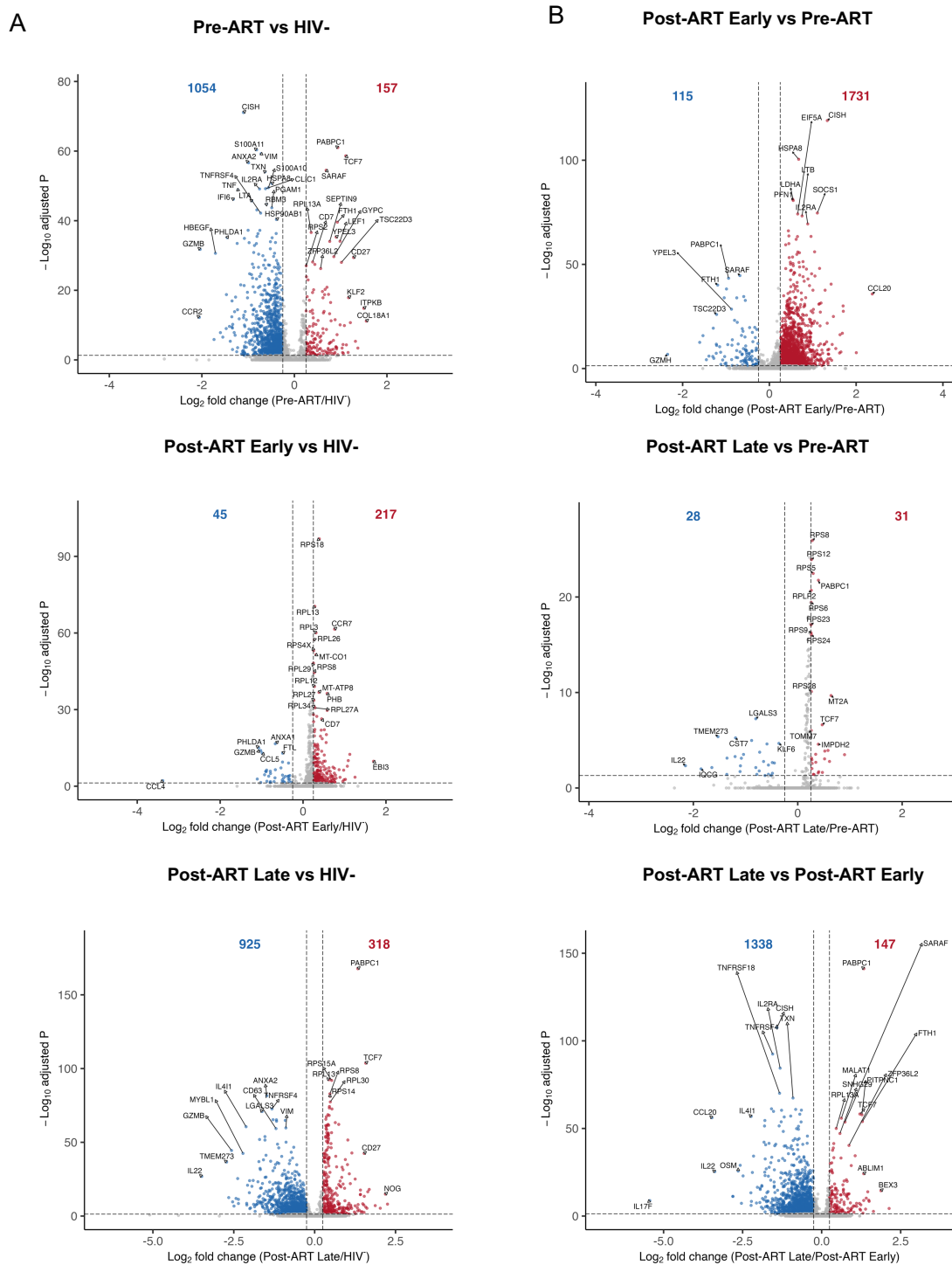
Supplemental Figure 3.2. Sample integration and batch correction for scRNA-seq of Mtb-specific CD4 T cells. UMAP visualization of integrated single-cell transcriptomes colored by experimental run (left) and by participant (right), after batch correction using a donor covariate and normalization with SCTransform in Seurat, demonstrating successful data integration across individuals and experimental batches.

Supplemental Figure 3.3



Supplemental Figure 3.3. Cluster-level gene expression and annotation of Mtb-specific CD4 T cell subsets. (A) Dot plot displaying normalized average expression of canonical helper T cell lineage and differentiation markers across identified clusters from scRNA-seq data. Dot color represents the scaled average expression level of each gene within a given cluster, while dot size indicates the proportion of cells in the cluster expressing that gene. (B) UMAP projections overlaid with expression patterns of select genes used for cluster annotation. Purple shading reflects the relative expression intensity of each gene, facilitating identification of transcriptional differences between clusters.

Supplemental Figure 3.4



Supplemental Figure 3.4. Volcano plots of differentially expressed genes between groups.

Volcano plots depicting DEGs from Mtb-specific CD4 T cells across all group comparisons as detailed in Figure 4. Each plot shows \log_2 FC versus $-\log_{10}$ p -value, with significantly upregulated genes highlighted in red and downregulated genes in blue. Non-significant genes are shown in grey. DEGs were identified using Seurat's FindMarkers function, applying thresholds of adjusted $p \leq 0.05$ and $|\log_2\text{FC}| > 0.25$. Volcano plots in panel A visually complement the MA plots in Figure 4D, whereas volcano plots in panel B complement the MA plots in Figure 4E.

CHAPTER 4. Discussion

4.1 Summary

The interplay between HIV and TB represents a significant challenge in global health, with HIV infection being the most potent risk factor for TB reactivation and disease progression [10]. This increased susceptibility is partially driven by the disruption of Mtb-specific CD4 T cell responses, particularly Th1 and Th17, which are essential, but not sufficient for protective immunity against Mtb^{9,65,97}. The integrated multi-omic cross-sectional and longitudinal study presented in this dissertation provides novel and comprehensive insight into how HIV infection and timing of ART initiation impact the functional and transcriptional profiles of Mtb-specific CD4 T cells. Together, the data offer a mechanistic framework for understanding the immune dysregulation that underpins the heightened TB risk in PWH.

In this dissertation, we examined the immunological changes of Mtb-specific CD4 T cell responses in HIV through both longitudinal and cross-sectional analyses, utilizing a robust profiling approach. In the longitudinal study detailed in Chapter 2, we uncovered changes in Mtb-specific CD4 T cells before and after HIV acquisition within the same individuals, providing a unique opportunity to assess early immune alterations without confounding from inter-individual variability. Functional assessments revealed that HIV infection significantly impaired the frequency and polyfunctionality of Mtb-specific CD4 T cells. Single-cell transcriptomic analysis of Mtb-specific CD4 T cells identified a conserved architecture comprising multiple functional subsets. However, HIV infection led to a depletion of effector subsets, such as Th1 and Th17 cells, and a concurrent expansion of less differentiated, stem-like populations. These shifts in cellular composition were accompanied by a general reduction in transcriptional activity and disruption of pathways associated with immune activation, migration, proliferation, and cytotoxic

responses.

In a complementary cross-sectional study, we compared Mtb-specific CD4 T cell responses across people without HIV and PWH who were either ART-naïve or had initiated ART early or late after infection. This design allowed us to examine how ART timing affected influences Mtb-specific CD4 T cell responses. Functional profiling showed reduced cytokine production and polyfunctional responses in ART-naïve individuals, complimenting the longitudinal findings, and those with delayed ART, while early-treated individuals retained responses more similar to those of people without HIV. Transcriptomic analysis further revealed that HIV-associated shifts in CD4 T cell states were more pronounced in those initiating ART later, reinforcing the critical window in which therapeutic intervention may mitigate immune dysfunction.

Our parallel analysis of resting bulk CD4 T cells using RNA-seq, ATAC-seq, and DNA methylation profiling demonstrated that epigenetic remodeling occurs early after HIV acquisition, even in the absence of widespread transcriptional and chromatin accessibility changes. Notably, we observed some shifts in DNA methylation, suggesting a priming or silencing of future transcriptional programs. However, out of >44 million loci detected, only 44,291 were differentially methylated, which is approximately 1% of loci. This dissociation between methylation and gene expression may represent a latent immune dysfunction that only becomes apparent upon antigen stimulation or a CD4 T cell memory-specific affect that is only clearly resolved in purified memory populations. These findings raise critical questions about the reversibility of these epigenetic changes in HIV.

In both the longitudinal and cross-sectional studies, HIV infection was associated with a notable depletion of key Mtb-specific CD4 T cell subsets, particularly Th1 and Th17 cells, which are critical for protective immunity against Mtb. In the cross-sectional cohort, we further observed a reduction

in Th17-like Tregs in PWH prior to initiation of ART, with these levels also lower in individuals who initiated ART at later stages. The depletion of this subset may have important implications for immune regulation and mucosal immunity, as Th17-like Tregs are known to balance effector responses and help maintain mucosal barrier function¹⁶⁵. The progressive loss of these cells in PWH suggests a widespread disruption in CD4 T cell subset diversity and function, contributing not only to impaired pathogen control but also to chronic immune activation and dysregulation.

4.2 Implications

These findings significantly expand our understanding of how HIV disrupts Mtb-specific CD4 T cell immunity. The longitudinal data provide direct evidence that HIV induces early functional and transcriptional impairments in antigen-specific CD4 T cells, including a loss of effector responses critical for controlling Mtb infection^{2,4,22,116}. The cross-sectional study complements this by showing that ART timing is a decisive factor in preserving or restoring these immune functions. Together, these results underscore the importance of initiating ART as early as possible after HIV diagnosis, not only to suppress viral replication but also to preserve the integrity of pathogen-specific immune responses^{77,81,83}.

Furthermore, the observed expansion of stem-like T cell populations and reduced effector function suggest that HIV infection skews the differentiation trajectory of Mtb-specific CD4 T cells. These stem-like cells may retain some capacity for self-renewal, but their failure to mature into functional effectors may contribute to TB susceptibility. The identification of epigenetic alterations also suggests that immune dysfunction begins before overt clinical symptoms, presenting a window for intervention. Understanding and targeting the pathways that underlie these epigenetic and transcriptional changes could lead to new therapeutic approaches aimed at enhancing immune resilience in PWH. For example, cytokine therapies might be useful in 'shocking' these stem-like

cells to differentiate into effector populations, thereby restoring Mtb-specific responses.

In conclusion, this body of work provides the first longitudinal, single-cell resolution analysis of how HIV impacts Mtb-specific CD4 T cell immunity. It reveals that HIV induces a shift toward less differentiated, transcriptionally restrained T cell states, and that early ART initiation can preserve the transcriptional program and functional capacity. These findings not only enhance our understanding of HIV/TB immunopathogenesis but also inform strategies for timing ART, designing therapeutic interventions, and developing predictive biomarkers aimed at mitigating TB risk in PWH.

4.3 Future Directions

Building on these insights, future research should investigate whether the stem-like Mtb-specific CD4 T cells observed in PWH can be directed toward functional differentiation with therapeutic cues. Delineating the molecular signals that promote or inhibit this process could inform interventions that restore protective immunity. Several immunomodulatory strategies are currently under investigation to enhance T cell function, including the use of checkpoint inhibitors (e.g., anti-PD-1, anti-CTLA-4), cytokine therapies (e.g., IL-7, IL-15), and metabolic reprogramming agents that may help reverse T cell exhaustion or enhance effector differentiation. These interventions, many of which are being tested in cancer and chronic infections, may have translational relevance in the context of HIV-TB co-infection and warrant future evaluation.

The role of ART timing should also be explored in greater depth, including its impact on tissue-resident immune responses, particularly within the lung, where TB immunity is most relevant. Prior studies have indicated discordance between blood and tissue immune profiles¹⁴⁹ and it remains unclear whether early ART similarly preserves localized immune function.

Fully uncovering the effects of ART timing on the preservation of CD4 T cell diversity, function,

and quantity would benefit from prospective studies involving individuals with precisely known timing of HIV exposure and infection. Ideally, such studies would involve participants initiating ART at varying time points while maintaining a uniform duration of HIV infection across groups, allowing for clearer dissection of the relative impacts of infection duration versus ART initiation on immune outcomes. While new prospective studies that delay ART initiation are not feasible due to current treatment guidelines advocating immediate ART upon diagnosis, existing cohorts such as the Mombasa Cohort may hold archived biospecimens suitable for retrospective analyses of these questions. Additionally, networks like the HIV Vaccine Trials Network and the AIDS Clinical Trials Group provide invaluable repositories of longitudinal samples that could support such investigations. Leveraging these resources could offer a more refined understanding of how ART timing influences CD4 T cell preservation and dysfunction, as well as aid in the identification of biomarkers predictive of immune resilience and response to early intervention strategies.

Although this dissertation provided transcriptional evidence for HIV-induced dysfunction in Mtb-specific CD4 T cells, we did not directly evaluate whether these changes were epigenetically programmed, as ATAC-seq or RRBS was not performed on antigen-specific cells. Future studies should address this important gap by applying epigenetic profiling techniques to Mtb-specific CD4 T cells, which could reveal whether observed gene expression differences reflect stable, heritable changes in chromatin accessibility or methylation. Such insights would be critical for determining the potential reversibility of HIV-associated immune alterations and identifying durable therapeutic targets.

Moreover, while this work has focused on CD4 T cells due to their central role in TB immunity, a more comprehensive understanding of the host response in PWH will require future studies to evaluate the contributions of other immune cell types. This includes CD8 T cells, non-conventional T cells such as MAIT and $\gamma\delta$ T cells, and innate populations like NK cells and monocyte-derived

macrophages. These cell types also play essential roles in controlling Mtb infection, and their function may likewise be compromised by HIV infection and modulated by ART timing. Employing a systems immunology approach that captures the full spectrum of cellular responses will be essential to fully understand the immune dysregulation that predisposes PWH to TB and to inform integrated therapeutic strategies.

In addition, future studies should evaluate the long-term effects of HIV on CD4 T cell responses across a broader array of antigens to determine whether the dysregulation observed in Mtb-specific T cells is antigen-specific or reflects a generalized immune dysfunction. The inclusion of tissue-specific analyses and longitudinal epigenetic profiling would help clarify whether the changes observed are reversible and how they correlate with disease outcomes. Expanding these approaches to larger and more diverse cohorts will enhance our understanding of HIV-associated immune dysregulation and may support the development of predictive biomarkers for TB risk in PWH.

Ultimately, integrating functional, transcriptional, and epigenetic analyses across both longitudinal and cross-sectional designs strengthens our understanding of the multifaceted impact of HIV on host CD4 T cell immunity. These findings emphasize not only the urgency of early ART but also the necessity of comprehensive immune monitoring to capture the nuanced effects of HIV on antigen-specific responses. By elucidating how HIV disrupts immune equilibrium at multiple levels and identifying the temporal windows where interventions can be most effective, this work lays a foundation for precision-based strategies aimed at restoring durable immune protection. These insights are especially critical in the global fight against TB, where HIV co-infection remains a major obstacle to disease control and elimination.

CHAPTER 5. References

- 1 *Coronavirus (COVID-19) dashboard*, <<https://covid19.who.int/>> (
- 2 Global tuberculosis report 2024. (World Health Organization, Geneva, 2024).
- 3 *WHO consolidated guidelines on tuberculosis (Module 1- Prevention): Tuberculosis preventative treatment*. second edition edn, 133 (World Health Organization, 2024).
- 4 Sutherland, I. Recent studies in the epidemiology of tuberculosis, based on the risk of being infected with tubercle bacilli. *Adv Tuberc Res* **19**, 1-63 (1976).
- 5 Menzies, N. A. *et al.* Progression from latent infection to active disease in dynamic tuberculosis transmission models: a systematic review of the validity of modelling assumptions. *Lancet Infect Dis* **18**, e228-e238 (2018). [https://doi.org:10.1016/S1473-3099\(18\)30134-8](https://doi.org:10.1016/S1473-3099(18)30134-8)
- 6 Tiemersma, E. W., van der Werf, M. J., Borgdorff, M. W., Williams, B. G. & Nagelkerke, N. J. Natural history of tuberculosis: duration and fatality of untreated pulmonary tuberculosis in HIV negative patients: a systematic review. *PLoS One* **6**, e17601 (2011). <https://doi.org:10.1371/journal.pone.0017601>
- 7 Sonnenberg, P. *et al.* How soon after infection with HIV does the risk of tuberculosis start to increase? A retrospective cohort study in South African gold miners. *J Infect Dis* **191**, 150-158 (2005). <https://doi.org:10.1086/426827>
- 8 (2024). WHO consolidated guidelines on tuberculosis (Module 4- Treatment): drug-sensitive and drug-resistant tuberculosis treatment, World Health Organization.

- 9 Narasimhan, P., Wood, J., Macintyre, C. R. & Mathai, D. Risk factors for tuberculosis. *Pulm Med* **2013**, 828939 (2013). <https://doi.org:10.1155/2013/828939>
- 10 Petruccioli, E. *et al.* Correlates of tuberculosis risk: predictive biomarkers for progression to active tuberculosis. *Eur Respir J* **48**, 1751-1763 (2016).
<https://doi.org:10.1183/13993003.01012-2016>
- 11 Scriba, T. J., Maseeme, M., Young, C., Taylor, L. & Leslie, A. J. Immunopathology in human tuberculosis. *Sci Immunol* **9**, eado5951 (2024).
<https://doi.org:10.1126/sciimmunol.ado5951>
- 12 Golden, M. P. & Vikram, H. R. Extrapulmonary tuberculosis: an overview. *Am Fam Physician* **72**, 1761-1768 (2005).
- 13 Ernst, J. D. The immunological life cycle of tuberculosis. *Nature Reviews Immunology* **12**, 581-591 (2012). <https://doi.org:10.1038/nri3259>
- 14 *Tuberculosis (TB): Clinical overview for health care providers.*
- 15 McKinney, J. D. *et al.* Persistence of Mycobacterium tuberculosis in macrophages and mice requires the glyoxylate shunt enzyme isocitrate lyase. *Nature* **406**, 735-738 (2000).
<https://doi.org:10.1038/35021074>
- 16 Fenton, M. J. & Vermeulen, M. W. Immunopathology of tuberculosis: roles of macrophages and monocytes. *Infect Immun* **64**, 683-690 (1996).
<https://doi.org:10.1128/iai.64.3.683-690.1996>
- 17 Cambier, C. J., Falkow, S. & Ramakrishnan, L. Host evasion and exploitation schemes of

Mycobacterium tuberculosis. *Cell* **159**, 1497-1509 (2014).

<https://doi.org:10.1016/j.cell.2014.11.024>

18 Cadena, A. M., Fortune, S. M. & Flynn, J. L. Heterogeneity in tuberculosis. *Nat Rev Immunol* **17**, 691-702 (2017). <https://doi.org:10.1038/nri.2017.69>

19 Russell, D. G., Barry, C. E., 3rd & Flynn, J. L. Tuberculosis: what we don't know can, and does, hurt us. *Science* **328**, 852-856 (2010). <https://doi.org:10.1126/science.1184784>

20 Pai, M. *et al.* Tuberculosis. *Nature Reviews Disease Primers* **2**, 16076 (2016). <https://doi.org:10.1038/nrdp.2016.76>

21 Cohen, S. B., Gern, B. H. & Urdahl, K. B. The Tuberculous Granuloma and Preexisting Immunity. *Annual Review of Immunology* **40**, 589-614 (2022).

<https://doi.org:https://doi.org/10.1146/annurev-immunol-093019-125148>

22 Flynn, J. L. & Chan, J. Immune cell interactions in tuberculosis. *Cell* **185**, 4682-4702 (2022). <https://doi.org:10.1016/j.cell.2022.10.025>

23 Kaplan, G. *et al.* Mycobacterium tuberculosis growth at the cavity surface: a microenvironment with failed immunity. *Infect Immun* **71**, 7099-7108 (2003).

<https://doi.org:10.1128/iai.71.12.7099-7108.2003>

24 Esmail, H. *et al.* Characterization of progressive HIV-associated tuberculosis using 2-deoxy-2-[(18)F]fluoro-D-glucose positron emission and computed tomography. *Nat Med* **22**, 1090-1093 (2016). <https://doi.org:10.1038/nm.4161>

25 García de Viedma, D., Marín, M., Ruiz Serrano, M. J., Alcalá, L. & Bouza, E. Polyclonal

- and Compartmentalized Infection by Mycobacterium tuberculosis in Patients with Both Respiratory and Extrapulmonary Involvement. *The Journal of Infectious Diseases* **187**, 695-699 (2003). <https://doi.org:10.1086/368368>
- 26 Dorman, S. E. *et al.* Xpert MTB/RIF Ultra for detection of Mycobacterium tuberculosis and rifampicin resistance: a prospective multicentre diagnostic accuracy study. *Lancet Infect Dis* **18**, 76-84 (2018). [https://doi.org:10.1016/s1473-3099\(17\)30691-6](https://doi.org:10.1016/s1473-3099(17)30691-6)
- 27 Suzana, S., Shanmugam, S., Latha, P. N. S. & Michael, J. S. Molecular genotyping to differentiate endogenous reactivation and exogenous reinfection of recurrent tuberculosis. *J Clin Tuberc Other Mycobact Dis* **13**, 17-21 (2018). <https://doi.org:10.1016/j.jctube.2018.10.001>
- 28 Pai, M., Riley, L. W. & Colford, J. M., Jr. Interferon-gamma assays in the immunodiagnosis of tuberculosis: a systematic review. *Lancet Infect Dis* **4**, 761-776 (2004). [https://doi.org:10.1016/s1473-3099\(04\)01206-x](https://doi.org:10.1016/s1473-3099(04)01206-x)
- 29 Villar-Hernández, R. *et al.* Tuberculosis: current challenges and beyond. *Breathe (Sheff)* **19**, 220166 (2023). <https://doi.org:10.1183/20734735.0166-2022>
- 30 Boehme, C. C. *et al.* Rapid molecular detection of tuberculosis and rifampin resistance. *N Engl J Med* **363**, 1005-1015 (2010). <https://doi.org:10.1056/NEJMoa0907847>
- 31 Gupta, A., Wood, R., Kaplan, R., Bekker, L.-G. & Lawn, S. D. Tuberculosis Incidence Rates during 8 Years of Follow-Up of an Antiretroviral Treatment Cohort in South Africa: Comparison with Rates in the Community. *PLOS ONE* **7**, e34156 (2012). <https://doi.org:10.1371/journal.pone.0034156>

- 32 Narayanan, S. *et al.* Impact of HIV infection on the recurrence of tuberculosis in South India. *J Infect Dis* **201**, 691-703 (2010). <https://doi.org:10.1086/650528>
- 33 Mezouar, S., Diarra, I., Roudier, J., Desnues, B. & Mege, J. L. Tumor Necrosis Factor-Alpha Antagonist Interferes With the Formation of Granulomatous Multinucleated Giant Cells: New Insights Into Mycobacterium tuberculosis Infection. *Front Immunol* **10**, 1947 (2019). <https://doi.org:10.3389/fimmu.2019.01947>
- 34 Church, L. W. P., Chopra, A. & Judson, M. A. Paradoxical Reactions and the Immune Reconstitution Inflammatory Syndrome. *Microbiology Spectrum* **5**, 10.1128/microbiolspec.tnmi1127-0033-2016 (2017). <https://doi.org:doi:10.1128/microbiolspec.tnmi7-0033-2016>
- 35 Franco, J. V. *et al.* Undernutrition as a risk factor for tuberculosis disease. *Cochrane Database Syst Rev* **6**, Cd015890 (2024). <https://doi.org:10.1002/14651858.CD015890.pub2>
- 36 Park, J. *et al.* Association of duration of undernutrition with occurrence of tuberculosis. *BMC Public Health* **22**, 2392 (2022). <https://doi.org:10.1186/s12889-022-14876-1>
- 37 Antonucci, G., Girardi, E., Raviglione, M. C. & Ippolito, G. Risk factors for tuberculosis in HIV-infected persons. A prospective cohort study. The Gruppo Italiano di Studio Tuberculosis e AIDS (GISTA). *Jama* **274**, 143-148 (1995). <https://doi.org:10.1001/jama.274.2.143>
- 38 Sterling, T. R. *et al.* Three months of rifapentine and isoniazid for latent tuberculosis infection. *N Engl J Med* **365**, 2155-2166 (2011). <https://doi.org:10.1056/NEJMoa1104875>
- 39 Shepardson, D. *et al.* Cost-effectiveness of a 12-dose regimen for treating latent

tuberculous infection in the United States. *Int J Tuberc Lung Dis* **17**, 1531-1537 (2013).

<https://doi.org:10.5588/ijtld.13.0423>

40 Assefa, Y., Assefa, Y., Woldeyohannes, S., Hamada, Y. & Getahun, H. 3-month daily rifampicin and isoniazid compared to 6- or 9-month isoniazid for treating latent tuberculosis infection in children and adolescents less than 15 years of age: an updated systematic review.

Eur Respir J **52** (2018). <https://doi.org:10.1183/13993003.00395-2018>

41 Menzies, D. *et al.* Four Months of Rifampin or Nine Months of Isoniazid for Latent Tuberculosis in Adults. *N Engl J Med* **379**, 440-453 (2018).

<https://doi.org:10.1056/NEJMoa1714283>

42 Paton, N. I. *et al.* Treatment Strategy for Rifampin-Susceptible Tuberculosis. *New England Journal of Medicine* **388**, 873-887 (2023). <https://doi.org:doi:10.1056/NEJMoa2212537>

43 Dookie, N. *et al.* The Changing Paradigm of Drug-Resistant Tuberculosis Treatment: Successes, Pitfalls, and Future Perspectives. *Clin Microbiol Rev* **35**, e0018019 (2022).

<https://doi.org:10.1128/cmr.00180-19>

44 Dorman, S. E. *et al.* High-dose rifapentine with or without moxifloxacin for shortening treatment of pulmonary tuberculosis: Study protocol for TBTC study 31/ACTG A5349 phase 3 clinical trial. *Contemporary Clinical Trials* **90**, 105938 (2020).

<https://doi.org:https://doi.org/10.1016/j.cct.2020.105938>

45 Pettit, A. C. *et al.* Rifapentine With and Without Moxifloxacin for Pulmonary Tuberculosis in People With Human Immunodeficiency Virus (S31/A5349). *Clinical Infectious*

Diseases **76**, e580-e589 (2022). <https://doi.org:10.1093/cid/ciac707>

46 Dorman, S. E. *et al.* Four-Month Rifapentine Regimens with or without Moxifloxacin for Tuberculosis. *New England Journal of Medicine* **384**, 1705-1718 (2021).

<https://doi.org:10.1056/NEJMoa2033400>

47 Saluzzo, F., Adepoju, V. A., Duarte, R., Lange, C. & Phillips, P. P. J. Treatment-shortening regimens for tuberculosis: updates and future priorities. *Breathe (Sheff)* **19**, 230028 (2023). <https://doi.org:10.1183/20734735.0028-2023>

48 Kroon, E. E. *et al.* An observational study identifying highly tuberculosis-exposed, HIV-1-positive but persistently TB, tuberculin and IGRA negative persons with M. tuberculosis specific antibodies in Cape Town, South Africa. *EBioMedicine* **61**, 103053 (2020).

<https://doi.org:10.1016/j.ebiom.2020.103053>

49 Azevedo-Pereira, J. M. *et al.* HIV/Mtb Co-Infection: From the Amplification of Disease Pathogenesis to an “Emerging Syndemic”. *Microorganisms* **11**, 853 (2023).

50 Getahun, H., Gunneberg, C., Granich, R. & Nunn, P. HIV Infection—Associated Tuberculosis: The Epidemiology and the Response. *Clinical Infectious Diseases* **50**, S201-S207 (2010). <https://doi.org:10.1086/651492>

51 Sterling, T. R., Pham, P. A. & Chaisson, R. E. HIV Infection—Related Tuberculosis: Clinical Manifestations and Treatment. *Clinical Infectious Diseases* **50**, S223-S230 (2010).

<https://doi.org:10.1086/651495>

52 Aaron, L. *et al.* Tuberculosis in HIV-infected patients: a comprehensive review. *Clinical*

Microbiology and Infection **10**, 388-398 (2004). [https://doi.org:https://doi.org/10.1111/j.1469-0691.2004.00758.x](https://doi.org/https://doi.org/10.1111/j.1469-0691.2004.00758.x)

53 Foreman, T. W. *et al.* CD4 T cells are rapidly depleted from tuberculosis granulomas following acute SIV co-infection. *Cell Rep* **39**, 110896 (2022).

<https://doi.org/10.1016/j.celrep.2022.110896>

54 Collins, K. R., Quiñones-Mateu, M. E., Toossi, Z. & Arts, E. J. Impact of tuberculosis on HIV-1 replication, diversity, and disease progression. *AIDS Rev* **4**, 165-176 (2002).

55 Whalen, C. *et al.* Accelerated course of human immunodeficiency virus infection after tuberculosis. *Am J Respir Crit Care Med* **151**, 129-135 (1995).

<https://doi.org/10.1164/ajrccm.151.1.7812542>

56 Goletti, D. *et al.* Effect of Mycobacterium tuberculosis on HIV replication. Role of immune activation. *J Immunol* **157**, 1271-1278 (1996).

57 Xun, J. *et al.* Mycobacterium tuberculosis co-infection is associated with increased surrogate marker of the HIV reservoir. *AIDS Research and Therapy* **17**, 63 (2020).

<https://doi.org/10.1186/s12981-020-00320-0>

58 Rosas-Taraco, A. G., Arce-Mendoza, A. Y., Caballero-Olín, G. & Salinas-Carmona, M. C. Mycobacterium tuberculosis Upregulates Coreceptors CCR5 and CXCR4 While HIV Modulates CD14 Favoring Concurrent Infection. *AIDS Research and Human Retroviruses* **22**, 45-51 (2006). <https://doi.org/10.1089/aid.2006.22.45>

59 He, X., Eddy, J. J., Jacobson, K. R., Henderson, A. J. & Agosto, L. M. Enhanced Human

Immunodeficiency Virus-1 Replication in CD4⁺ T Cells Derived From Individuals With Latent Mycobacterium tuberculosis Infection. *J Infect Dis* **222**, 1550-1560 (2020).

<https://doi.org:10.1093/infdis/jiaa257>

60 Wong, M. E., Jaworowski, A. & Hearps, A. C. The HIV Reservoir in Monocytes and Macrophages. *Frontiers in Immunology* **Volume 10 - 2019** (2019).

<https://doi.org:10.3389/fimmu.2019.01435>

61 Liu, C. H., Liu, H. & Ge, B. Innate immunity in tuberculosis: host defense vs pathogen evasion. *Cellular & Molecular Immunology* **14**, 963-975 (2017).

<https://doi.org:10.1038/cmi.2017.88>

62 O'Garra, A. *et al.* The immune response in tuberculosis. *Annu Rev Immunol* **31**, 475-527 (2013). <https://doi.org:10.1146/annurev-immunol-032712-095939>

63 Flynn, J. L. *et al.* An essential role for interferon gamma in resistance to Mycobacterium tuberculosis infection. *J Exp Med* **178**, 2249-2254 (1993).

<https://doi.org:10.1084/jem.178.6.2249>

64 Flynn, J. L. *et al.* Tumor necrosis factor-alpha is required in the protective immune response against Mycobacterium tuberculosis in mice. *Immunity* **2**, 561-572 (1995).

[https://doi.org:10.1016/1074-7613\(95\)90001-2](https://doi.org:10.1016/1074-7613(95)90001-2)

65 Jasenosky, L. D., Scriba, T. J., Hanekom, W. A. & Goldfeld, A. E. T cells and adaptive immunity to Mycobacterium tuberculosis in humans. *Immunol Rev* **264**, 74-87 (2015).

<https://doi.org:10.1111/imr.12274>

- 66 Wolf, A. J. *et al.* Initiation of the adaptive immune response to *Mycobacterium tuberculosis* depends on antigen production in the local lymph node, not the lungs. *J Exp Med* **205**, 105-115 (2008). <https://doi.org:10.1084/jem.20071367>
- 67 Ozbek, N. *et al.* Interleukin-12 receptor beta 1 chain deficiency in a child with disseminated tuberculosis. *Clin Infect Dis* **40**, e55-58 (2005). <https://doi.org:10.1086/427879>
- 68 Jung, S. M., Han, M., Kim, E. H., Jung, I. & Park, Y.-B. Comparison of developing tuberculosis following tumor necrosis factor inhibition and interleukin-6 inhibition in patients with rheumatoid arthritis: a nationwide observational study in South Korea, 2013–2018. *Arthritis Research & Therapy* **24**, 157 (2022). <https://doi.org:10.1186/s13075-022-02842-6>
- 69 Fallahi-Sichani, M., Flynn, J. L., Linderman, J. J. & Kirschner, D. E. Differential Risk of Tuberculosis Reactivation among Anti-TNF Therapies Is Due to Drug Binding Kinetics and Permeability. *The Journal of Immunology* **188**, 3169-3178 (2012). <https://doi.org:10.4049/jimmunol.1103298>
- 70 MacMicking, J. D. Cell-Autonomous Effector Mechanisms against *Mycobacterium tuberculosis*. *Cold Spring Harbor Perspectives in Medicine* **4** (2014). <https://doi.org:10.1101/cshperspect.a018507>
- 71 Ehlers, S. Role of tumour necrosis factor (TNF) in host defence against tuberculosis: implications for immunotherapies targeting TNF. *Ann Rheum Dis* **62 Suppl 2**, ii37-42 (2003). https://doi.org:10.1136/ard.62.suppl_2.ii37
- 72 Day, T. A. *et al.* Secondary lymphoid organs are dispensable for the development of T-

cell-mediated immunity during tuberculosis. *Eur J Immunol* **40**, 1663-1673 (2010).

<https://doi.org:10.1002/eji.201040299>

73 Russell, D. G. Who puts the tubercle in tuberculosis? *Nat Rev Microbiol* **5**, 39-47 (2007).

<https://doi.org:10.1038/nrmicro1538>

74 Lin, P. L. & Flynn, J. L. CD8 T cells and Mycobacterium tuberculosis infection. *Semin Immunopathol* **37**, 239-249 (2015). <https://doi.org:10.1007/s00281-015-0490-8>

75 Lu, L. L. *et al.* A Functional Role for Antibodies in Tuberculosis. *Cell* **167**, 433-443.e414 (2016). <https://doi.org:https://doi.org/10.1016/j.cell.2016.08.072>

76 Okoye, A. A. & Picker, L. J. CD4(+) T-cell depletion in HIV infection: mechanisms of immunological failure. *Immunol Rev* **254**, 54-64 (2013). <https://doi.org:10.1111/imr.12066>

77 Geldmacher, C. *et al.* Early depletion of Mycobacterium tuberculosis-specific T helper 1 cell responses after HIV-1 infection. *J Infect Dis* **198**, 1590-1598 (2008).

<https://doi.org:10.1086/593017>

78 Geldmacher, C. *et al.* Preferential infection and depletion of Mycobacterium tuberculosis-specific CD4 T cells after HIV-1 infection. *J Exp Med* **207**, 2869-2881 (2010).

<https://doi.org:10.1084/jem.20100090>

79 Murray, L. W. *et al.* Human Immunodeficiency Virus Infection Impairs Th1 and Th17 Mycobacterium tuberculosis-Specific T-Cell Responses. *J Infect Dis* **217**, 1782-1792 (2018).

<https://doi.org:10.1093/infdis/jiy052>

80 Bunjun, R. *et al.* Th22 Cells Are a Major Contributor to the Mycobacterial CD4(+) T

Cell Response and Are Depleted During HIV Infection. *J Immunol* **207**, 1239-1249 (2021).

<https://doi.org:10.4049/jimmunol.1900984>

81 Day, C. L. *et al.* HIV-1 Infection Is Associated with Depletion and Functional Impairment of Mycobacterium tuberculosis-Specific CD4 T Cells in Individuals with Latent Tuberculosis Infection. *J Immunol* **199**, 2069-2080 (2017).

<https://doi.org:10.4049/jimmunol.1700558>

82 Sutherland, R. *et al.* Impaired IFN-gamma-secreting capacity in mycobacterial antigen-specific CD4 T cells during chronic HIV-1 infection despite long-term HAART. *AIDS* **20**, 821-829 (2006). <https://doi.org:10.1097/01.aids.0000218545.31716.a4>

83 Day, C. L. *et al.* Functional Capacity of Mycobacterium tuberculosis-Specific T Cell Responses in Humans Is Associated with Mycobacterial Load. *The Journal of Immunology* **187**, 2222-2232 (2011). <https://doi.org:10.4049/jimmunol.1101122>

84 Amelio, P. *et al.* HIV Infection Functionally Impairs Mycobacterium tuberculosis-Specific CD4 and CD8 T-Cell Responses. *J Virol* **93** (2019). <https://doi.org:10.1128/JVI.01728-18>

85 Hileman, C. O. & Funderburg, N. T. Inflammation, Immune Activation, and Antiretroviral Therapy in HIV. *Curr HIV/AIDS Rep* **14**, 93-100 (2017).

<https://doi.org:10.1007/s11904-017-0356-x>

86 Li, J. Z. *et al.* Antiretroviral Therapy Reduces T-cell Activation and Immune Exhaustion Markers in Human Immunodeficiency Virus Controllers. *Clin Infect Dis* **70**, 1636-1642 (2020).

<https://doi.org:10.1093/cid/ciz442>

87 Blanc, F.-X. *et al.* Earlier versus Later Start of Antiretroviral Therapy in HIV-Infected Adults with Tuberculosis. *New England Journal of Medicine* **365**, 1471-1481 (2011).

<https://doi.org:doi:10.1056/NEJMoa1013911>

88 Bohórquez, J. A., Jagannath, C., Xu, H., Wang, X. & Yi, G. T Cell Responses during Human Immunodeficiency Virus/Mycobacterium tuberculosis Coinfection. *Vaccines (Basel)* **12** (2024). <https://doi.org:10.3390/vaccines12080901>

89 Chiacchio, T. *et al.* Impact of antiretroviral and tuberculosis therapies on CD4+ and CD8+ HIV/M. tuberculosis-specific T-cell in co-infected subjects. *Immunology Letters* **198**, 33-43 (2018). <https://doi.org:https://doi.org/10.1016/j.imlet.2018.04.001>

90 Riou, C. *et al.* Restoration of CD4+ Responses to Copathogens in HIV-Infected Individuals on Antiretroviral Therapy Is Dependent on T Cell Memory Phenotype. *The Journal of Immunology* **195**, 2273-2281 (2015). <https://doi.org:10.4049/jimmunol.1500803>

91 Gantner, P. *et al.* HIV rapidly targets a diverse pool of CD4(+) T cells to establish productive and latent infections. *Immunity* **56**, 653-668.e655 (2023). <https://doi.org:10.1016/j.immuni.2023.01.030>

92 Sun, M. *et al.* Specific CD4+ T cell phenotypes associate with bacterial control in people who ‘resist’ infection with Mycobacterium tuberculosis. *Nature Immunology* **25**, 1411-1421 (2024). <https://doi.org:10.1038/s41590-024-01897-8>

93 Sun, W. *et al.* Phenotypic signatures of immune selection in HIV-1 reservoir cells.

Nature **614**, 309-317 (2023). <https://doi.org/10.1038/s41586-022-05538-8>

94 Naidoo, K. K. *et al.* Early Initiation of Antiretroviral Therapy Preserves the Metabolic Function of CD4+ T Cells in Subtype C Human Immunodeficiency Virus 1 Infection. *J Infect Dis* **229**, 753-762 (2024). <https://doi.org/10.1093/infdis/jiad432>

95 Initiation of Antiretroviral Therapy in Early Asymptomatic HIV Infection. *New England Journal of Medicine* **373**, 795-807 (2015). <https://doi.org/doi:10.1056/NEJMoa1506816>

96 Pai, M. *et al.* Tuberculosis. *Nat Rev Dis Primers* **2**, 16076 (2016).
<https://doi.org/10.1038/nrdp.2016.76>

97 Sakai, S., Mayer-Barber, K. D. & Barber, D. L. Defining features of protective CD4 T cell responses to Mycobacterium tuberculosis. *Curr Opin Immunol* **29**, 137-142 (2014).
<https://doi.org/10.1016/j.coi.2014.06.003>

98 McClelland, R. S. *et al.* A 15-year study of the impact of community antiretroviral therapy coverage on HIV incidence in Kenyan female sex workers. *AIDS* **29**, 2279-2286 (2015).
<https://doi.org/10.1097/qad.0000000000000829>

99 Finak, G. *et al.* Mixture models for single-cell assays with applications to vaccine studies. *Biostatistics* **15**, 87-101 (2014). <https://doi.org/10.1093/biostatistics/kxt024>

100 Lin, L. *et al.* COMPASS identifies T-cell subsets correlated with clinical outcomes. *Nat Biotechnol* **33**, 610-616 (2015). <https://doi.org/10.1038/nbt.3187>

101 Zheng, G. X. Y. *et al.* Massively parallel digital transcriptional profiling of single cells. *Nature Communications* **8**, 14049 (2017). <https://doi.org/10.1038/ncomms14049>

102 Satija, R., Farrell, J. A., Gennert, D., Schier, A. F. & Regev, A. Spatial reconstruction of single-cell gene expression data. *Nature Biotechnology* **33**, 495-502 (2015).

<https://doi.org:10.1038/nbt.3192>

103 Aran, D. *et al.* Reference-based analysis of lung single-cell sequencing reveals a transitional profibrotic macrophage. *Nature Immunology* **20**, 163-172 (2019).

<https://doi.org:10.1038/s41590-018-0276-y>

104 Regev, A. *et al.* The Human Cell Atlas. *eLife* **6**, e27041 (2017).

<https://doi.org:10.7554/eLife.27041>

105 Choudhary, S. & Satija, R. Comparison and evaluation of statistical error models for scRNA-seq. *Genome Biol* **23**, 27 (2022). <https://doi.org:10.1186/s13059-021-02584-9>

106 Finak, G. *et al.* MAST: a flexible statistical framework for assessing transcriptional changes and characterizing heterogeneity in single-cell RNA sequencing data. *Genome Biol* **16**, 278 (2015). <https://doi.org:10.1186/s13059-015-0844-5>

107 Bibby, J. A. *et al.* Systematic single-cell pathway analysis to characterize early T cell activation. *Cell Reports* **41** (2022). <https://doi.org:10.1016/j.celrep.2022.111697>

108 Lin, L. *et al.* COMPASS identifies T-cell subsets correlated with clinical outcomes. *Nature Biotechnology* **33**, 610-616 (2015). <https://doi.org:10.1038/nbt.3187>

109 Bibby, J. A. *et al.* Systematic single-cell pathway analysis to characterize early T cell activation. *Cell Rep* **41**, 111697 (2022). <https://doi.org:10.1016/j.celrep.2022.111697>

110 Reiss, S. *et al.* Comparative analysis of activation induced marker (AIM) assays for

sensitive identification of antigen-specific CD4 T cells. *PLoS One* **12**, e0186998 (2017).

<https://doi.org:10.1371/journal.pone.0186998>

111 Barham, M. S. *et al.* Activation-Induced Marker Expression Identifies Mycobacterium tuberculosis-Specific CD4 T Cells in a Cytokine-Independent Manner in HIV-Infected Individuals with Latent Tuberculosis. *Immunohorizons* **4**, 573-584 (2020).

<https://doi.org:10.4049/immunohorizons.2000051>

112 Luckheeram, R. V., Zhou, R., Verma, A. D. & Xia, B. CD4⁺T cells: differentiation and functions. *Clin Dev Immunol* **2012**, 925135 (2012). <https://doi.org:10.1155/2012/925135>

113 Cooper, A. M. *et al.* Disseminated tuberculosis in interferon gamma gene-disrupted mice. *J Exp Med* **178**, 2243-2247 (1993). <https://doi.org:10.1084/jem.178.6.2243>

114 Ray, J. C., Flynn, J. L. & Kirschner, D. E. Synergy between individual TNF-dependent functions determines granuloma performance for controlling Mycobacterium tuberculosis infection. *J Immunol* **182**, 3706-3717 (2009). <https://doi.org:10.4049/jimmunol.0802297>

115 Scanga, C. A. *et al.* Depletion of CD4(+) T cells causes reactivation of murine persistent tuberculosis despite continued expression of interferon gamma and nitric oxide synthase 2. *J Exp Med* **192**, 347-358 (2000). <https://doi.org:10.1084/jem.192.3.347>

116 Grant Nicole, L. *et al.* Mycobacterium tuberculosis-Specific CD4 T Cells Expressing Transcription Factors T-Bet or ROR γ T Associate with Bacterial Control in Granulomas. *mBio* **14**, e00477-00423 (2023). <https://doi.org:10.1128/mbio.00477-23>

117 Khader, S. A. *et al.* IL-23 and IL-17 in the establishment of protective pulmonary CD4+

T cell responses after vaccination and during Mycobacterium tuberculosis challenge. *Nat Immunol* **8**, 369-377 (2007). <https://doi.org:10.1038/ni1449>

118 Okamoto Yoshida, Y. *et al.* Essential role of IL-17A in the formation of a mycobacterial infection-induced granuloma in the lung. *J Immunol* **184**, 4414-4422 (2010).

<https://doi.org:10.4049/jimmunol.0903332>

119 Mpande, C. A. M. *et al.* Functional, Antigen-Specific Stem Cell Memory (T(SCM)) CD4(+) T Cells Are Induced by Human Mycobacterium tuberculosis Infection. *Front Immunol* **9**, 324 (2018). <https://doi.org:10.3389/fimmu.2018.00324>

120 Orlando, V. *et al.* Human CD4 T-Cells With a Naive Phenotype Produce Multiple Cytokines During Mycobacterium Tuberculosis Infection and Correlate With Active Disease. *Frontiers in Immunology* **9** (2018). <https://doi.org:10.3389/fimmu.2018.01119>

121 Lyadova, I. & Nikitina, I. Cell Differentiation Degree as a Factor Determining the Role for Different T-Helper Populations in Tuberculosis Protection. *Front Immunol* **10**, 972 (2019). <https://doi.org:10.3389/fimmu.2019.00972>

122 Caccamo, N., Joosten, S. A., Ottenhoff, T. H. M. & Dieli, F. Atypical Human Effector/Memory CD4(+) T Cells With a Naive-Like Phenotype. *Front Immunol* **9**, 2832 (2018). <https://doi.org:10.3389/fimmu.2018.02832>

123 Zhao, X., Shan, Q. & Xue, H.-H. TCF1 in T cell immunity: a broadened frontier. *Nature Reviews Immunology* **22**, 147-157 (2022). <https://doi.org:10.1038/s41577-021-00563-6>

124 Ljungberg, J. K., Kling, J. C., Tran, T. T. & Blumenthal, A. Functions of the WNT

Signaling Network in Shaping Host Responses to Infection. *Front Immunol* **10**, 2521 (2019).

<https://doi.org:10.3389/fimmu.2019.02521>

125 Gattinoni, L., Ji, Y. & Restifo, N. P. Wnt/beta-catenin signaling in T-cell immunity and cancer immunotherapy. *Clin Cancer Res* **16**, 4695-4701 (2010). <https://doi.org:10.1158/1078-0432.CCR-10-0356>

126 Mukherjee, T. & Balaji, K. N. The WNT Framework in Shaping Immune Cell Responses During Bacterial Infections. *Front Immunol* **10**, 1985 (2019).

<https://doi.org:10.3389/fimmu.2019.01985>

127 Valverde-Villegas, J. M., Matte, M. C., de Medeiros, R. M. & Chies, J. A. New Insights about Treg and Th17 Cells in HIV Infection and Disease Progression. *J Immunol Res* **2015**,

647916 (2015). <https://doi.org:10.1155/2015/647916>

128 Tolomeo, M. & Cascio, A. The Complex Dysregulations of CD4 T Cell Subtypes in HIV Infection. *International Journal of Molecular Sciences* **25**, 7512 (2024).

129 DaFonseca, S. *et al.* Impaired Th17 polarization of phenotypically naive CD4⁺ T-cells during chronic HIV-1 infection and potential restoration with early ART. *Retrovirology* **12**, 38

(2015). <https://doi.org:10.1186/s12977-015-0164-6>

130 McKinstry, K. K. *et al.* Effector CD4 T-cell transition to memory requires late cognate interactions that induce autocrine IL-2. *Nature Communications* **5**, 5377 (2014).

<https://doi.org:10.1038/ncomms6377>

131 Dang, E. V. *et al.* Control of T(H)17/T(reg) balance by hypoxia-inducible factor 1. *Cell*

146, 772-784 (2011). <https://doi.org:10.1016/j.cell.2011.07.033>

132 Knight, M. & Stanley, S. HIF-1alpha as a central mediator of cellular resistance to intracellular pathogens. *Curr Opin Immunol* **60**, 111-116 (2019).

<https://doi.org:10.1016/j.coi.2019.05.005>

133 Duette, G. *et al.* Induction of HIF-1alpha by HIV-1 Infection in CD4(+) T Cells Promotes Viral Replication and Drives Extracellular Vesicle-Mediated Inflammation. *mBio* **9** (2018).

<https://doi.org:10.1128/mBio.00757-18>

134 Marchingo, J. M. & Cantrell, D. A. Protein synthesis, degradation, and energy metabolism in T cell immunity. *Cell Mol Immunol* **19**, 303-315 (2022).

<https://doi.org:10.1038/s41423-021-00792-8>

135 Turner, M. Regulation and function of poised mRNAs in lymphocytes. *Bioessays* **45**, e2200236 (2023). <https://doi.org:10.1002/bies.202200236>

136 Masopust, D. & Schenkel, J. M. The integration of T cell migration, differentiation and function. *Nature Reviews Immunology* **13**, 309-320 (2013). <https://doi.org:10.1038/nri3442>

137 Corn, R. A. *et al.* T cell-intrinsic requirement for NF-kappa B induction in postdifferentiation IFN-gamma production and clonal expansion in a Th1 response. *J Immunol*

171, 1816-1824 (2003). <https://doi.org:10.4049/jimmunol.171.4.1816>

138 Oh, H. & Ghosh, S. NF-κB: roles and regulation in different CD4(+) T-cell subsets.

Immunol Rev **252**, 41-51 (2013). <https://doi.org:10.1111/imr.12033>

139 Wong, L. M. & Jiang, G. NF-κβ sub-pathways and HIV cure: A revisit. *eBioMedicine* **63**

(2021). <https://doi.org:10.1016/j.ebiom.2020.103159>

140 Ross, S. H. & Cantrell, D. A. Signaling and Function of Interleukin-2 in T Lymphocytes. *Annu Rev Immunol* **36**, 411-433 (2018). <https://doi.org:10.1146/annurev-immunol-042617-053352>

141 Taniguchi, T. & Minami, Y. The IL-2/IL-2 receptor system: A current overview. *Cell* **73**, 5-8 (1993). [https://doi.org:https://doi.org/10.1016/0092-8674\(93\)90152-G](https://doi.org:https://doi.org/10.1016/0092-8674(93)90152-G)

142 Tkaczuk, J. *et al.* Effect of Anti-IL-2R α Antibody on IL-2-induced Jak/STAT Signaling. *American Journal of Transplantation* **2**, 31-40 (2002). <https://doi.org:https://doi.org/10.1034/j.1600-6143.2002.020107.x>

143 Adankwah, E., Seyfarth, J., Phillips, R. & Jacobsen, M. Aberrant cytokine milieu and signaling affect immune cell phenotypes and functions in tuberculosis pathology: What can we learn from this phenomenon for application to inflammatory syndromes? *Cellular & Molecular Immunology* **18**, 2062-2064 (2021). <https://doi.org:10.1038/s41423-021-00695-8>

144 Kumararatne, D. S. *et al.* Specific lysis of mycobacterial antigen-bearing macrophages by class II MHC-restricted polyclonal T cell lines in healthy donors or patients with tuberculosis. *Clin Exp Immunol* **80**, 314-323 (1990). <https://doi.org:10.1111/j.1365-2249.1990.tb03287.x>

145 Canaday, D. H. *et al.* CD4(+) and CD8(+) T cells kill intracellular Mycobacterium tuberculosis by a perforin and Fas/Fas ligand-independent mechanism. *J Immunol* **167**, 2734-2742 (2001). <https://doi.org:10.4049/jimmunol.167.5.2734>

146 Kaufmann, S. H. Cell-mediated immunity: dealing a direct blow to pathogens. *Curr Biol*

9, R97-99 (1999). [https://doi.org:10.1016/s0960-9822\(99\)80059-1](https://doi.org:10.1016/s0960-9822(99)80059-1)

147 Dotiwala, F. & Lieberman, J. Granulysin: killer lymphocyte safeguard against microbes. *Current Opinion in Immunology* **60**, 19-29 (2019).

<https://doi.org:https://doi.org/10.1016/j.coi.2019.04.013>

148 Zou, S. *et al.* The Role of CD4(+)CD8(+) T Cells in HIV Infection With Tuberculosis. *Front Public Health* **10**, 895179 (2022). <https://doi.org:10.3389/fpubh.2022.895179>

149 Du Bruyn, E. *et al.* Comparison of the frequency and phenotypic profile of Mycobacterium tuberculosis-specific CD4 T cells between the site of disease and blood in pericardial tuberculosis. *Front Immunol* **13**, 1009016 (2022).

<https://doi.org:10.3389/fimmu.2022.1009016>

150 Seder, R. A., Darrah, P. A. & Roederer, M. T-cell quality in memory and protection: implications for vaccine design. *Nature Reviews Immunology* **8**, 247-258 (2008).

<https://doi.org:10.1038/nri2274>

151 Morou, A. *et al.* Altered differentiation is central to HIV-specific CD4+ T cell dysfunction in progressive disease. *Nature Immunology* **20**, 1059-1070 (2019).

<https://doi.org:10.1038/s41590-019-0418-x>

152 Wilkinson, K. A. *et al.* Effect of treatment of latent tuberculosis infection on the T cell response to Mycobacterium tuberculosis antigens. *J Infect Dis* **193**, 354-359 (2006).

<https://doi.org:10.1086/499311>

153 Riou, C., Jhilmeet, N., Rangaka, M. X., Wilkinson, R. J. & Wilkinson, K. A.

Tuberculosis Antigen-Specific T-Cell Responses During the First 6 Months of Antiretroviral Treatment. *The Journal of Infectious Diseases* **221**, 162-167 (2019).

<https://doi.org:10.1093/infdis/jiz417>

154 Wang, X.-M. *et al.* Global transcriptomic characterization of T cells in individuals with chronic HIV-1 infection. *Cell Discovery* **8**, 29 (2022). <https://doi.org:10.1038/s41421-021-00367-x>

155 Collora, J. A., Liu, R., Albrecht, K. & Ho, Y. C. The single-cell landscape of immunological responses of CD4+ T cells in HIV versus severe acute respiratory syndrome coronavirus 2. *Curr Opin HIV AIDS* **16**, 36-47 (2021).

<https://doi.org:10.1097/coh.0000000000000655>

156 Kim, D. *et al.* TopHat2: accurate alignment of transcriptomes in the presence of insertions, deletions and gene fusions. *Genome Biology* **14**, R36 (2013).

<https://doi.org:10.1186/gb-2013-14-4-r36>

157 Hsu, F. *et al.* The UCSC Known Genes. *Bioinformatics* **22**, 1036-1046 (2006).

<https://doi.org:10.1093/bioinformatics/btl048>

158 Lawrence, M. *et al.* Software for Computing and Annotating Genomic Ranges. *PLOS Computational Biology* **9**, e1003118 (2013). <https://doi.org:10.1371/journal.pcbi.1003118>

159 Robinson, M. D., McCarthy, D. J. & Smyth, G. K. edgeR: a Bioconductor package for differential expression analysis of digital gene expression data. *Bioinformatics* **26**, 139-140 (2009). <https://doi.org:10.1093/bioinformatics/btp616>

- 160 Zhang, Y. *et al.* Model-based Analysis of ChIP-Seq (MACS). *Genome Biology* **9**, R137 (2008). <https://doi.org:10.1186/gb-2008-9-9-r137>
- 161 Heinz, S. *et al.* Simple Combinations of Lineage-Determining Transcription Factors Prime cis-Regulatory Elements Required for Macrophage and B Cell Identities. *Molecular Cell* **38**, 576-589 (2010). <https://doi.org:https://doi.org/10.1016/j.molcel.2010.05.004>
- 162 Chang, E., Cavallo, K. & Behar, S. M. CD4 T cell dysfunction is associated with bacterial recrudescence during chronic tuberculosis. *Nature Communications* **16**, 2636 (2025). <https://doi.org:10.1038/s41467-025-57819-1>
- 163 Doitsh, G. & Greene, Warner C. Dissecting How CD4 T Cells Are Lost During HIV Infection. *Cell Host & Microbe* **19**, 280-291 (2016). <https://doi.org:https://doi.org/10.1016/j.chom.2016.02.012>
- 164 Pawlowski, A., Jansson, M., Sköld, M., Rottenberg, M. E. & Källenius, G. Tuberculosis and HIV Co-Infection. *PLOS Pathogens* **8**, e1002464 (2012). <https://doi.org:10.1371/journal.ppat.1002464>
- 165 Thomas, R., Qiao, S. & Yang, X. Th17/Treg Imbalance: Implications in Lung Inflammatory Diseases. *International Journal of Molecular Sciences* **24**, 4865 (2023).